Flocculation performance of lignin-acrylamide derivatives

A thesis presented to

The Faculty of Graduate Studies of

Lakehead University

by

Malak Aldajani

Supervisor Dr. Pedram Fatehi

In partial fulfillment of the requirements

for the degree of

Master of Science in Chemistry Department

August 2019

Abstract

Wastewater produced in different industries contains fine suspended particles that raise a number of environmental concerns due to their potential toxicity and physicochemical properties and make their removal from industrial wastewater a challenging process. Synthetic polymers are commonly used as flocculants in colloidal systems due to their effectiveness at low dosages and their inertness to pH changes. However, in addition to their high costs, these synthetic polymers are toxic and nonbiodegradable. These disadvantages of synthetic flocculants can be overcome by using flocculants derived from natural sources. Lignin, after cellulose, is the most abundant biopolymer; it's an inexpensive raw material, and readily available as a by-product of pulping processes. Kraft lignin does not possess suitable properties to be used as a flocculant, however, lignin attributes can be changed by means of chemical modification. In this thesis, kraft lignin-acrylamide polymer was produced and then hydrolyzed to a product with properties that favor its use as a flocculant. The flocculant performance of hydrolyzed kraft lignin-acrylamide polymer was compared with analyzed kraft lignin-acrylamide and polyacrylamide polymers synthesized under the same conditions, in an alumina suspension. Alternatively, kraft lignin was modified via carboxymethylation and oxidation, and subsequently polymerized with acrylamide monomer to produce an effective flocculant for alumina suspension. The properties of the resulting polymers were characterized using different methods including TGA, DSC, elemental analysis, molecular weight analysis, and NMR. All of these methods illustrated remarkable changes in the chemical and physical properties of kraft lignin after modification. The flocculant properties of the produced polymers were investigated in alumina suspension by studying a) the adsorption behavior of polymer on alumina particles, b) the effect of modified lignin on the zeta potential of alumina suspension, c) the affinity of the modified polymers to alter the relative turbidity of alumina

colloids. The flocculation of the lignin polymers in alumina suspension was also analyzed by an FBRM. The results obtained demonstrated that modified lignin could indeed act as an effective flocculant in an alumina suspension with its performance being mainly dependent on charge density, molecular weight, and affinity to decrease the zeta potential of the alumina suspension. Modified lignin with a higher charge density showed high adsorption on alumina particles and significantly reduced the relative turbidity of the suspension. This work demonstrates the potential of using renewable and inexpensive material, i.e., kraft lignin, in the production of environmentally friendly flocculants.

Acknowledgments

First and foremost, I would like to thank my supervisor Dr. Pedram Fatehi, for his help, and guidance throughout my research. I would also like to thank my committee members, Dr. C. Gottardo, Dr. E. Rezaei, and chemistry program coordinator Dr. R. Mawhinney for their support, and advice.

Additionally, I would like to thank Dr. Fatehi's lab members for helping me through my graduate studies when help was needed and keeping the time spent in the lab interesting. I also wish to thank my family and friends for all of their love and support.

Dedications

I would like to dedicate my thesis to my parents for their love, endless support, and encouragement.

Table of Contents

List of tables

List of figures

List of schemes

List of abbreviations

KL	Kraft lignin
KL-AM	Kraft lignin-acrylamide
HKL-AM	Hydrolyized kraft lignin-acrylamide
OKL	Oxidized kraft lignin
CMKL	Carboxymethylated lignin
OKL-AM	Oxidized kraft lignin-acrylamide
CMKL-AM	Carboxymethylated kraft lignin-acrylamide
AM	Acrylamide
DADMAC	Diallyldimethyl ammonium chloride
DDJ	Dynamic draining jar
FBRM	Focused beam reflectance measurement
FTIR	Fourier transform infrared spectrophotometry
GPC	Gel permeation chromatography
M_N	Number-average molecular weight
Mw	Weight-average molecular weight
NMR	Nuclear magnetic resonance
PDA	Photometric dispersion analysis
$K_2S_2O_8$	Potassium persulfate

List of equations

Chapter 1: Introduction

1.1 Overview

Industrial effluents is a major environmental issue around the world that is growing with the growth of population and increased material consumption (Lee and Chong, 2014). These effluents contain heavy metals, dyes, inorganic, and organic particles, and some of these contaminants are known to be toxic and carcinogenic (Razali and Ariffin, 2015). The properties of these particles affect their behavior in solid-liquid phase and thus their removal. The presence of surface charges and the small size of these particles makes it hard to bring them close to form a heavy mass for settlement, and this makes the filtration process challenging for industry (Radoiu et al., 2004). Different methods have been utilized to remove colloidal particles from wastewater, such as coagulation, flocculation, membrane filtration, adsorption, solvent extraction, floatation, and biological methods (Divakaran and Sivasankara Pillai, 2001; Nasser and James, 2006). Flocculation is the most commonly used solid/liquid separation method for the removal of colloids and organic matter suspended in industrial wastewater. This method is simple, efficient, and has been successfully used in the treatment of wastewater effluents, such as that of pulp mills, textile, oily wastewater, and sanitary landfill leachates (Ahmad et al., 2005; Wong et al., 2006; Yue et al., 2008; Razali and Ariffin, 2015a).

Synthetic polymers are heavily used as flocculants in industry. However, due to the environmental concerns associated with the use of synthetic polymers, the search for efficient, bio-based flocculants has become a topic of research. For many years, flocculants based on biopolymers such as cellulose, starch, chitosan, and guar gum have been researched for their potential use in industry (Singh et al., 2000; Renault et al., 2009; Ben et al., 2011; Wang et al., 2012). However, these biopolymers are widely used in other applications such as fermentation processes, pharmaceutical,

papermaking, and agricultural industries, which limits their availability to be used as flocculants (Wang et al., 2011)

In this context, lignin as a biopolymer has a great potential to be used in flocculants production. Currently, lignin is produced in large quantity as a by-product of pulping processes and is considered an underutilized material in the pulping industry (Hatakeyama, 2009). Lignin in its native state has poor interaction with colloidal particles, including those of aluminum oxide (alumina) suspensions due to its limited functional groups. Different studies have investigated the performance of lignin-based flocculants in bentonite and kaoline suspensions (Hasan and Fatehi, 2019; Price and Fatehi, 2018). However, very few studies were reported on the performance of lignin-based flocculants in alumina suspension (Kong et al., 2018; Kazzaz et al., 2018). In this MSc study, the performance of hydrolyzed lignin-acrylamide polymer in alumina suspension was studied in comparison with unhydrolyzed polymer and polyacrylamide (PAM). Anionic lignin acrylamide polymers were produced via oxidation, carboxymethylation of lignin, and subsequent polymerization with acrylamide monomer (AM). Their performance in alumina suspension was also assessed. The effect of polymer properties, such as charge density and molecular weight on their flocculation performance, were investigated. Adsorption of lignin-acrylamide based flocculants on alumina particles were also reported. Different mechanisms such as charge neutralization, bridging, and electrostatic patching have been proposed in the literature to explain flocs formation, and destabilization of colloidal particles by polymers. These flocculation mechanisms are crucially dependent on polymers adsorption (Szyguła et al., 2009; Razali et al., 2011). Adsorption of polymers on the particles' surface occurs in different ways, including electrostatic interaction and hydrogen bonding. The extent of adsorption not only depends on polymer characteristics but also the properties of colloidal particles (Petzold et al., 2003; Szyguła

et al., 2009; Rabiee, 2010). The adsorption of charged polymers on alumina particles also affects their electrokinetic potential, which influences the flocculation process (Petzold et al., 2003).

The main focus of this dissertation is to asses the performance of anionic lignin-acrylamide based flocculants in alumina suspension. In this chapter (Chapter 1) a summary of this work is given. Furthermore, the objectives and novelty of this work are presented.

Chapter two discusses the literature review on lignin properties, different chemical modification methods, methods to characterize lignin-based polymers, and the different methods to assess the flocculation performance of polymers.

In chapter three, the main focus was on the production and hydrolysis of lignin-acrylamide polymers under different conditions. The effect of various polymerization conditions on the characteristics of lignin-acrylamide polymer was also presented. The properties of polymers and their adsorption analysis on alumina were reported. The characteristics of the products were investigated using ^{1}H NMR, FTIR, elemental analyzer, TGA, and DSC. The polymers' effect on the alumina suspension's zeta potential, relative turbidity, and alumina removal from suspension was discussed. The properties of polymers and their performance under shear forces were also reported using FBRM.

Chapter four investigates the production of anionic flocculants via polymerization of oxidized, and carboxymethylated lignin with acrylamide. The properties of polymers were analyzed, and the flocculation performance of produced copolymers was investigated via zeta potential, turbidity analysis, adsorption analysis, and FBRM. The ability of the polymers to remove alumina was also investigated.

Chapter five represents the overall conclusions of the thesis and presents recommendations for future work.

1.2. Questions to investigate

1. What will be the effect of hydrolysis conditions on lignin-acrylamide properties such as charge density, and how this will influence their flocculation efficiency in alumina suspension?

2. What processes can be followed for the production of pretreated anionic lignin?

3. How will the flocculation performance of modified anionic lignin-acrylamide polymers differ in alumina suspension based on their properties?

1.3. Novelty of study

This study is novel as it will present results for the

1.investigation on the effect of different hydrolysis conditions on the properties of lignin-acrylamide polymers and their performance in alumina suspension

2.the production of novel products via polymerization of oxidized and carboxymethylated lignin with acrylamide monomer.

3. investigation on the performance of anionic lignin-acrylamide based flocculants in alumina suspension.

References

Ahmad, A. L., Ismail, S., & Bhatia, S. (2005). Optimization of coagulation− flocculation process for palm oil mill effluent using response surface methodology. *Environmental science & technology*, *39*(8), 2828-2834.

Ben, W., Yulian, Z., Chunbao, M., 2011. Preparation of Cationic Chitosan-Polyacrylamide Flocculant and Its Properties in Wastewater Treatment. *Journal Ocean University China (Oceanic and Coastal Sea Research)*,10 (2), 42-46.

Bolto, B., & Gregory, J. (2007). Organic polyelectrolytes in water treatment. *Water research*, *41*(11), 2301-2324.

Divakaran, R., & Pillai, V. S. (2001). Flocculation of kaolinite suspensions in water by chitosan. *Water Research*, *35*(16), 3904-3908.

Hasan, A., & Fatehi, P. (2019). Cationic kraft lignin-acrylamide copolymer as a flocculant for clay suspensions:(2) Charge density effect. *Separation and Purification Technology*, *210*, 963-972.

Hatakeyama, H., & Hatakeyama, T. (2009). Lignin structure, properties, and applications. In *Biopolymers* (pp. 1-63). Springer, Berlin, Heidelberg.

Kazzaz, A. E., Feizi, Z. H., & Fatehi, P. (2018). Interaction of sulfomethylated lignin and aluminum oxide. *Colloid and Polymer Science*, *296*(11), 1867-1878.

Kong, F., Wang, S., Gao, W., & Fatehi, P. (2018). Novel pathway to produce high molecular weight kraft lignin–acrylic acid polymers in acidic suspension systems. *RSC Advances*, *8*(22), 12322-12336.

Lee, C. S., Robinson, J., & Chong, M. F. (2014). A review on application of flocculants in wastewater treatment. *Process Safety and Environmental Protection*, *92*(6), 489-508.

Nasser, M. S., & James, A. E. (2006). The effect of polyacrylamide charge density and molecular weight on the flocculation and sedimentation behavior of kaolinite suspensions. *Separation and purification technology*, *52*(2), 241-252.

Petzold, G., Mende, M., Lunkwitz, K., Schwarz, S., & Buchhammer, H. M. (2003). Higher efficiency in the flocculation of clay suspensions by using combinations of oppositely charged polyelectrolytes. *Colloids and Surfaces A: Physicochemical and Engineering Aspects*, *218*(1-3), 47-57.

Price, J. T., Gao, W., & Fatehi, P. (2018). Lignin-g-poly (acrylamide)-g-poly (diallyl dimethyl-ammoniumchloride):Synthesis,Characterization,andApplications. *ChemistryOpen*, *7*(8) , 645-65

Rabiee, A. (2010). Acrylamide-based anionic polyelectrolytes and their applications: A survey. *Journal of Vinyl and Additive Technology*, *16*(2), 111-119.

Radoiu, M. T., Martin, D. I., Calinescu, I., & Iovu, H. (2004). Preparation of polyelectrolytes for wastewater treatment. *Journal of Hazardous Materials*, *106*(1), 27-37.

Razali, M. A. A., & Ariffin, A. (2015). Polymeric flocculant based on cassava starch grafted polydiallyldimethylammonium chloride: flocculation behavior and mechanism. *Applied Surface Science*, *351*, 89-94.

Renault, F., Sancey, B., Badot, P. M., & Crini, G. (2009). Chitosan for coagulation/flocculation processes–an eco-friendly approach. *European Polymer Journal*, *45*(5), 1337-1348.

Singh, R. P., Karmakar, G. P., Rath, S. K., Karmakar, N. C., Pandey, S. R., Tripathy, T., ... & Lan, N. T. (2000). Biodegradable drag reducing agents and flocculants based on polysaccharides: materials and applications. *Polymer Engineering & Science*, *40*(1), 46-60.

Szyguła, A., Guibal, E., Palacín, M. A., Ruiz, M., & Sastre, A. M. (2009). Removal of an anionic dye (Acid Blue 92) by coagulation-flocculation using chitosan. *Journal of Environmental Management*, *90*(10), 2979-2986.

Wang, J. P., Chen, Y. Z., Wang, Y., Yuan, S. J., Sheng, G. P., & Yu, H. Q. (2012). A novel efficient cationic flocculant prepared through grafting two monomers onto chitosan induced by Gamma radiation. *RSC Advances*, *2*(2), 494-500.

Wang, J. P., Chen, Y. Z., Wang, Y., Yuan, S. J., Sheng, G. P., & Yu, H. Q. (2012). A novel efficient cationic flocculant prepared through grafting two monomers onto chitosan induced by Gamma radiation. *RSC Advances*, *2*(2), 494-500.

Wong, S. S., Teng, T. T., Ahmad, A. L., Zuhairi, A., & Najafpour, G. (2006). Treatment of pulp and paper mill wastewater by polyacrylamide (PAM) in polymer induced flocculation. *Journal of Hazardous Materials*, *135*(1-3), 378-388.

Yue, Q. Y., Gao, B. Y., Wang, Y., Zhang, H., Sun, X., Wang, S. G., & Gu, R. R. (2008). Synthesis of polyamine flocculants and their potential use in treating dye wastewater. *Journal of Hazardous Materials*, *152*(1), 221-227.

Chapter 2: Literature review

2.1. Introduction

The growing awareness concerning human effects on the environment and depletion of fossil fuel resources has driven research to find safe, bio-based, and renewable alternatives in the last two decades. The production of biofuels and biomaterials will contribute to a sustainable and greener economy (Kamm and Kamm, 2004; Elmekawy et al., 2013).

In this perspective, interest in biomass resources and biorefining processes has increased over the last decade. Biorefining processes are based on the utilization of biomass by different conversion processes, including thermal, thermochemical, and biochemical to produce valuable products. Lignocellulosic biomass is the most abundantly available material on earth, which makes it a sustainable platform for the production of chemicals, fuels, energy, and bio-based products (Elmekawy et al., 2013). Lignocellulosic biomass consists of carbohydrate polymers (cellulose, hemicellulose) and an aromatic polymer (lignin) (Kamm and Kamm, 2004). Lignin plays a significant role in plants. It constitutes, with cellulose and hemicellulose, the structural cell wall of vascular plants to control fluid flow and provide plants with structural rigidity and resistance to microbial decay (Hatakeyama and Hatakeyama, 2009). Lignin can be extracted from wood, annual crops, such as wheat straw, or agricultural residue, such as sugar cane bagasse. The percentage of lignin in plants varies considerably based on plant species. In general, softwood species have more lignin compared to hardwood species (Inwood, 2014).

Most biorefining processes focus on the utilization of cellulose and hemicellulose while lignin has been considered as a low-value residue. A large quantity of lignin is produced every year as a by-product of different biorefining and pulping processes (Mai et al., 2000). Most of the lignin is

either incinerated to produce low-cost fuel or chemically degraded to a low molecular weight aromatic compounds. However, only 2% of lignin has been commercialized for the production of value-added products (Laurichesse and Avérous, 2014). The polymeric structure of lignin and its renewable resources create great potential for lignin-based products. However, the utilization of lignin is hindered by its unclearly defined structure and its variability according to the origin, fragmentation, and separation processes (Vishtal and Kraslawski, 2011).

2.2. Lignin structure

Lignin has an amorphous and polyphenolic structure (Scheme 2.1) composed of phenylpropane units that are connected by carbon-carbon and ether bonds, mostly alkyl-aryl ether bonds. Phenylpropane units are generated from three alcohol precursors (monolignols), *p*-coumaryl, coniferyl, and sinapyl alcohol (Hatakeyama and Hatakeyama, 2009; El Mansouri et al., 2011). During biological lignification processes, these monolignols are cross-linked through radical coupling reaction to form a multibranched and three-dimensional structure consisting of three types of lignin units called *p*-hydroxyphenyl, guaiacyl, and syringyl units, as shown in Scheme 2.2.
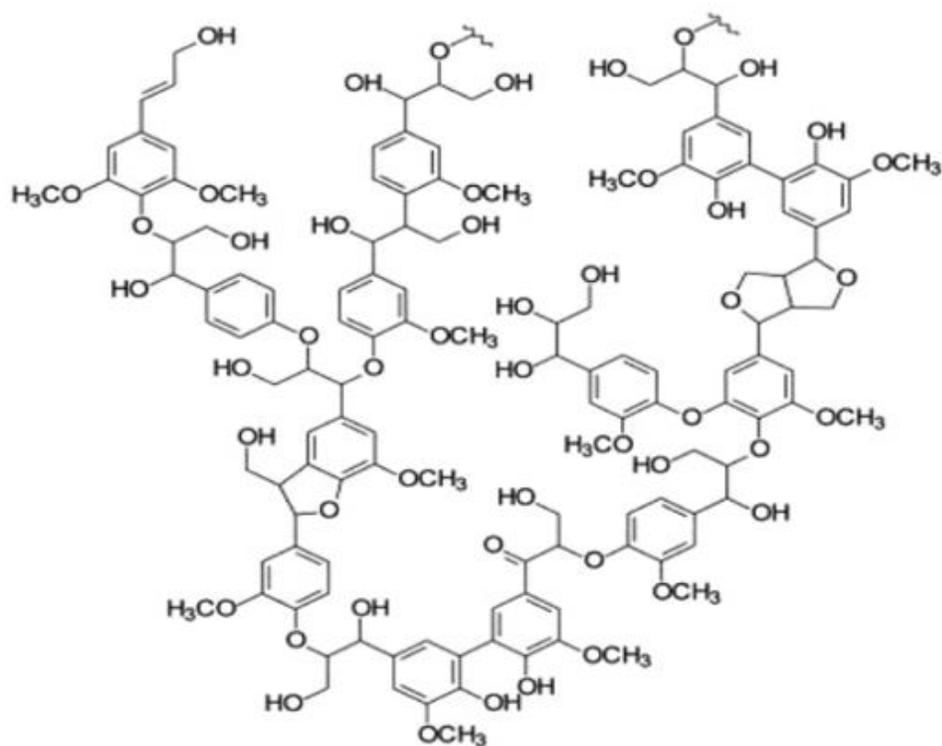
Scheme 2.1. Structure of native lignin (Lewinsky, 2007)
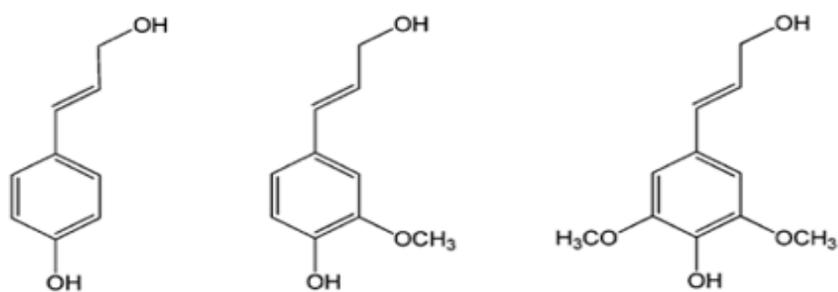
Scheme 2.2. Phenyl propene units. *P*- hydroxy phenylpropene (H), guaiacol(G), Syringyl (S), (from left to right) (Inwood, 2014).

9

Lignin structure lacks order and pattern. The type of lignocellulosic species, environment, and extraction methods influence lignin compositions, content, size, amount, and degree of cross-linkage. For example, softwood lignin mostly consists of G units while hardwood lignin shows a more heterogeneous structure of S, and G units and low amount of H units. Due to extensive research, the monomeric units of lignin have been defined; whereas, the polymeric structure of lignin has not been fully elucidated (El Mansouri et al., 2011).

2.3. Lignin production

The main production of lignin happens in the pulping industry as a by-product, estimated between 30 to 50 million tons per year as a non-commercialized waste product (Varanasi et al., 2013). Also to meet the goal of replacing 30% of fossil fuel with biofuel by the year of 2030, about 223 million tons of lignin are expected to be generated as a by-product of fermentation processes (Sahoo et al., 2011). However, only 2% of lignin is utilized and used commercially, and the rest is incinerated as a solid fuel to generate energy for the pulping process (Sahoo et al., 2011).

Kraft and sulfite pulping processes are the two main techniques to produce lignin. In the sulfite pulping process, sulfur dioxide and a base containing magnesium, calcium, sodium, or ammonium, are used to produce paper products, which also results in lignin generation (Arkell et al., 2014). In the process, lignin is sulfonated, degraded, and solubilized, producing what is called lignosulfonate (Vishtal and Kraslawski, 2011). Lignosulfonate is water-soluble because of its anionic sulfonic acid groups and a variety of other functional groups such as carboxylic groups, and phenolic hydroxyl groups (Arekogh et al., 2010). It also has a relatively high molecular weight ranging from 1,000 to 150,000 g/mol (Vishtal and Kraslawski, 2011). As a result of the properties mentioned

above, lignosulfonates can be used as dispersing agents, cement additives, surfactants, adhesives, and binders for drilling agents (Vishtal and Kraslawski, 2011; Laurichesse and Avérous, 2014). However, lignosulfonate only accounts for 10 % of lignin production in the world. Due to environmental problems associated with the sulfite pulping process, most of the pulp mills around the world are kraft based operations (Kuzmenko, 2010).

In the kraft process, 90 to 95 % of lignin in wood is dissolved using an aqueous solution of NaOH and N_2S (Chakra and Raqauskas, 2004). Kraft lignin has a high proportion of condensed structure and high levels of phenolic hydroxyl groups due to the extensive cleavage of β-aryl bonds during the cooking process. This condensed structure of kraft lignin limits its reactivity and solubility in water (Vishtal and Kraslawski, 2011). As a result, kraft lignin has not found uses as a high value-added product (Zakzeski et al., 2010). However, by developing a better understanding of lignin structure and continuing the research on lignin utilization, the potential of lignin as a renewable, and widely available material can be unlocked (Varanasi et al., 2013). Besides limited reactivity, kraft lignin's low molecular weight and hydrophobicity are the two main factors limiting kraft lignin utilization. However, these limitations can be overcome by chemical modification of lignin (Ahvazi et al., 2011).

2.4. Chemical modification of lignin

While lignin is currently used as an additive or filler, it has not been exploited comprehensively as a raw material for chemical production due to its complicated and condensed structure. The inter-unit connections in lignin structure by a multitude of ether and carbon-carbon bonds occupy reactive sites, which limit lignin solubility and reactivity (Yuan et al., 2010). However, various methods have been employed to alter lignin structure, and hence its chemical and physical properties. In general, lignin reactivity is based on hydroxyl groups both aliphatic and aromatic

and specific positions (mainly ortho position) of the aromatic ring. As a result, the chemical modification of lignin happens by modifying hydroxyl groups or creating new reactive sites through grafting and polymerization reactions (Yuan et al., 2010).

The main approach to modify lignin structure in the past was lignin fragmentation. This approach degrades lignin to fractions with lower molecular weight to increase the number of phenolic hydroxyl groups and minimize the stereo- hindrance effect for further chemical modification (Hu et al., 2011). Lignin degradation, as a resource for low molar mass compounds, has gained high interest, especially with limited fossil fuel resources. Lignin degradation is utilized to obtain a variety of compounds such as aldehydes, hydroxylated and simple aromatics, vanillin, quinines, aliphatic acids, and many other chemical compounds. Different enzymatic and thermochemical fragmentation pathways and their effect on lignin structure have been widely investigated (Negrão et al., 2012; Laurichesse and Avérous, 2014).

One of the commonly used modification methods is the demethylation of lignin to remove methyl groups that hinder lignin reactivity by blocking reactive sites. Sulfur mediated demethylation is the most reported method to remove methyl groups (An et al., 1995; Wu and Zhan, 2001). Other methods, including phenolation and sulfonation, have been widely investigated in the literature. Phenolation or phenolysis is the thermal treatment of lignin with phenol in an acidic medium resulting in the condensation of phenol with lignin aromatic ring and side-chain (Effendi et al., 2008). It is one of the most used methods for lignin modification to increase the content of phenolic hydroxyl groups and thus lignin reactivity improvement (Hu et al., 2011). Phenolated lignin is mostly used as a phenol substitute in the production of phenol-formaldehyde resins (Inwood, 2014). Sulfonation of lignin involves the introduction of sulfonic acid groups to the aromatic ring of lignin, leading to high solubility and charge density (Inwood, 2014). Part of the work in this

thesis would be focused on chemical modification methods such as lignin oxidation and carboxymethylation.

2.4.1. Lignin oxidation

Lignin oxidation makes valuable lignin-based material by increasing lignin's reactivity and solubility in water (Villar et al., 2001). Different oxidation pathways via nitrobenzene, metal oxides, oxygen, and air were reported (Sun et al., 1995; Laurichesse and Avérous, 2014; Mahmood et al., 2016). These methods preserve lignin's aromatic ring and produce valuable products such as aldehydes (vanillin and syringic), acids (vanillic and syringic acids), polyfunctional monomeric, and fine chemicals (Laurichesse and Avérous, 2014). The yield of oxidation products mostly depends on the type of oxidant used in the reaction and the catalyst. The resulting bio-based compounds can be successfully incorporated into the pharmaceutical and chemical industry (Pang et al., 2008). The most valuable product of lignin oxidation is vanillin, which is used as an intermediate to generate a variety of products that are used as a treatment for Parkinson disease, hypertension, and respiratory system infections. Other uses are as an antifoaming agent in the preparation of tanning creams and herbicides. Moreover, syringaldehyde, vanillic acid, and its esters have similar disinfectant properties, so they have similar applications (Villar et al., 2001).

Compared to the previously mentioned pathways, H_2O_2 is a common reagent to oxidize lignin under mild conditions. Ouyang et al. (2010) studied the H_2O_2 oxidation of wheat straw soda lignin by microwave irradiation, which facilitated the degradation of lignin to smaller fractions with lower M_W and narrower molecular weight distribution (Ouyang et al., 2010). Degradation of lignin macromolecules by H_2O_2 involves the cleavage of ether bonds (β-O-4) that occupies most of the reactive sites in lignin structure and increases the content of phenolic hydroxyl groups for further chemical modifications. At higher H_2O_2 dosage, longer reaction time or higher temperature, the

reaction involves the opening of aromatic ring and formation of a partial quinoid, which decreases the content of reactive phenolic hydroxyl groups (Laurichesse and Avérous, 2014). In another study, Dalimova (2005) investigated the effect of H_2O_2 oxidation on the structure of hydrolyzed lignin of cottonseed husks at 90 °C. The significant increase in the carbonyl and carboxyl groups indicates the cleavage of ester and ether bonds in lignin macromolecules, which increases lignin's solubility in water. In another report, H_2O_2 oxidation of black kraft liquor of Caribbean pine wood species in the presence of ferrous ions converted black liquor's lignin into compounds with a lower molecular weight (Araujo et al., 2002).

2.4.2. Lignin carboxymethylation

Carboxymethylation of lignin is an important etherification method to produce a water-soluble product from lignin. Phenolic hydroxyl groups react with haloacetic acid in an alkaline medium to obtain carboxymethylated lignin with a low content of phenolic hydroxyl groups. The degree of carboxymethylation depends on the hydroxyl group substitution with carboxymethyl groups. The reaction led to an increase in the average molecular weight and charge density of lignin. Different examples of lignin carboxymethylation were reported in the literature; most of them were carboxymethylations of lignin from nonwood species (Hon, 2017). Cerrutti et al. (2012) reported the carboxymethylation of sugarcane bagasse lignin produced by organosolv process, and the product was used as an effective stabilizing agent in ceramic suspensions. In another study, kraft lignin of beech and spruce was carboxymethylated with bromoacetic acid, and the product was used as a dispersant in a graphite suspension (Can et al., 2012). In another report, carboxymethylation of hardwood kraft lignin was investigated, and the resultant anionic polymer was used as a dispersant in clay suspension (Scheme 2.1) (Konduri et al., 2015).
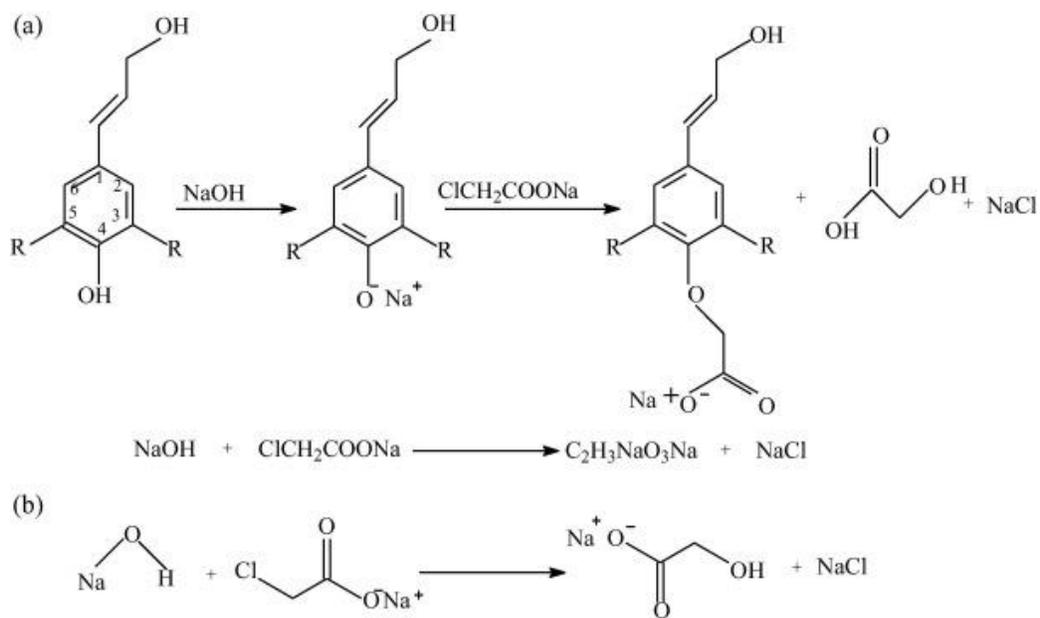
Scheme 2.3. a) Carboxymethylation of lignin, b) Possible undesired reactions. "R" can be OCH_3 or H (Konduri et al, 2015).

2.5. Lignin-vinyl monomers polymerization

As previously mentioned, chemical modification methods would only moderately change lignin molecular weight, charge density, and solubility, still limiting its potential use in industry. Some applications, including flocculation, depend on key parameters such as polymer's molecular weight and charge density, which greatly influences the adsorption and conformation of polymers on suspended particles (Wong et al., 2006; Zhu et al., 2009). Polymerization of lignin and vinyl monomers; acrylic acid, acrylamide, acrylonitrile, and methacrylate, have been investigated in the literature as a way to impart lignin with properties that favor its application as a flocculant or a dispersant without adversely affecting the molecular structure of lignin (Mohamad et al., 2010). Various studies have investigated polymerization reactions through different pathways, such as UV radiation (Rosu et al., 2009), mechanical activation (Huang et al., 2009), and chemo-enzymes (Mai et al., 2000), to produce polymers for various applications in industry. However, for industrial

purposes, free radical polymerization is considered as the most efficient and cost-effective method for the production of flocculants. The polymerization reaction involves the use of a free radical initiator (e.g., potassium persulfate ceric ammonium nitrate, or hydrogen peroxide) to generate free radicals on the lignin backbone that react with the monomer. Acrylamide, in particular, is an attractive monomer given its high reactivity and low cost, and it's resulting homopolymer (PAM) has been widely used in industry as a flocculant for wastewater and as a strength additive in papermaking processes as illustrated in Table 2.1 (Qian et al., 2004; Wang, 2016).

Table 2.1. Different applications of lignin-vinyl monomers

Lignin type	Monomer	Application	Reference
Kraft lignin	Acrylic acid	Additive in hydrocarbon drilling operations	(Ibrahim et al., 2006)
Soda lignin	Acrylamide	Dry strength additive for papermaking	(Wang, 2016)
Kraft lignin	Acrylic acid	Dispersant for cement admixture	(Kong et al., 2015)
Kraft lignin	Methacrylate	Binder applications	(Holmberg et al., 2016)
kraft lignin	Acrylic acid	Dispersants for drilling mud	(Zahran and Basuni, 2014)
Kraft lignin	Acrylonitrile	Carbon fibers	(Youe et al., 2012)
EH	Acrylamide	Flocculant for dye wastewater	(Fang, 2009)
Sodium lignosulfonate	Acrylamide	Thinner for drilling mud	(Abdel, 2015)
lignosulfonate	Acrylic acid	Dust depresant	(Ye et al., 2014)

2.6. Applications of acrylamide polymers

As stated above, acrylamide is both highly reactive, and cost-effective monomer. As such, it has been widely used for the polymerization of different bio-based materials (Smith et al., 1991). Similar to polyacrylamide (PAM), acrylamide-based polymers are used in a wide range of applications, including being used in soil erosion, sugar manufacture, production of concrete, plastic, cosmetics, grout, as flocculants in wastewater treatment, and as drilling fluid additives (Smith and Oehme, 1991; Isikgor et al., 2015). Lignin-acrylamide polymer has also been used as a paper strength additive (Wang et al., 2016). For example, adding 1 wt.% of soda lignin-acrylamide polymer to the soda pulping increased the strength of the resulting paper to 15 % (Wang et al., 2016). The increase in paper strength was mainly attributed to the hydrogen bonding between the hydroxyl groups in cellulose fibers and amide groups in soda lignin acrylamide polymer (Wang et al., 2016). In previous studies, enzymatically hydrolyzed lignin was used in the removal of dye (Acid Red 274) present in wastewater effluents. The removal of dye increased from 30 to 85 % by increasing the concentration of the polymer from 50 to 200 mg/L (Fang et al., 2009). In other work, lignosulfonate was polymerized with acrylamide using hydrogen peroxide as initiator, and the product was used as a thinner for drilling mud (Abdel, 2015). The polymerization reaction increased the viscosity of lignin-acrylamide polymer to 50 % compared to unmodified lignin because amide groups were less hydrophilic than the carboxylic groups in acrylic acid which was found to be advantageous in this particular application (Abdel, 2015).

2.7. Bio-based flocculants

Various studies have investigated free radical polymerization of biopolymers such as cellulose, starch, and chitosan with vinyl monomers to produce bio-based flocculants with higher efficiency, better properties, and longer shelf life, which can replace synthetic flocculants. Bioflocculants that

are based on polysaccharides gained a lot of interest as these flocculants are safe, biodegradable, and fairly shear-stable compared to synthetic polymers (Lee et al., 2014). Machida et al. (1971) investigated the graft polymerization of cellulose and acrylamide, and the resultant polymer was tested in kaoline suspension, where the grafting ratio of acrylamide monomer significantly influenced the flocculation rate in kaoline suspension. Cellulose- acrylamide polymers with higher grafting ratios were found to accelerate the flocculation process remarkably, and, once the aggregates were formed, could hardly be redispersed due to increased hydrogen bonding (Machida et al., 1971). In another study, starch and polyacrylamide polymer were synthesized by a novel method involving the combination of free radical polymerization and microwave radiation, and the produced polymer had maximum flocculation efficiency in kaoline suspension (Mishra et al., 2011). The performance of chitosan-acrylamide polymer as a flocculant in wastewater was investigated by Zhang et al. (2011), where polymers with high grafting ratios had up to 70% kaoline removal. However, polysaccharides-based biopolymers have extensive applications, including cosmetics, medicine, and food. As lignin gained more recognition as a bio-based polymer with great potential, more studies are being conducted on the performance of lignin-based polymers as bio-based flocculants (Laurichesse and Avérous, 2014). The performance of cationic lignin-acrylamide based polymers in kaoline and bentonite suspensions was investigated (Hassan and Fatehi, 2018). It was found that the polymer's charge density mainly influenced the flocculation efficiency, and the relative turbidity of kaoline and bentonite suspensions was reduced to 0.61 and 0.32, respectively, by highly charged cationic polymers (Hassan and Fatehi, 2018). In another report that investigated lignin and acrylic acid polymerization, the performance of the produced polymer compared to polyacrylic acid polymer was evaluated in alumina suspension

(Kong et al., 2018). Lignin-acrylic acid polymer was more efficient flocculant compared to polyacrylic acid, which shows its potential to be used as a green flocculant (Kong et al., 2018).

2.8. Fundamentals

2.8.1. Zeta potential

Zeta potential is a term used to express a physical property exhibited by colloidal systems that can be used to measure the stability of a suspension (Araki et al., 1992). Colloidal particles develop a net surface charge as a result of functional groups of colloidal particles dissociated in a suspension. These surface charges affect the distribution of counterions around each particle resulting in an increased concentration of counterions surrounding each particle. Thus, an electrical double layer is formed around each particle. This electrical double layer consists of an inner region called stern layer, consisting of counter ions that are firmly attached to the surface of particles, and an outer region of less firmly attached ions (diffuse layer). Ions within the boundary of the diffuse layer (slipping plane) move with particles when they travel in the medium as a result of Brownian motion or sedimentation. Zeta potential is defined as the electrical potential at the slipping plane as illustrated in Figure 2.1. The magnitude of zeta potential is used to determine the stability of a system. For example, if two adjacent particles have a sufficiently high zeta potential of the same sign, agglomeration will not take place as a result of electrostatic repulsion forces between the particles (Riddick,1961; Araki et al., 1992).

On the other hand, particles with a lower zeta potential tend to agglomerate as a result of weak repulsion forces (Araki et al., 1992). In a report, carboxymethylated lignin reduced the zeta potential of ceramic suspension from -20 to -30 mV, creating a stable system (Traiphol et al., 2010). However, the effect of anionic lignin-acrylamide based flocculants with different charge

densities and molecular weight on the zeta potential of alumina suspension has not been studied, and is addressed in this work.
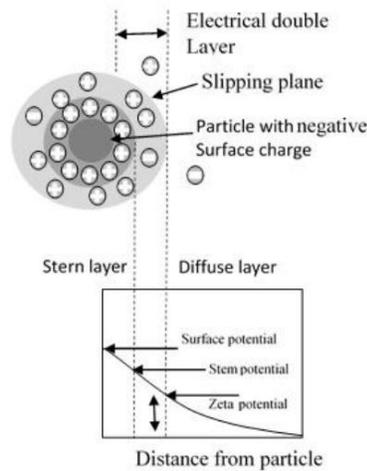
Figure 2.1. electrical double layer surrounding the particle in an aqueous medium (Araki et al., 1992).

2.8.2. Adsorption

Adsorption of polymers on the surface of colloidal particles changes the surface morphology and chemistry of particles, and thus the interparticle forces between them. It can also facilitate their removal or increase the stability of the suspension (dispersibility) based on the polymer characteristics (Rabie, 2010). Polymers containing polyacrylamide chains adsorb on the surface of suspended particles through different mechanisms such as hydrogen bonding, van der Waals forces, or hydrophobic interaction (Rabie, 2010). In the case of polymers having the same charge (negative) as suspended particles, adsorption happens through ion bonding. Cationic di- or trivalent ions, such as calcium, magnesium, and aluminum ions, promote adsorption by bridging between carboxylate groups in anionic polyacrylamide chains and anionic surface sites (Lee et al., 2014). In a suspension where particles have an opposite charge from flocculant, polymer

adsorptions happen through electrostatic interaction. When electrostatic interaction is the main affinity of adsorption, the impact of salts in suspension become significant. The adsorption of the polymer decreases as the salt concentration increases due to screening effect between the ionic segment of the polymer and the dissolved ions. The screening effect on adsorption becomes less significant when there are additional interaction forces between polymers and suspended particles such as hydrogen bonding or hydrophobic interaction (Rabie, 2010; Lee et al., 2014).

2.8.3. Impact of polymer charge density and molecular weight on adsorption

Polymer properties; molecular weight, charge density, and suspended particle properties all are significant factors that determine the type of interparticle forces, and the amount of adsorbed polymer. In previous studies, it was shown that polymers with a high molecular weight and low charge density adsorb on the surface of suspended particles in the form of tails and loops, which enables polymers to extend into the solution and interact with other particles forming bridging bonds (Zhou et al., 2007; Miranda et al., 2008). In the case of polymers with low or medium molecular weight and high charge density, the polymer takes a flatter configuration on the surface of particles, leading to the destabilization of the suspended particles via charge neutralization or patching mechanisms (Miranda et al., 2008). Patching mechanisms occur when polymers with a high charge density and low molecular weight adsorb on the surface of low charge sites and form patches that reduces particle surface charge. Previous studies on the effect of synthetic polymers, such as polyacrylamide or polyacrylic acids in alumina suspension flocculation show the significance of polymer charge density (Miranda et al., 2008). The flocculation mechanism in these systems mainly occurred through charge neutralization, confirmed by zeta potential analysis, where the lowest relative turbidity for alumina suspension was achieved at the zeta potential of 0 mV (Wiśniewska et al., 2015; Wiśniewska et al., 2016; Kazzaz et al., 2018).

2.8.4. Relative turbidity

Given that the turbidity of a suspension is influenced by the size and the number of suspended particles, one way of assessing the efficiency of the flocculation process is to monitor the clarity (turbidity) of the suspension. For example, the flocculation efficiency of cationic lignin and [2-(methacryloyloxy) ethyl] trimethyl ammonium chloride (METAC) polymer in the removal of azo-dyes was investigated, and the removal of anionic azo-dyes increased in a concentration-dependent manner (Wang et al., 2018). In another study, the effect of cationic lignin-acrylamide (AM)-(2-methacryloyloxyethyl) trimethyl ammonium chloride (DMC) polymer in kaoline and bentonite suspensions was investigated, and the relative turbidity of kaolin and bentonite suspensions decreased to 0.61 and 0.32, respectively, resulting in 71 wt.%, and 84 wt.% kaoline and bentonite removal, respectively (Hasan and Fatehi, 2018). The performance of lignin-based flocculants is affected by polymer characteristics, such as charge density, molecular weight, and functional groups (Liimatainen et al., 2009). Different factors such as shear rate and pH of the medium also affect the relative turbidity of the suspension (Petzold et al., 2005; Wang et al., 2016). However, how anionic lignin-acrylamide based flocculants alter the relative turbidity of alumina suspension has not been investigated yet.

2.8.5. Alumina removal

Aluminum oxide (alumina) is widely used in different industries, such as minerals and ceramic processes, due to its thermal stability, mechanical strength, and large surface area. Therefore, the wastewater produced by these industries contains alumina particles that need to be treated. The effect of anionic polyacrylic acid polymers on alumina removal was investigated as a function of alumina suspension pH (Wiśniewska et al., 2013). It was found that the removal of alumina increased from pH 3 to pH 6, where 80% of alumina removal was achieved. Above pH 8, the

removal of alumina decreased significantly as a result of the electrostatic repulsion between anionic polymers and negatively charged alumina particles (Wiśniewska et al., 2013). In another report, the effect of cationic polyacrylamide polymers on alumina removal was investigated where the molecular weight of polymers had a significant impact on alumina removal (Wiśniewska et al., 2014). Modified lignin has a great potential to be used in the removal of different industrial effluents, including alumina, due to its properties such as charge density, its hydrophilic and hydrophobic groups (Suteu et al., 2010). Several studies were conducted on the removal of industrial effluents, such as bentonite and kaoline, using lignin-based polymers (Konduri and Fatehi, 2018; Hasan and Fatehi, 2019). Different studies have also examined the use of lignin-based polymers as dispersants in alumina suspensions (He and Fatehi, 2015; Alzahrani, 2018). However, studies on the removal of alumina by lignin-based flocculants are limited. Kazzaz et al. (2018) studied the use of oxidized sulfomethylated lignin as a flocculant in alumina suspension. It was shown that charge neutralization had a significant effect on alumina removal.

2.8.6. Focused beam reflectance measurement (FBRM)

One of the most important parameters in investigating the efficiency of flocculation process is to study the characteristics of flocs. The flocculation behavior of anionic lignin-acrylamide based flocculants was investigated in alumina suspension under shear forces using focused beam reflectance measurement (FBRM). FBRM is a non-imaging laser scanning microscopy to monitor the flocculation process. This methodology allows us to investigate, and optimize, the flocculation process by studying the increase in flocs size, and determining flocculant optimal dosage (Zhu et al., 2011; Blanco et al., 2002). Flocculants in a suspension operate via different mechanisms depending on the polymer structure, molecular weight, the charge density of the polymer, and charge density of the suspension (Zou et al., 2011). FBRM also examines the effect of shear forces

on flocs formation, breakage, and re-flocculation process, which would enable identifying the flocculation mechanism and flocs properties. This technique operates by using a highly focused laser beam that scans across particles in a suspension at a fixed speed (Blanco et al., 2002). By measuring the duration of the backscattered light from particles and multiplying it by the velocity of the laser, a geometric characteristic of particles, called chord length, is obtained. Chord length is the length between the two edges of a particle in a suspension. Thousands of chord length measurements are taken per 5 or 10 seconds, generating a histogram in which the chord length of the particles is distributed over a range of 0.5 to 2000 mm (Blanco et al., 2002). This allows us to investigate the flocculation behavior by minoring the increase in the mean chord length of particles or even targeting the increase in a specific size region throughout the whole experiment. Also by increasing or decreasing shear forces, the deflocculation and re-flocculation behavior of a system can be examined.

2.9. Methods to characterize polymers

2.9.1. Elemental analysis

Elemental analysis is a method by which the organic elements of a sample are determined. In this method, samples are combusted in a furnace at 1200 ºC in the presence of oxygen, and various traps. The products of combustion including nitric oxide, sulphur dioxide, water, and carbon dioxide are collected, and the masses of these products are used to determine the mass fraction of carbon, hydrogen, nitrogen, and sulphur in an unknown sample (Das et al., 2013). This technique is used in a range of applications such as polymers, food, and pharmaceuticals to assure the purity of the sample and to determine the chemical formula of a product by considering the weight percentage and the atomic weight of each element (Fadeeva et al., 2008).

2.9.2. Molecular weight determination (GPC)

Gel permeation chromatography is a powerful, and versatile analytical method used to characterize the molecular weight of polymers (Choi et al., 2001). GPC can obtain different characteristics such as weight average molecular weight (Mw), number average molecular weight (Mn), and polydispersity (Mw/Mn). This technique is based on separating molecules in solution depending on their effective size (Kostanski et al., 2004). In this method, a column consisting of porous gel particles is used. Thus, when a sample with different polymeric molecules goes through the column, large molecules elute first as they cannot pass through pores, while the smaller particles pass through pores and elute later. The elution behavior of the tested sample is shown in chromatogram that represents the time for molecules of a particular size to elute the column (retention time). By using standard polymers, such as polyethylene oxide, a calibration curve can be generated by correlating retention time and size of polymer, and this correlation can be used to determine the molecular weight distribution of polymers. Furthermore, the molecules eluted from the column can be detected by different detectors including refractive index (RI), multi-angle laser detector, and ultraviolet (UV) viscometer (Bernd, 1995).

2.9.3. Charge density analysis

The charge density of a material is defined as the quantity of electrical charge attached to it (Nasser and James, 2006). In a colloidal system, the charge density of a polymer plays an important role as it is responsible for how particles interact in a suspension. Also, measuring the charge density of a polymer can determine the efficiency of a reaction, and if charged groups are attached to or detached from the starting material in a reaction. In many studies, the charge density of polymers was measured using a particle charge detector (PCD), which is based on the neutralization of charged groups in a polymer by using a standard solution of a polymer with an opposite charge

(Lou et al., 2013). In a study, polydiallyldimethylammonium chloride (PDADMAC) was used as a standard solution to neutralize anionic polymers. By considering the volume of PDADMAC added for neutralization and the mass of dried polymer added to the cell of PCD, the charge density of the polymer can be measured (Lou et al., 2013).

2.9.4. Fourier transform infrared spectrophotometer (FTIR)

FTIR is a simple and rapid method that is used in polymer science, organic synthesis, and petrochemical engineering to identify the functional groups in a sample. When infrared radiation passes through a sample, some of the radiation is absorbed by the sample, and some of it passes through (transmittance). The resultant infrared spectrum represents absorption peaks corresponding to the vibration frequencies of bonds between atoms in a material. As each material has a unique combination of atoms, two different materials cannot produce the same spectrum (Zhang and Cresswell, 2016). According to the literature, FTIR can be used for both qualitative and quantitative analysis of functional groups (Faix and Bottcher, 1993).

2.10. Methods to determine the thermal stability of products

2.10.1. Thermo-gravimetric analysis (TGA)

Thermogravimetric analysis investigates the thermal stability of a product, by monitoring the mass of a sample while gradually increasing the temperature. The sample is placed in a furnace where it is subjected to thermal changes in a controlled atmosphere, and the weight of the sample is measured on an analytical balance placed outside the furnace. The mass loss of the sample is reported as a function of temperature and/or time. This mass loss indicates the gradual degradation of the sample at specific temperatures including the loss of water or solvent (Kostanski et al., 2004; Choi et al., 2001). In this work, TGA results for modified lignin are reported.

2.10.2. Differential scanning calorimetry (DSC)

Differential scanning calorimetry is a method used to study the thermal transition of polymers or the changes that take place when the polymer is heated, such as the melting temperature of crystalline polymers or glass transition temperature (Gabbott et al., 2008). The instrument contains two pans; each one located on top of a heater. One pan is the reference pan, and the other pan contains the polymer sample. The instrument is monitored by a computer, which keeps a constant heating rate for the two pans throughout the analysis, for example, 10 °C per minute. One pan contains the sample and the other pan is empty; the heater underneath the pan containing the sample releases more heat, so that the two pans heat at the same rate. The computer monitors how much more heat is put out, and provides a plot of the amount of heat absorbed by the polymer or heat flow against temperature. The heat flow is shown as units of heat supplied, q, per unit of time, as illustrated in equation 2.1 (Gabbott et al., 2008; Khaldi et al., 2016). The heat flow of the sample divided by the heating rate provides the heat capacity, C_P, which is the amount of heat needed to get a certain temperature increase.

$$\frac{Heat}{Time} = \frac{q}{t} = heat\ flow \tag{2.1}$$

$$\frac{Temperature\ increase}{Time} = \frac{\Delta T}{t} = heating\ rate \tag{2.2}$$

$$\frac{\frac{q}{t}}{\frac{\Delta T}{t}} = \frac{q}{t} = C_P = heat\ capacity \tag{2.3}$$

The instrument also provides the polymer's glass transition temperature, where the polymer changes from a glassy state to a rubbery state. At this temperature, the heat flow increases indicating more heat absorbed by the polymer or increased heat capacity. Polymers have a higher heat capacity above their glass transition temperature than below it, and this is used to indicate the glass transition temperature of polymers as illustrated in Figure 2.2. (Gabbott et al., 2008).
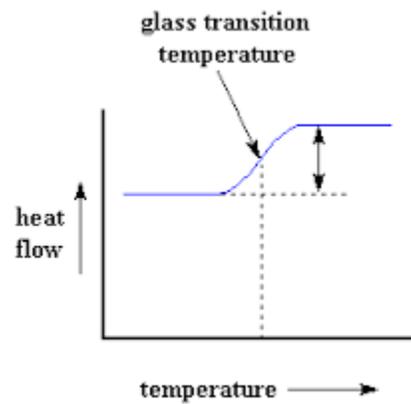
Figure 2.2. Heat flow as a function of temperature (Gabbott et al., 2008).

References

Abdel, M., Zahran, H., & Basuni, M. M. (2015). Study on Graft-Copolymerization of Sodium Lignosulfonates with acrylic monomers. *BioResources,* 68(9), 35-40.

Ahvazi, B., Wojciechowicz, O., Ton-That, T. M., & Hawari, J. (2011). Preparation of lignopolyols from wheat straw soda lignin. *Journal of Agricultural and Food Chemistry*, *59*(19), 10505-10516.

Alkhalifa, Z. (2017). Copolymerization of pretreated kraft lignin and acrylic acid to produce flocculants for suspension and solution systems. Lakehead university. Mater thesis.

Alzahrani, P. (2018). Dispersion and flocculation affinity of anionically charged kraft lignin. Lakehead university. Mater thesis.

An, X. N., Schroeder, H. A., & Thompson, G. E. (1995). Demethylated kraft lignin as a substitute for phenol in wood adhesive. *Crops and Products*, 3, 36-42.

Araki, J., Wada, M., Kuga, S., & Okano, T. (1998). Flow properties of microcrystalline cellulose suspension prepared by acid treatment of native cellulose. *Colloids and Surfaces A: Physicochemical and Engineering Aspects*, *142*(1), 75-82.

Araujo, E., Rodríguez-Malaver, A., González, A. M., Rojas, O. J., Peñaloza, N., Bullón, J., Lara, M. A., & Dmitrieva, N. (2002) Fenton's reagent–mediated degradation of residual kraft black liquor. *Appl. Biochem. Biotech.* 97, 91-103.

Areskogh, D., Li, J., Gellerstedt, G., & Henriksson, G. (2010). Structural modification of commercial lignosulphonates through laccase catalysis and ozonolysis. *Industrial Crops and Products*, *32*(3), 458-466.

Arkell, A., Olsson, J., & Wallberg, O. (2014). Process performance in lignin separation from softwood black liquor by membrane filtration. *Chemical Engineering Research and Design*, *92*(9), 1792-1800.

Aro, T., & Fatehi, P. (2017). Production and application of lignosulfonates and sulfonated lignin. *ChemSusChem*, *10*(9), 1861-1877.

Blanco, A., Fuente, E., Negro, C., & Tijero, J. (2002). Flocculation monitoring: focused beam reflectance measurement as a measurement tool. *Canadian journal of chemical engineering*, 80(4), 734-740.

Brend, T. (1995). Determination of MWD and chemical composition of polymers by chromatographic techniques. *Progress in Polymer Science*, *20*(4), 615-650.

Cerrutti, B. M., De Souza, C. S., Castellan, A., Ruggiero, R., & Frollini, E. (2012). Carboxymethyl lignin as stabilizing agent in aqueous ceramic suspensions. *Industrial Crops and Products*, *36*(1), 108-115.

Cerrutti, B. M., De Souza, C. S., Castellan, A., Ruggiero, R., & Frollini, E. (2012). Carboxymethyl lignin as stabilizing agent in aqueous ceramic suspensions. *Industrial Crops and Products*, *36*(1), 108-115.

Chakar, F. S., & Ragauskas, A. J. (2004). Review of current and future softwood kraft lignin process chemistry. *Industrial Crops and Products*, *20*(2), 131-141.

Chen, R. L., Kokta, B. V., Daneault, C., & Valade, J. L. (1986). Some water-soluble copolymers from lignin. *Journal of Applied Polymer Science*, *32*(5), 4815-4826.

Choi, J. W., Faix, O., & Meier, D. (2001). Characterization of residual lignins from chemical pulps of spruce (Picea abies L.) and beech (Fagus sylvatica L.) by analytical pyrolysis–gas chromatography/mass spectrometry. *Holzforschung*, *55*(2), 185-192.

Choi, J. W., Faix, O., & Meier, D. (2001). Characterization of residual lignins from chemical pulps of spruce (Picea abies L.) and beech (Fagus sylvatica L.) by analytical pyrolysis–gas chromatography/mass spectrometry. *Holzforschung*, *55*(2), 185-192.

Da Silva, L. G., Ruggiero, R., Gontijo, P. D. M., Pinto, R. B., Royer, B., Lima, E. C., ... & Calvete, T. (2011). Adsorption of Brilliant Red 2BE dye from water solutions by a chemically modified sugarcane bagasse lignin. *Chemical Engineering Journal*, *168*(2), 620-628.

Dalimova, G. N. (2005). Oxidation of hydrolyzed lignin from cotton-seed husks by hydrogen peroxide. *Chemistry of natural compounds*, *41*(1), 85-87.

Das, D., Dash, U., Meher, J., & Misra, P. K. (2013). Improving stability of concentrated coal–water slurry using mixture of a natural and synthetic surfactants. *Fuel Processing Technology*, *113*, 41-51.

Effendi, A., Gerhauser, H., & Bridgwater, A. V. (2008). Production of renewable phenolic resins by thermochemical conversion of biomass: a review. *Renewable and Sustainable Energy Reviews*, *12*(8), 2092-2116.

El Mansouri, N. E., & Salvadó, J. (2006). Structural characterization of technical lignins for the production of adhesives: Application to lignosulfonate, kraft, soda-anthraquinone, organosolv and ethanol process lignins. *Industrial Crops and Products*, *24*(1), 8-16.

El Mansouri, N. E., Yuan, Q., & Huang, F. (2011). Characterization of alkaline lignins for use in phenol-formaldehyde and epoxy resins. *BioResources*, *6*(3), 2647-2662.

El Mansouri, N. E., Yuan, Q., & Huang, F. (2011). Characterization of alkaline lignins for use in phenol-formaldehyde and epoxy resins. *BioResources*, *6*(3), 2647-2662.

ElMekawy, A., Diels, L., De Wever, H., & Pant, D. (2013). Valorization of cereal based biorefinery byproducts: reality and expectations. *Environmental Science & Technology*, *47*(16), 9014-9027.

Elumalai, S., & Pan, X. J. (2011). Chemistry and reactions of forest biomass in biorefining. *Sustainable Production of Fuels, Chemicals, and Fibers from Forest Biomass*, 109-144.

Fadeeva, V. P., Tikhova, V. D., & Nikulicheva, O. N. (2008). Elemental analysis of organic compounds with the use of automated CHNS analyzers. *Journal of Analytical Chemistry*, *63*(11), 1094-1106.

Faix, O., & Böttcher, J. H. (1993). Determination of phenolic hydroxyl group contents in milled wood lignins by FTIR spectroscopy applying partial least-squares (PLS) and principal components regression (PCR). *Holzforschung-International Journal of the Biology, Chemistry, Physics and Technology of Wood*, *47*(1), 45-49.

Fang, R., Cheng, X. S., Fu, J., & Zheng, Z. B. (2009). Research on the graft copolymerization of EH-lignin with acrylamide. *BioResources*, 1(1), 17-22.

Fatehi, P., & Chen, J. (2016). Extraction of technical lignins from pulping spent liquors, challenges and opportunities. In *Production of Biofuels and Chemicals from Lignin* (pp. 35-54). Springer, Singapore.

Gabbott, P., & Bottom, R. (2008). Thermogravimetric analysis (chapter 3). In *Principles and Applications of Thermal Analysis*. Blackwell Publishing Ltd., 87-118.

Gan, L. H., Zhou, M. S., & Qiu, X. Q. (2012). Preparation of water-soluble carboxymethylated lignin from wheat straw alkali lignin. In *Advanced Materials Research* (Vol. 550, pp. 1293-1298). Trans Tech Publications.

Gan, L. H., Zhou, M. S., & Qiu, X. Q. (2012). Preparation of water-soluble carboxymethylated lignin from wheat straw alkali lignin. In *Advanced Materials Research*, 550, 1293-1298.

Hasan, A., & Fatehi, P. (2019). Cationic kraft lignin-acrylamide copolymer as a flocculant for clay suspensions:(2) Charge density effect. *Separation and Purification Technology*, *210*, 963-972.

Hasan, A., & Fatehi, P. (2019). Flocculation of kaolin particles with cationic lignin polymers. *Scientific Reports*, *9*(1), 2672.

Hatakeyama, H., & Hatakeyama, T. (2009). Lignin structure, properties, and applications. In *Biopolymers* (pp. 1-63). Springer, Berlin, Heidelberg.

He, W., & Fatehi, P. (2015). Preparation of sulfomethylated softwood kraft lignin as a dispersant for cement admixture. *RSC Advances*, *5*(58), 47031-47039.

Holmberg, A. L., Nguyen, N. A., Karavolias, M. G., Reno, K. H., Wool, R. P., & Epps III, T. H. (2016). Softwood lignin-based methacrylate polymers with tunable thermal and viscoelastic properties. *Macromolecules*, *49*(4), 1286-1295.

Hon, D. N. S. (2017). Chemical modification of cellulose. In *Chemical Modification of Lignocellulosic Materials* (pp. 97-127). Routledge.

Hu, L., Pan, H., Zhou, Y., & Zhang, M. (2011). Methods to improve lignin's reactivity as a phenol substitute and as replacement for other phenolic compounds: A brief review. *BioResources*, *6*(3), 3515-3525.

Huang, Z., Liang, X., Hu, H., Gao, L., Chen, Y., & Tong, Z. (2009). Influence of mechanical activation on the graft copolymerization of sugarcane bagasse and acrylic acid. *Polymer Degradation and Stability*, *94*(10), 1737-1745.

Ibrahim, M. N. M., Ahmed-Haras, M. R., Sipaut, C. S., Aboul-Enein, H. Y., & Mohamed, A. A. (2010). Preparation and characterization of a newly water soluble lignin graft copolymer from oil palm lignocellulosic waste. *Carbohydrate Polymers*, *80*(4), 1102-1110.

Ibrahim, M., Azreena, N., Azreena, N., & Ismail, M. S. (2006). Lignin graft copolymer as a drilling mud thinner for high temperature well. *Journal of Applied Sciences*, 1-6.

Inwood, J. (2014). Sulfonation of kraft lignin to water-soluble value-added products. Lakehead university. Mater thesis.

Isikgor, F. H., & Becer, C. R. (2015). Lignocellulosic biomass: a sustainable platform for the production of bio-based chemicals and polymers. *Polymer Chemistry*, *6*(25), 4497-4559.

Juan, F. A. N., & Huaiyu, Z. H. A. N. (2008). Optimization of synthesis of spherical lignosulphonate resin and its structure characterization. *Chinese Journal of Chemical Engineering*, *16*(3), 407-410.

Kadla, J. F., Kubo, S., Venditti, R. A., Gilbert, R. D., Compere, A. L., & Griffith, W. (2002). Lignin-based carbon fibers for composite fiber applications. *Carbon*, *40*(15), 2913-2920.

Kadla, J. F., Kubo, S., Venditti, R. A., Gilbert, R. D., Compere, A. L., Griffith, W. (2002). Lignin-based carbon fibers for composite fiber application. *Carbon*., 44, 2913-2920.

Kamm, B., & Kamm, M. (2004). Principles of biorefineries. *Applied Microbiology and Biotechnology*, *64*(2), 137-145.

Kazzaz, A. E., Feizi, Z. H., & Fatehi, P. (2018). Interaction of sulfomethylated lignin and aluminum oxide. *Colloid and Polymer Science*, *296*(11), 1867-1878.

Khaldi-Hansen, E., Schulze, M., & Kamm, B. (2016). Qualitative and quantitative analysis of lignins from different sources and isolation methods for an application as a biobased chemical resource and polymeric material. *Analytical Techniques and Methods for Biomass* 223 (1), 15-44

Konduri, M. K., & Fatehi, P. (2018). Designing anionic lignin based dispersant for kaolin suspensions. *Colloids and Surfaces A: Physicochemical and Engineering Aspects*, *538*, 639-650.

Konduri, M. K., Kong, F., & Fatehi, P. (2015). Production of carboxymethylated lignin and its application as a dispersant. *European Polymer Journal*, *70*, 371-383.

Kong, F., Wang, S., Gao, W., & Fatehi, P. (2018). Novel pathway to produce high molecular weight kraft lignin–acrylic acid polymers in acidic suspension systems. *RSC advances*, *8*(22), 12322-12336.

Kong, F., Wang, S., Price, J. T., Konduri, M. K., & Fatehi, P. (2018). Water soluble kraft lignin–acrylic acid copolymer: Synthesis and characterization. *Green Chemistry*, *17*(8), 4355-4366.

Kostanski, L. K., Keller, D. M., & Hamielec, A. E. (2004). Size-exclusion chromatography—a review of calibration methodologies. *Journal of Biochemical and Biophysical Methods*, *58*(2), 159-186.

Kuzmenko, O. (2010). Feasibility study for acidic biorefinery concept. Department of Chemical Technology, Lappeenranta University of Technology, Lappeenranta, Finland. Master Thesis.

Laurichesse, S., & Avérous, L. (2014). Chemical modification of lignins: Towards biobased polymers. *Progress in Polymer Science*, *39*(7), 1266-1290.

Lee, C. S., Robinson, J., & Chong, M. F. (2014). A review on application of flocculants in wastewater treatment. *Process Safety and Environmental Protection*, *92*(6), 489-508.

Lewinsky, A. A. (2007). *Hazardous materials and wastewater: treatment, removal and analysis*. Nova Publishers.

Liimatainen, Henrikki, et al. "Fibre floc morphology and dewaterability of a pulp suspension: Role of flocculation kinetics and characteristics of flocculation agents." *BioResources* 4.2 (2009): 640-658.

Lou, H., Lai, H., Wang, M., Pang, Y., Yang, D., Qiu, X., ... & Zhang, H. (2013). Preparation of lignin-based superplasticizer by graft sulfonation and investigation of the dispersive performance and mechanism in a cementitious system. *Industrial & Engineering Chemistry Research*, *52*(46), 16101-16109.

Machida, S., Narita, H., & Katsura, T. (1971). Flocculation properties of cellulose-acrylamide graft copolymers. *Die Angewandte Makromolekulare Chemie: Applied Macromolecular Chemistry and Physics*, *20*(1), 47-56.

Machida, S., Narita, H., & Katsura, T. (1971). Flocculation properties of cellulose-acrylamide graft copolymers. *Die Angewandte Makromolekulare Chemie: Applied Macromolecular Chemistry and Physics*, *20*(1), 47-56.

Mahmood, N., Yuan, Z., Schmidt, J., & Xu, C. C. (2016). Depolymerization of lignins and their applications for the preparation of polyols and rigid polyurethane foams: A review. *Renewable and Sustainable Energy Reviews*, *60*, 317-329.

Mai, C., Milstein, O., & Hüttermann, A. (2000). Chemoenzymatical grafting of acrylamide onto lignin. *Journal of Biotechnology*, *79*(2), 173-183.

Matsushita, Y. (2015). Conversion of technical lignins to functional materials with retained polymeric properties. *Journal of Wood Science*, *61*(3), 230.

Meister, J. J., Patil, D. R., & Channell, H. (1984). Properties and applications of lignin–acrylamide graft copolymer. *Journal of Applied Polymer Science*, *29*(11), 3457-3477.

Miranda, R., Blanco, A., Fuente, E. D. L., & Negro, C. (2008). Separation of contaminants from deinking process water by dissolved air flotation: effect of flocculant charge density. *Separation Science and Technology*, *43*(14), 3732-3754.

Mishra, S., Mukul, A., Sen, G., & Jha, U. (2011). Microwave assisted synthesis of polyacrylamide grafted starch (St-g-PAM) and its applicability as flocculant for water treatment. *International Journal of Biological Macromolecules*, *48*(1), 106-111.

Mohamad, I. M., Ahmed-Haras, M. R., Sipaut, C. S., Aboul-Enein, H. Y., & Mohamed, A. A. (2010). Preparation and characterization of a newly water soluble lignin graft copolymer from oil palm lignocellulosic waste. *Carbohydrate polymers*, *80*(4), 1102-1110.

Mohan, D., Pittman Jr, C. U., & Steele, P. H. (2006). Single, binary and multi-component adsorption of copper and cadmium from aqueous solutions on Kraft lignin—a biosorbent. *Journal of Colloid and Interface Science*, *297*(2), 489-504.

Nasser, M. S., & James, A. E. (2006). The effect of polyacrylamide charge density and molecular weight on the flocculation and sedimentation behaviour of kaolinite suspensions. *Separation and Purification Technology*, *52*(2), 241-252.

Negrão, D. R., Sain, M., Leão, A. L., Sameni, J., Jeng, R., Jesus, J. P., & Monteiro, R. T. (2015). Fragmentation of Lignin from Organosolv Black Liquor by White Rot Fungi. *BioResources,10*(1), 1553-1573

Ouyang, X., Zaixiong, L. I. N., Yonghong, D. E. N. G., Dongjie, Y. A. N. G., & Xueqing, Q. I. U. (2010). Oxidative degradation of soda lignin assisted by microwave irradiation. *Chinese Journal of Chemical Engineering*, *18*(4), 695-702.

Pang, Y. X., Qiu, X. Q., Yang, D. J., & Lou, H. M. (2008). Influence of oxidation, hydroxymethylation and sulfomethylation on the physicochemical properties of calcium lignosulfonate. *Colloids and Surfaces A: Physicochemical and Engineering Aspects*, *312*(2-3), 154-159.

Petzold, K., Schwikal, K., Günther, W., & Heinze, T. (2005, December). Carboxymethyl Xylan-Control of Properties by Synthesis. In *Macromolecular symposia* ,232 (1), 27-36.

Price, J. T., Gao, W., & Fatehi, P. (2018). Lignin-g-poly (acrylamide)-g-poly (diallyl dimethyl-ammonium chloride)Synthesis, Characterization, and Applications. *ChemistryOpen*, 7(8), 645-658.

Qian, J. W., Xiang, X. J., Yang, W. Y., Wang, M., & Zheng, B. Q. (2004). Flocculation performance of different polyacrylamide and the relation between optimal dose and critical concentration. *European Polymer Journal*, *40*(8), 1699-1704.

Rabiee, A. (2010). Acrylamide-based anionic polyelectrolytes and their applications: A survey. *Journal of Vinyl and Additive Technology*, *16*(2), 111-119.

Riddick, T. M. (1961). Zeta potential and its application to difficult waters. *Journal-American Water Works Association*, *53*(8), 1007-1030.

Robinson, C. F., Waxweiler, R. J., & Fowler, D. P. (1986). Mortality among production workers in pulp and paper mills. *Scandinavian Journal of Work, Environment & Health*, *12*(6), 552-560.

Rosu, L., Cascaval, C. N., & Rosu, D. (2009). Effect of UV radiation on some polymeric networks based on vinyl ester resin and modified lignin. *Polymer Testing*, *28*(3), 296-300.

Sahoo, S., Seydibeyoğlu, M. Ö., Mohanty, A. K., & Misra, M. (2011). Characterization of industrial lignins for their utilization in future value added applications. *Biomass and Bioenergy*, *35*(10), 4230-4237.

Smith, E. A., & Oehme, F. W. (1991). Acrylamide and polyacrylamide: Review of Production, Use, Environmental Fate and Neurotoxicity. *Reviews On Environmental Health*. 1991, 9(4), 342-762.

Sun, R., Lawther, J. M., & Banks, W. B. (1995). The effect of alkaline nitrobenzene oxidation conditions on the yield and components of phenolic monomers in wheat straw lignin and compared to cupric (II) oxidation. *Industrial Crops and Products*, *4*(4), 241-254.

Suteu, D., Malutan, T., & Bilba, D. (2010). Removal of reactive dye Brilliant Red HE-3B from aqueous solutions by industrial lignin: Equilibrium and kinetics modeling. *Desalination*, *255*(1-3), 84-90.

Traiphol, N., Suntako, R., & Chanthornthip, K. (2010). Roles of polymeric dispersant charge density on lead zirconate titanate aqueous processing. *Ceramics International*, *36*(7), 2147-2153.

Varanasi, P., Singh, P., Auer, M., Adams, P. D., Simmons, B. A., & Singh, S. (2013). Survey of renewable chemicals produced from lignocellulosic biomass during ionic liquid pretreatment. *Biotechnology for Biofuels*, *6*(1), 14.

Villar, J. C., Caperos, A., & García-Ochoa, F. (1997). Oxidation of hardwood kraft-lignin to phenolic derivatives. Nitrobenzene and copper oxide as oxidants. *Journal of Wood Chemistry and Technology*, *17*(3), 259-285.

Vishtal, A. G., & Kraslawski, A. (2011). Challenges in industrial applications of technical lignins. *BioResources*, *6*(3), 3547-3568.

Wang, B., Zhang, Y., & Miao, C. (2011). Preparation of cationic chitosan-polyacrylamide flocculant and its properties in wastewater treatment. *Journal of Ocean University of China*, *10*(1), 42-46.

Wang, G., & Jing, Y. (2014). Synthesis and application of a cationic polyacrylamide dry strength agent with anionic content. *BioResources*, *9*(1), 1111-1120.

Wang, J. P., Chen, Y. Z., Yuan, S. J., Sheng, G. P., & Yu, H. Q. (2009). Synthesis and characterization of a novel cationic chitosan-based flocculant with a high water-solubility for pulp mill wastewater treatment. *Water research*, *43*(20), 5267-5275.

Wang, S., Kong, F., Fatehi, P., & Hou, Q. (2018). Cationic high molecular weight lignin polymer: a flocculant for the removal of anionic azo-dyes from simulated wastewater. *Molecules*, *23*(8), 2005.

Wang, S., Sun, Y., Kong, F., Yang, G., & Fatehi, P. (2016). Preparation and characterization of lignin-acrylamide copolymer as a paper strength additive. *BioResources*, *11*(1), 1765-1783.

Wang, S., Sun, Y., Kong, F., Yang, G., & Fatehi, P. (2016). Preparation and characterization of lignin-acrylamide copolymer as a paper strength additive. *BioResources*, *11*(1), 1765-1783.

Wiśniewska, M., Chibowski, S., & Urban, T. (2014). Effect of the presence of cationic polyacrylamide on the surface properties of aqueous alumina suspension-stability mechanism. *Applied Surface Science*, *320*, 843-851.

Wiśniewska, M., Chibowski, S., & Urban, T. (2015). Impact of anionic and cationic polyacrylamide on the stability of aqueous alumina suspension—comparison of adsorption mechanism. *Colloid and Polymer Science*, *293*(4), 1171-1179.

Wiśniewska, M., Chibowski, S., Urban, T., Sternik, D., & Terpiłowski, K. (2016). Impact of anionic polyacrylamide on stability and surface properties of the Al 2 O 3–polymer solution system at different temperatures. *Colloid and Polymer Science*, *294*(9), 1511-1517.

Wiśniewska, M., Terpiłowski, K., Chibowski, S., Urban, T., Zarko, V. I., & Gun'Ko, V. M. (2013). Effect of polyacrylic acid (PAA) adsorption on stability of mixed alumina-silica oxide suspension. *Powder Technology*, *233*(1), 190-200.

Wong, S. S., Teng, T. T., Ahmad, A. L., Zuhairi, A., & Najafpour, G. (2006). Treatment of pulp and paper mill wastewater by polyacrylamide (PAM) in polymer induced flocculation. *Journal of Hazardous Materials*, *135*(1-3), 378-388.

Wu, S., & Zhan, H. (2001). Characteristics of demethylated wheat straw soda lignin and its utilization in lignin-based phenolic formaldehyde resins. *Cellulose Chemistry and Technology*, *35*(3-4), 253-262.

Ye, D. Z., Jiang, X. C., Xia, C., Liu, L., & Zhang, X. (2012). Graft polymers of eucalyptus lignosulfonate calcium with acrylic acid: Synthesis and characterization. *Carbohydrate Polymers*, *89*(3), 876-882.

Ye, L., Ma, C., Zhang, M. H., & Zhang, X. (2014). The graft polymers from different species of lignin and acrylic acid: Synthesis and mechanism study. *International journal of biological macromolecules*, *63*, 43-48.

Youe, W. J., Lee, S. M., Lee, S. S., Lee, S. H., & Kim, Y. S. (2016). Characterization of carbon copolymer nanofiber mats produced from electrospun lignin-g-polyacrylonitrile copolymer. *International journal of biological macromolecules*, *82*, 497-504.

Yuan, B., Shang, Y., Lu, Y., Qin, Z., Jiang, Y., Chen, A., ... & Cheng, R. (2010). The flocculating properties of chitosan-graft-polyacrylamide flocculants (I)—effect of the grafting ratio. *Journal of applied polymer science*, *117*(4), 1876-1882.

Yuan, T. Q., Xu, F., & Sun, R. C. (2013). Role of lignin in a biorefinery: separation characterization and valorization. *Journal of Chemical Technology & Biotechnology*, *88*(3), 346-352.

Zahran, M. A., & Basuni, M. M. (2014). Preparation and evaluation of some graft copolymers and their applications in drilling fluid. *International Journal of Academic Research*, *6* (3), 264-254.

Zahran, M. A., & Basuni, M. M. (2014). Preparation and evaluation of some lignin graft copolymers and their applications in drilling. *International Journal of Academic Research*, *6*(3). 32-53.

Zakzeski, J., Bruijnincx, P. C., Jongerius, A. L., & Weckhuysen, B. M. (2010). The catalytic valorization of lignin for the production of renewable chemicals. *Chemical Reviews*, *110*(6), 3552-3599.

Zhang, W.X., Shang, Y.B., Yuan, B., Jiang, Y.X., Lu, Y.B., Qin, Z.Q., Chen, A.M., Qian, X.Z.,

Zhou, M., Qiu, X., Yang, D., Lou, H., & Ouyang, X. (2007). High-performance dispersant of coal–water slurry synthesized from wheat straw alkali lignin. *Fuel Processing Technology*, *88*(4), 375-382.

Zhu, Z., Li, T., Lu, J., Wang, D., & Yao, C. (2009). Characterization of kaolin flocs formed by polyacrylamide as flocculation aids. *International Journal of mineral processing*, *91*(3-4), 94-99.

Zou, J., Zhu, H., Wang, F., Sui, H., & Fan, J. (2011). Preparation of a new inorganic–organic composite flocculant used in solid–liquid separation for waste drilling fluid. *Chemical Engineering Journal, 171*(1), 350-356.

Chapter 3

3.1. Abstract

Flocculation is a widely applied method for industrial wastewater treatment, and alumina has been recognized as a major part of industrial effluents. Lignin is a natural polymer with great potential to be explored in different applications and used in the production of bio-based flocculants. Vinyl monomers' and bio-polymers' polymerization reactions were proven to produce polymers with properties that allow them to be applied in industrial processes where the polymer properties become compatible with the process. A polymers charge density is one of the significant parameters that affect its flocculation performance, especially in suspensions with charged colloidal particles. Hydrolysis reactions can increase polymer charge density and thus improve their flocculation performance. The effect of different reaction parameters on the molecular weight, charge density, grafting ratio, and yield of kraft lignin-acrylamide, KL-AM, were investigated in this work. The optimal polymerization conditions were found to be 7 mol/mol AM/ KL ratio, 80 °C, 3 h, 3 wt. % of $K_2S_2O_8$ based on lignin's dried mass. KL-AM polymer with the grafting ratio of 280 % and a molecular weight of 1, 064 Kg/mol was hydrolyzed under a variety of conditions. The partially hydrolyzed polymer had a charge density of - 3.62 meq/g and 601 kg/mol molecular weight. The adsorption analysis for hydrolyzed lignin acrylamide polymer (HKL-AM) was higher (16 mg/g) than that of other polymers indicating that charge density plays a significant role in alumina particles and polymers interaction. Furthermore, HKL-AM's high charge density improved its performance in changing the zeta potential and relative turbidity of the suspension. The flocs chord length of HKL-AM was pronouncedly increased from 23 μm to 132 μm, and flocs had higher strength and a re-flocculation tendency.

3.2. Introduction

The increased demand for consumable products worldwide has raised energy and material consumption as well as waste generation. As a result, more strict regulations are under implementation to reduce the generation of waste or to find ways to process waste. Among the different methods used for wastewater treatment, flocculation is the most effective and widely used method (Renault et al., 2009). Industrial wastewater generally consists of tiny suspended organic, inorganic, and metal particles. Bringing these particles to settlement is a difficult task due to their colloidal properties and the presence of surface charges, which increases the repulsion forces between particles making them stable for a long time (Bratby, 2006). The flocculants used in wastewater treatment are generally categorized into three main groups: inorganic flocculants, biopolymers, and synthetic polymers. Inorganic flocculants are widely used due to their low cost and ease of use (Wang et al., 2011; Zhong et al., 2003). However, they have low efficiency, high sensitivity to pH, and they create a great amount of sludge and secondary pollution (Bratby, 2006; Sharma et al., 2006). Natural polymers, such as starch, and chitosan, are widely consumed in other applications, such as agricultural, medicine, and food, which limits their availability for other uses. On the other hand, synthetic polymers, while very effective flocculants, represent health and environmental issues as some of these polymers are highly toxic, carcinogenic, and non-biodegradable (Brostow et al., 2009).

Therefore,, the development of biobased flocculants that minimize the risk of environmental and health issues is highly desireable. As natural polymers have moderate efficiency and a short shelf life, graft polymerization of biopolymers and vinyl monomers has been proven as an effective method to enhance the flocculation performance of biopolymers. This combination of natural polymers and vinyl monomers can increase the shelf life of biopolymers while producing more

environmentally friendly flocculants (Lee et al., 2012). Graft polymers and their applications in wastewater treatment have been widely investigared in the past. One of the highly used monomers in graft polymerization is acrylamide, which is inexpensive and a water-soluble monomer. The acrylamide-starch polymer (Mishra et al., 2011) and hydroxypropyl methylcellulose-acrylamide copolymer were produced and had promising flocculation results in a kaoline suspension (Das et al., 2013). Also, carboxymethyl chitosan-acrylamide polymer was used as a flocculant in the textile wastewater treatment and had 93% dye removal from a simulated solution (Yang et al., 2013).

While biopolymers, such as chitosan and starch, are highly utilized in many applications, lignin has been neglected and considered as a low-value material. Most of the lignin that is produced as a byproduct of pulping processes are either incinerated to produce low-cost fuel or chemically degraded to low molecular weight aromatic compounds (Mai et al., 2000). It was reported that only 2% of lignin had been used commercially for the formation of flocculants, surfactants, adhesives, dispersants, and antioxidants in plastics (Laurichesse and Avérous, 2014). Graft polymerization reactions of lignin and acrylamide were introduced in the literature as an alternative to branch lignin into macromolecules under mild conditions, and impart lignin with properties that favor its use as flocculants. Rong et al. (2013) investigated the graft polymerization of acrylamide onto lignin for treating pulp and paper industrial sludge (PPIS). In this case, the final product was also used as an aid for aluminum sulfate and poly aluminum chloride in humic acid water treatment (Rong et al., 2013). In another study, lignin, chitosan were polymerized with acrylamide, and the produced polymers were reported to provide 99% and 76% dye removal (Lou et al., 2018). In another report, lignin isolated from enzymatically hydrolyzed corn stalk was polymerized with acrylamide, and the polymer was used in dye wastewater treatment (Fang et al., 2009). In other studies, cationic lignin-acrylamide based flocculants were tested in bentonite and kaoline

suspensions, and the polymers had high flocculation efficiency (Price et al., 2018; Hasan and Fatehi, 2019).

In addition, hydrolysis reactions have been considered as a means to improve the charge density of polymers while shortening their molecular weights. It was reported that the hydrolysis of polyvinylamide polymers imparts the polymers with an enhanced set of performance characteristic (e.g., higher charge density) compared to the unhydrolyzed one (Moens and Smets, 1957). Such polymers with different degrees of hydrolysis and chemical compositions have great potential for many applications such as flocculation, paper, and textile processing, recovery of minerals, and intensification of petroleum production (Abidinet et al., 2012; Lee et al., 2014). Since the use of anionic lignin-acrylamide flocculants in alumina suspension has not been reported, the work presented herein focuses on the hydrolysis of kraft lignin acrylamide polymer under different conditions and assessing their performance in alumina suspension. The effect of different reaction parameters on the properties of lignin-acrylamide polymer such as charge density, molecular weight, grafting ratio, and solubility are also reported. Polymer characteristics were investigated using Fourier transform infrared (FTIR), proton nuclear magnetic resonance (^{1}H-NMR), thermogravimetric analysis (TGA), elemental analysis, and differential scanning analysis (DSC). The effect of polymers characteristics on the suspension zeta potential, relative turbidity, flocs strength and recoverability was examined.

3.3. Materials and methods

3.3.1. Materials

Unwashed dried softwood kraft lignin (KL) was supplied by FPInnovations from its pilot plant facilities located in Thunder Bay, ON. Canada and was used as received. Sulphuric acid (98 wt.%)

obtained from Sigma Aldrich and was diluted to 1 M concentration before use. Sodium hydroxide, acrylamide (AM), potassium chloride (99%), potassium hydroxide solution (8 M), para-hydroxybenzoic acid, alumina particles, potassium persulfate ($K_2S_2O_8$), and poly diallyl dimethyl ammonium chloride (PDADMAC, 100,000-200,000 g/mol, 20 wt.% in water), deuterated water (D_2O) were all purchased from Sigma-Aldrich. Dialysis membrane (molecular weight cut-off of 1000 g/mol) was obtained from Spectrum Labs Inc., USA.

3.3.2. Lignin-acrylamide polymerization

Polymerization reactions were carried out in a three-neck flask equipped with a magnetic stirrer at 280 rpm and a reflux condenser under N_2. First, 2.0 g of KL and an appropriate amount of AM were dissolved in 45 mL of deionized water. Then, the pH of the reaction mixture was adjusted to 10, and the solution was purged under N_2 for half an hour. An appropriate amount of $K_2S_2O_8$ as an initiator was added to the solution. The flask was immersed in a water bath equipped with a thermometer to maintain a specific reaction temperature, and the reaction was performed in the absence of oxygen by keeping a continuous supply of N_2 throughout the reaction. The polymerization was carried out under different temperatures, times, pH, and AM/KL molar ratios to obtain the optimal conditions of KL-AM polymerization. After completion, the flask was immersed in cold water and acidified to pH 1.5 using H_2SO_4. The precipitated polymer was separated from homopolymer (polyacrylamide) by a centrifuge. The pH of the sample then was adjusted to 7, and the sample was dialyzed using dialysis membranes for two days to separate inorganic impurities and unreacted AM monomers. The sample was then dried at 105 °C, and KL-AM polymer was obtained. KL-AM polymer, which was generated under the conditions of 7 AM/lignin molar ratio, 80 °C, 3 h, pH 10, had the highest charge density and molecular weight

and was used for further characterization. The yield of the polymer was calculated according to the following equation (3.1):

$$Y\% = \frac{w_2}{w_0 + w_1} \times 100 \qquad\qquad (3.1)$$

where W_0 is the weight of kraft lignin used in the reaction (g), W_1 is the weight of used acrylamide monomer (g), and W_2 is the weight of KL-AM polymer (g).

The homopolymer (PAM) was synthesized under nitrogen following the optimal reaction conditions mentioned above for KL-AM polymer. For the homopolymer purification, dialysis membranes were used for two days, changing the distilled water every 6 hours.

3.3.3. Lignin-acrylamide polymer hydrolysis

KL-AM polymer that was generated under the optimal conditions (7 AM/ KL molar ratio, 80 °C, 3 h, 3 wt. % of $K_2S_2O_8$ based on lignin mass) was selected for hydrolysis experiments to investigate the effect of different hydrolysis conditions on KL-AM polymer. In this set of experiments, a 4% aqueous solution containing KL-AM polymer was prepared, and different concentrations of sodium hydroxide solutions were added to the reaction mixture, and the reaction was carried under different temperatures and times. The produced solutions were then acidified by lowering the pH of the solution to 1.5 and centrifuged to separate the hydrolyzed products. The products were then dialyzed by mixing the sample with 100 mL of water and placing the sample in a tubular dialysis membrane in deionized water. The water of this dialysis process was changed every 6 h for two days. The collected solutions were dried in a 105 °C oven, and the dried samples were denoted as HKL-AM polymers.

3.3.4. Molecular weight determination (GPC)

For molecular weight analysis, 30 mg of the samples were dissolved in 10 mL of 0.1 M NaNO$_3$ solution, and the solution was stirred at 200 rpm for 24 h at room temperature. The samples were filtered using a 13 mm diameter nylon filter with a 0.2 μm pore size, and the filtered solutions were used for analysis. The molecular weight of KL-AM was measured using a gel permeation chromatography, Malvern, GPCmax VE2001 Module, Viscotek system equipped with viscometer and RI detectors. Polyanalytic columns were used at 35 °C, and 0.1 mol L^{-1} of the NaNO$_3$ solution was used as a solution with a flow rate of 0.7 mL min^{-1}. Polyethylene oxide was used as a standard in this system.

3.3.5. Elemental analysis and grafting ratio analysis

The elemental analysis of the polymers was performed using an elemental analyzer, Elementar Vario EL Cube (Jahan et al., 2012). In preparation, the sample was first dried in a 60 °C oven overnight to remove any moisture, and then approximately 2 mg of the dried sample was weighed and transferred to the carousel chamber of the elemental analyzer, where the sample was combusted at 1200 °C. The generated gases were reduced to determine the organic components of the sample (Alkhalifa, 2017).

The nitrogen content of the sample indicates the grafting ratio of AM to lignin. As the element nitrogen is absent in KL, the content of nitrogen in the sample is derived from AM and used to determine the grafting ratio of AM. The grafting ratio was calculated following equation (3.2) (Fang et al., 2009):

$$Grafting\ ratio\ mol\ \% = \frac{\frac{N}{14} \times M_w}{100 - N/14 \times M_w} \times 100 \qquad (3.2)$$

N is the nitrogen content of the sample (wt%), and Mw is the molecular weight of AM, 71.08 g mol $^{-1}$.

3.3.6. Fourier Transform Infrared Spectroscopy (FTIR) analysis

FTIR analysis of the polymers was performed using a Bruker Tensor 37, Germany, ATR accessory. In this test, 50 mg of each sample was dried in a 60 ℃ oven overnight. Each spectrum was recorded in the range from 500 cm^{-1} to 4000 cm^{-1} in the transmittance mode with 1 cm^{-1} resolution.

3.3.7. Thermogravimetric Analysis (TGA)

Thermogravimetric analysis of polymers was carried out using thermogravimetric analyzer, TGA (i-1000 series, Instrument Specialist Inc) to determine the thermal stability of these samples. Approximately, 8-10 mg of each sample was dried at 60 ℃ for 48 h to remove any moisture. The analysis was performed under nitrogen at a steady flow rate of 100 mL min^{-1}. Each sample was heated from 25 ℃ to 800 ℃ at the heating flow rate of 5℃ min^{-1}.

3.3.8. Differential scanning analysis (DSC)

Thermal behavior of KL, KL-AM, and HKL-AM was analyzed using a differential scanning calorimeter, DSC (TA instrument Q2000, using an RC standard cell). The samples were dried at 60 ℃ for two days. 8 – 10 mg of the samples were placed into a Tzero aluminum pan, and the analysis was performed in the range of 50 – 250 ºC at 50 mL/min nitrogen and 5 ºC/min.

3.3.9.Charge density and solubility analysis

To measure the charge density and solubility of polymers, approximately 0.2 g of the polymer was dissolved in 19.8 mL of distilled deionized water to make a 1 wt.% solution. The solutions were

immersed into a water bath shaker (Innova 3100, Brunswick Scientific, Edison, NJ, USA) and shaken (150 rpm) at 30 °C for 1 h. Then, the suspension was centrifuged at 1000 rpm for 5 mins. The supernatant was separated and used for solubility and charge density determination. The charge density of the polymer was measured using a particle charge detector, Mütek PCD 04 Particle Charge Detector, with 0.005 M PDADMAC solution according to equation (3.3) (Huang et al., 2013; Ma, 2011).

$$Charge\ density\ \left(\frac{meq}{g}\right) = \frac{PDADMAC\ volum\ (mL) \times\ PDADMAC\ constration\ (\frac{mol}{L})}{mass\ of\ lignin\ in\ the\ titrator\ (g)} \times\ dilution\ factor\ (if\ any)$$

(3.3)

For solubility measurements, the concentration of the polymer in the supernatant was determined by drying the supernatant and measuring polymer solubility following equation (3.4) :

$$Solubility\ (wt.\%) = \frac{Mass\ of\ dissolved\ lignin}{Intial\ mass\ of\ lignin} \times 100 \tag{3.4}$$

3.3.10. Phenolate and carboxylate group analysis

The phenolic hydroxyl and carboxylate group contents of KL, KL-AM, HKL-AM polymers were measured using a potentiometric titration method (Kondure et al., 2015) by an automatic potentiometer (Metrohm, 728 Tirado, Switzerland). In this set of experiments, 0.06 g of the sample was dissolved in 1 mL of potassium hydroxide (0.8 M), and 4 mL of para-hydroxybenzoic acid (0.5%) was used as an internal standard. 100 mL of deionized water was added to the mixture and titrated against HCl (0.1 M) solution. The content of phenolic hydroxyl and carboxylate groups was determined based on the following equations (3.5) and (3.6).

$$Phenolic\ hydroxyl\ groups\ (mmol/g) = \frac{[(V'_2 - V'_1) - (V_2 - V_1)] \times C}{m} \tag{3.5}$$

$$Carboxylate\ groups\ (mmol/g) = \frac{[(V'_3 - V'_2) - (V_3 - V_2)] \times C}{m} \tag{3.6}$$

where C is the concentration of HCl standard solution (0.1 M), and m is the dried mass of kraft

lignin (g). V_1, V_2, and V_3 represent the first, second and third endpoint volumes of HCl solution

(mL) in the blank titration, and $V_{1'}$, $V_{2'}$, and $V_{3'}$ represent the first, second and third endpoint

volumes of HCl solution (mL) used in the measurement.

3.3.11. H-NMR

KL-AM sample was dried overnight at 105 °C to remove any moisture. The sample was dissolved

into D_2O at 40-50 mg/mL concentration. The solution was stirred for 30 min, and the ^{1}H-NMR

spectra of the samples were recorded at room temperature using an INOVA-500 MHz instrument

(Varian, USA) with a 45° pulse, and the interpulse delay time of 1.0 s.

3.3.12. Zeta potential analysis

The zeta potential of alumina suspension was analyzed using a NanoBrook Zeta PALS

(Brookhaven Instruments Corp, USA). In this analysis, 5 g of alumina were added to 200 mL of

deionized water (25 g/L) and stirred at 300 rpm overnight. The pH of alumina suspensions was

adjusted to 6 using H_2SO_4 (0.1 M). Different concentrations of the polymers (2-64 mg/g) were

maintained in a 50 mL of alumina suspension, and the solutions were stirred at 250 rpm, and room

temperature for 1 h. After stirring, 1 mL of the samples were mixed with 20 mL of KCl (0.1 mM)

solution and used for zeta potential analysis. Zeta potential measurements were carried out at a

constant electrical field of 8.4 V/cm, and room temperature. The values were reported as a mean

of three measurements.

3.3.13. Adsorption analysis

In this set of experiments, the adsorption of KL, KL-AM, HKL-AM, and PAM polymers on alumina particles was investigated at pH 6. Different dosages of polymers were added to 50 mL alumina (1 g/L), and the mixture was stirred at 200 rpm for 30 min and room temperature. The samples were centrifuged at 1500 rpm for 10 min, and then the samples were filtered using Whatman filters#1. Polymers concentration remaining in the filtrate samples was measured using a UV-Vis spectrophotometer at 280 nm and room temperature. The adsorption amount was calculated based on the difference in solutions concentrations before and after filtration following equation (3.7):

$$\text{Adsorbed amount}(\frac{\text{mg}}{\text{g}}) = \frac{v(C_0 - C)}{m} \tag{3.7}$$

where C_o and C represent the concentration of lignin samples (mg/L) before and after filtration, m is the weight of alumina (g), and v is the initial volume of the polymer (mL).

3.3.14. Turbidity analysis

The flocculation of alumina suspensions was investigated using a photometric dispersion analyzer (PDA 3000, Rank Brothers Ltd) that is connected to a dynamic drainage jar (DDJ) fitted with a 70 mm mesh screen (Wang et al., 2009). In this set of experiments, 480 mL of distilled water was first poured into the DDJ and water was circulated from DDJ to PDA through a plastic tube (3 mm) until a flow rate of 20 mL/min was obtained with the help of a peristaltic pump. Then, 20 mL of alumina suspension (25 g/L) was added to the DDJ container to make a 1 g/L concentration of alumina in DDJ. The presence of the alumina reduced the PDA's initial DC voltage (V_0) to a new voltage (Vi). After 100 s, lignin polymers with different concentrations were added to the alumina suspension in DDJ, and this caused an increase in PDA's DC voltage from V_i to the voltage of the

final suspension (V_f). The flocculation performance of PAM, KL-AM, and HKL-AM in alumina suspension was assessed by the relative turbidity (τ_r) of suspensions according to equation 3.8 (Wang et al., 2009; Xiao et al., 2010)

$$\text{Relative turbidity} = \frac{\tau_f}{\tau_i} = \frac{\ln(V_0/V_f)}{\ln(V_0/V_i)} \qquad (3.8)$$

where τ_f represents the final suspension turbidity, and τ_i is the initial suspension turbidity.

3.3.15. Focused beam reflectance measurement (FBRM)

The flocculation of alumina suspension by KL-AM, HKL-AM, and PAM was studied under dynamic conditions. The change in the size of alumina particles was monitored using FBRM (Mettler-Toledo E25). The optimal dosage for each flocculant was studied by preparing 200 mL of alumina suspension (25 g/L) and placing the suspension in a 500 mL beaker at a constant stirring of 250 rpm to keep the suspension homogenized. Different dosages of the polymers (0.2-20 mg/g) were added to the alumina suspensions at a time interval of 30 seconds. Various data in a graphical representation of the chord length distribution was obtained. Flocs strength was analyzed by adding polymers at optimal dosages of polymers and 250 rpm and monitoring the changes in flocs chord length. To analyze flocs recoverability, the deflocculation process was induced by increasing the stirring speed to 750 rpm for 2 min. Then, the stirring speed was reduced again to 250 rpm. The data obtained from deflocculation and re-flocculation curves for flocs chord length were adjusted to empirical equations to determine flocculation (T_{df}), and re-flocculation (T_{rf}) parameters (s) according to the following equations (Alfano et al., 1998; Alfano et al., 1999).

$$y = C_0 + A \cdot e^{-\frac{t}{Tdf}} \qquad (3.9)$$

$$y = c_\infty - k \cdot e^{-\frac{t}{Trf}} \qquad (3.10)$$

where A is a pre-exponential factor (mm), C_0 and c_∞ are numerical constants,(mm), k is pre-exponential factor (mm), T_{df} is de-flocculation parameter(s), T_{rf} is re-flocculation parameter (s), and y is mean chord size (mm).

3.3.16. Alumina removal

The effect of polymers on alumina removal was investigated by mixing different dosages (0.2 and 20 mg/g) of polymers and 50 mL of alumina suspension (1 g/L) at 30 °C and pH 6 for 2 h. After mixing, the suspensions were allowed to settle for 1 h. 10 mL of each sample was collected before and after settlement and oven-dried at 105 °C. The alumina particle's concentrations were tested to investigate the removal of alumina by developing a mass balance. All reported values are the mean of three experiments.

3.4. Results and discussion

3.4.1. Lignin acrylamide polymerization

The polymerization of kraft lignin and acrylamide occurred via free radical polymerization where $K_2S_2O_8$ was used as an initiator. When heated, $K_2S_2O_8$ produces sulfate radicals in the solution. The sulfate radicals react with lignin's phenolic hydroxyl groups to create phenoxy radicals that serve as reaction sites for acrylamide (AM) monomers, or propagated acrylamide chains as shown in the reaction Scheme 3.1 (Wang et al., 2016).

$$K_2S_2O_8 \xrightarrow{\triangle} 2K^+ + 2SO_4^{2-} \xrightarrow{\triangle} 2SO_4^{-\bullet} \qquad (1)$$

$$n\ CH_2{=}\overset{\displaystyle \overset{CONH_2}{|}}{CH} \xrightarrow{SO_4^{-\bullet}} {\left(CH_2{-}\overset{\displaystyle \overset{CONH_2}{|}}{CH}\right)}_n \qquad (2)$$

homopolymer

Lignin ... Lignin ... Lignin

$$\xrightarrow{SO_4^{-\bullet}} \qquad \xrightarrow{n\ CH_2{=}\overset{\overset{CONH_2}{|}}{CH}} \qquad (3)$$
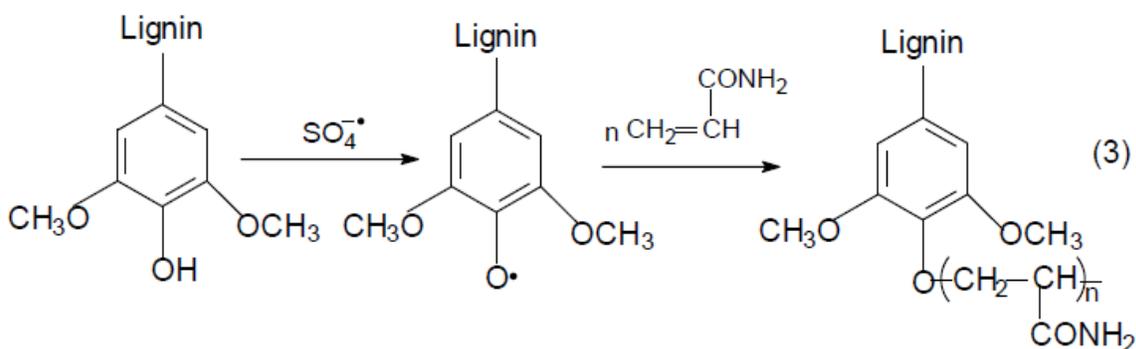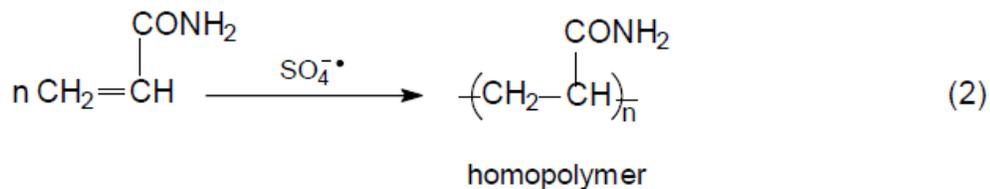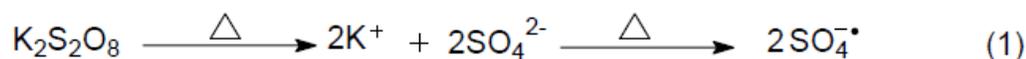
Scheme 3.1. Polymerization of KL and AM.

The effect of reaction parameters on the produced KL-AM's charge density, molecular weight, yield of production, and grafting ratio was investigated to determine the optimal conditions for polymerization. The basic conditions for these experiments were 2 AM/KL molar ratio, 3 wt.% $K_2S_2O_8$ (based on lignin weight), and 80 °C.

Effect of reaction parameters on polymerization reaction

3.4.2. Effect of pH

KL-AM polymerization reaction was carried at different pHs to determine the impact of solution pH on the reaction. The molecular weight, charge density, grafting ratio, yield, and solubility of KL-AM polymer as a function of reaction pH was presented in Figure 3.1. At lower pH, hydrogen

ions catalyze the thermal decomposition of potassium persulfate to potassium disulfate and oxygen, which results in lower molecular weight, grafting ratio, and yield as represented in Figure 3.1.a, and 3.1.b, respectively (Lin, 2001). From pH 2 to 10, there was a graduate increase in the polymer's molecular weight, grafting ratio, yield, and charge density. Such growth in polymer's molecular weight, grafting ratio, and yield can be attributed to the increased dissociation of lignin's phenolic hydroxyl groups at higher pH, which increases the reactive sites of lignin and facilitates its polymerization with AM (Kong et al., 2015). The polymerization reached a maximum (i.e., highest molecular weight, grafting ratio, and yield) at pH 10, which correspond to the pKa of phenolic hydroxyl groups of KL (Ragnar et al., 2002). Acrylamide is a neutral monomer (i.e., with no charges), thus the noticeable increase in polymer charge density is attributed to the attachment and subsequent hydrolysis of the amide groups to negatively charged carboxylic groups when the reaction is conducted under alkaline conditions (Kurenkov et al., 2000). The drop in polymer molecular weight at a pH higher than 10 can be attributed to the excessive hydrolysis of acrylamide at higher pH, which lowers the polymer's molecular weight. The decrease in polymer grafting ratio and yield at pH higher than 10 can be attributed to the formation of more homopolymer (PAM) than KL-AM polymer, as it was reported in different studies that the homopolymerization of acrylamide is favored at pH higher than 10 (Kurenkov et al., 2000; Nakabayashi and Mori, 2013). The solubility of the polymer reaches 100 % at pH> 6 as a result of increased grafting ratio of acrylamide, which contains polar amide groups, as shown in Figure 3.1.c.

a

b
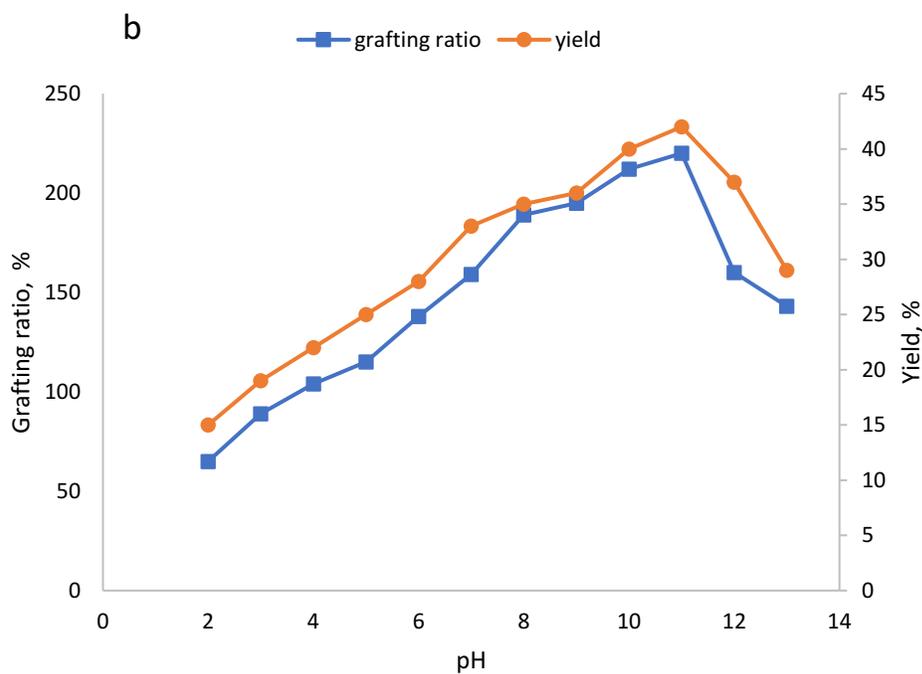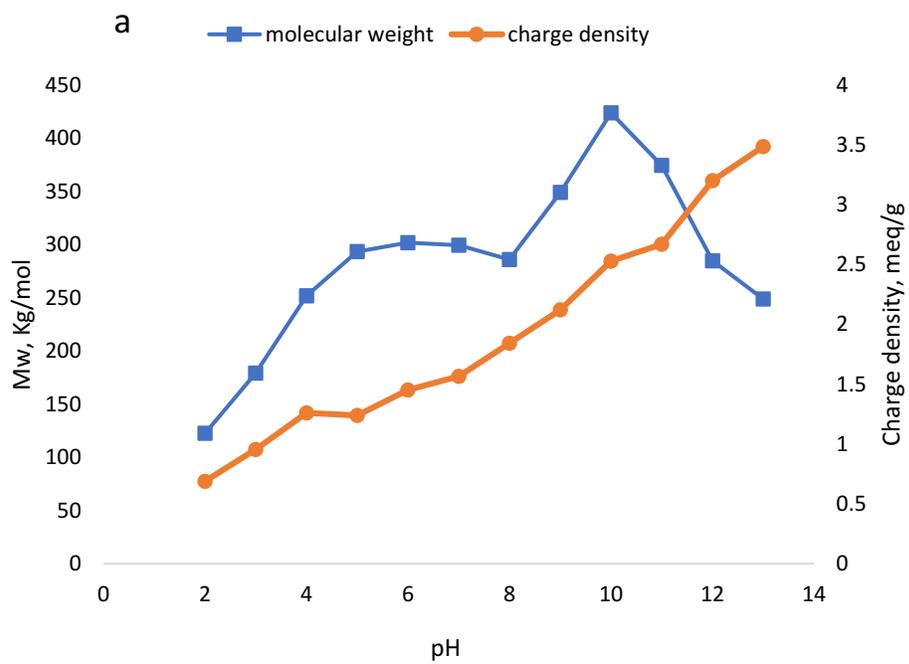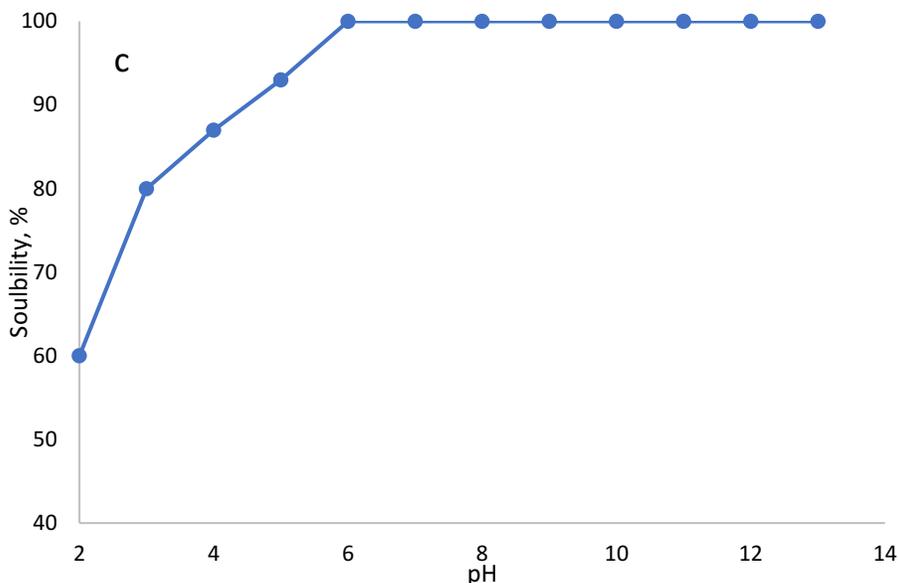
Figure 3.1. The effect of solution pH on KL-AM polymer's, a) molecular weight and charge density, b) grafting ratio and yield, c) solubility.

3.4.3. Effect of AM/lignin molar ratio

The molar ratio of AM to lignin is another important factor that affects the polymerization reaction. Figure 3.2.a, and 3.2.b, respectively, show a significant increase in the grafting ratio of AM/lignin and polymer's molecular weight as the concentration of AM monomers increases in the solution. This increase in AM concentration facilitates the reaction of KL-AM. As the monomer concentration increases, it becomes easier for lignin molecules to come into contact with vinyl monomers, as indicated in previous studies (Fang et al., 2009). This increase in grafting ratio was associated with a decrease in lignin's phenolic hydroxyl group content as its shown in Figure 3.2.a. According to previous studies on lignin and vinyl monomers polymerization, the majority of polymerization takes place on lignin's phenolic hydroxyl groups, which lower the contents of phenolic hydroxyl groups as the grafting ratio of AM increases (Liu et al., 2018; Kong et al., 2015).

Reaction yield also increased significantly when AM/lignin ratio was not more than 7 mol/mol. When AM ratio was greater than 7 mol/mol, we noticed a decrease in polymers' grafting ratio and Mw. This noticeable decrease probably indicates that more AM monomers were homopolymerized to polyacrylamide where homopolymerization reaction competed with KL-AM formation based on previous studies (Kong et al., 2015; Wang et al., 2016). This decrease was also observed in the reaction yield at a ratio greater than 7 mol/mol. This drop in yield could be a result of less KL-AM polymerization or the result of a significant increase in water solubility of KL-AM with long chains of AM attached to lignin, which ould make it difficult to separate the product from the aqueous solution (Fang et al., 2015). Polymer's charge density reached a maximum of – 2.24 meq/g at 7 mol/mol. After this ratio, the increase in the charge density was unremarkable as AM grafting ratio dropped.
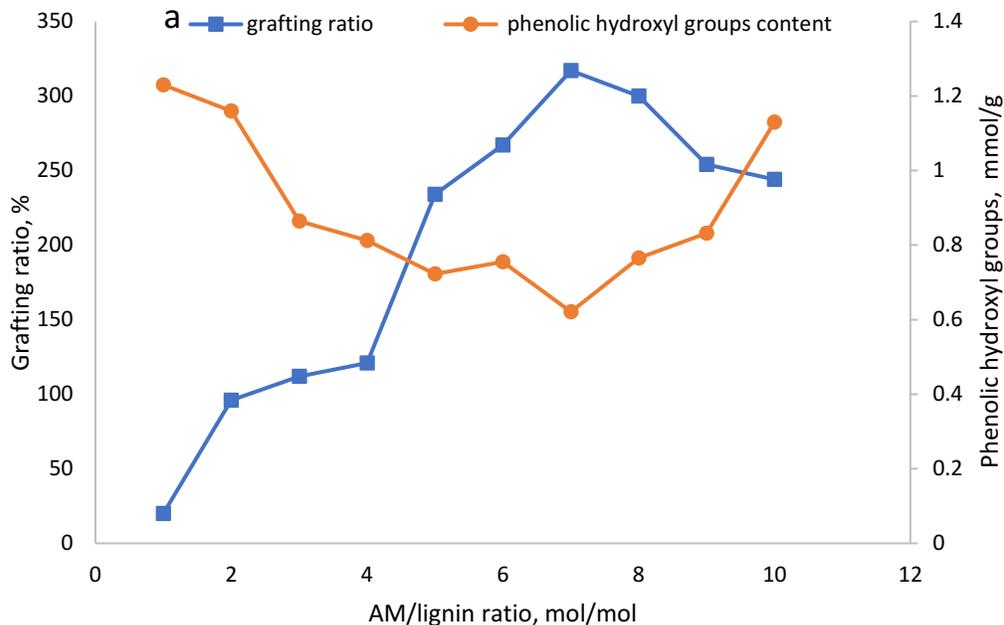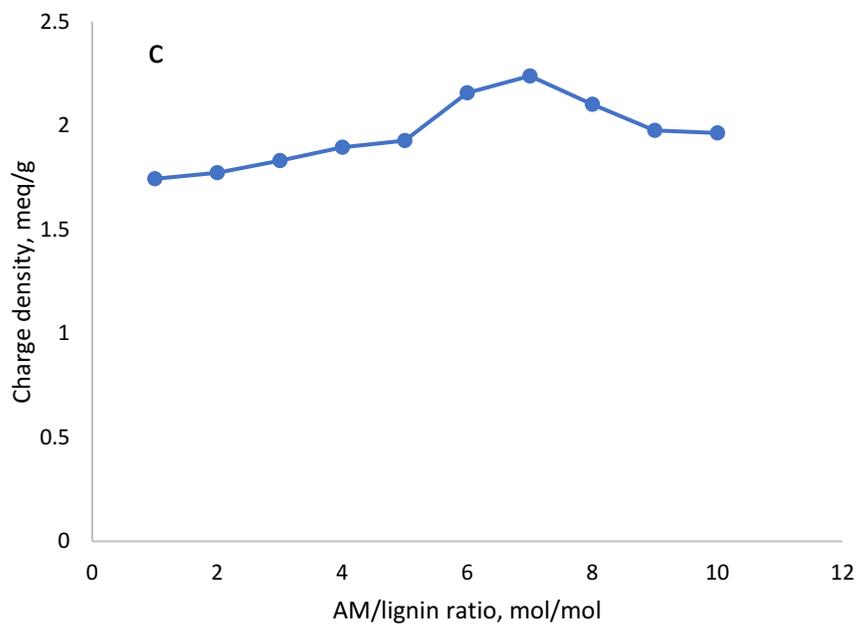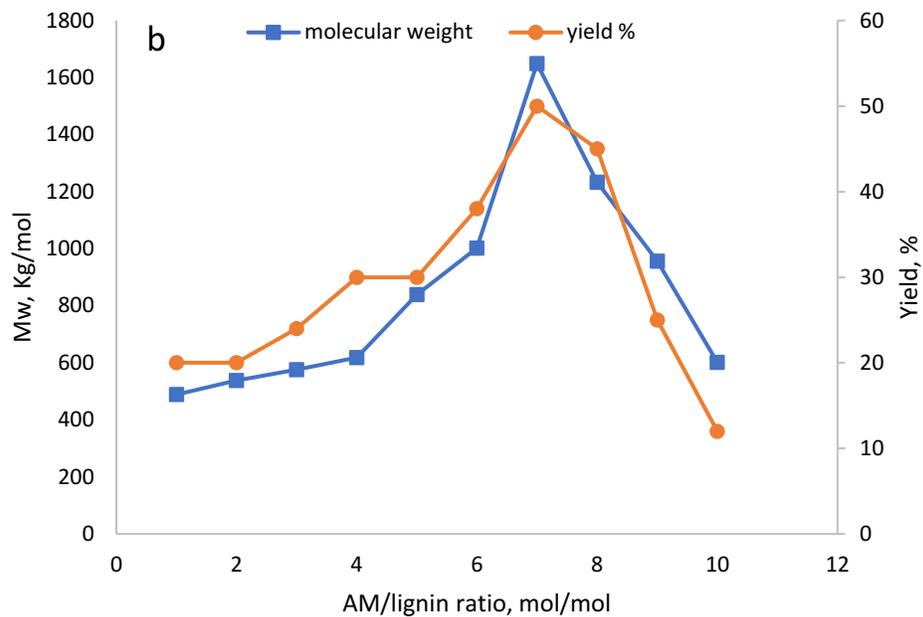
Figure 3.2. The effect of AM/lignin molar ratio on KL-AM polymer's, a) grafting ratio and phenolic hydroxyl groups content, b) Mw, and yield, c) charge density.

3.4.4. Effect of temperature

The effect of reaction temperature on the KL-AM's grafting ratio and yield was presented in Figure 3.3.a. We can see that the grafting ratio and yield increased rapidly as the reaction temperature increased. The highest grafting ratio and yield were both obtained at 80 °C. The same trend was also observed for polymer's molecular weight and charge density, as shown in Figure 3.3.b, where we see a progressive increase via elevating the reaction temperature. At low reaction temperature, the decomposition of the initiator was hampered, which restrained the polymerization and resulted in a lower grafting ratio, molecular weight, and yield.

On the contrary, a very high reaction temperature can cause the decomposition of the initiator very rapidly and increases the possibility for radical transfer, which leads to a lower yield and grafting ratio. At the reaction temperature of 90 °C, KL-AM polymer with a lower molecular weight and charge density was obtained, which could be attributed to a lower grafting ratio, as shown in Figure 3b.
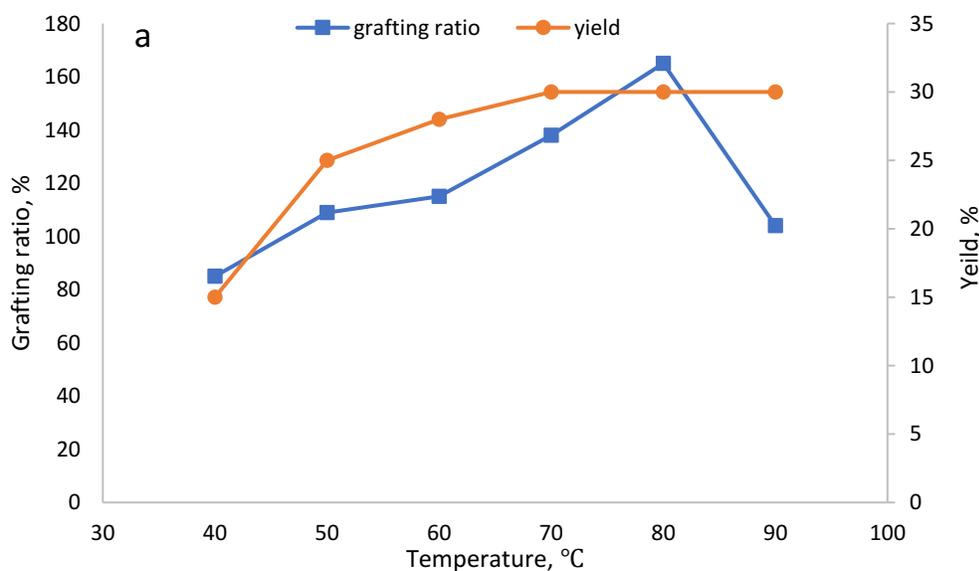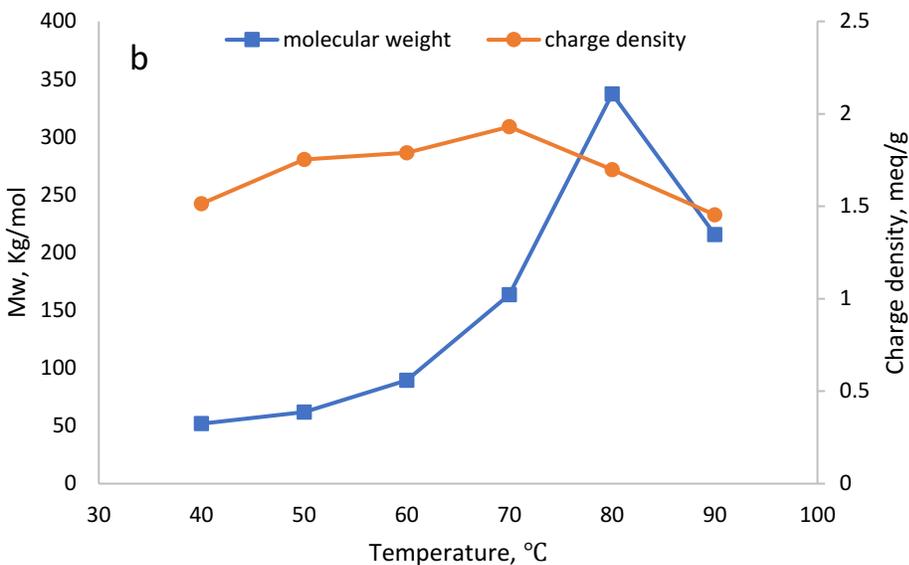
Figure 3.3. The effect of reaction temperature on KL-AM polymer's, a) grafting ratio, and yield, b) Mw and charge density.

3.4.5. Effect of time

The effect of reaction time on KL-AM's molecular weight, yield, and charge density was shown in Figure 3.4. As the reaction time increased from 1 to 6 h, a slight increase in polymer's charge density was observed after 3 h of reaction. The molecular weight and yield improved rapidly as the reaction time increased from 1 to 3 h. When the reaction time was further increased, the growth in both molecular weight and yield were unremarkable. This noticed behavior is similar to the pattern of radical polymerization where the reaction mostly takes place in the period of initiation, and the rate of polymerization is high at first (Buback, 1990). As the concentration of monomer and initiator declined within a period of time, it was found prolonging the reaction time more than 3 h had an unremarkable effect on the growth of polymer yield and molecular weight.
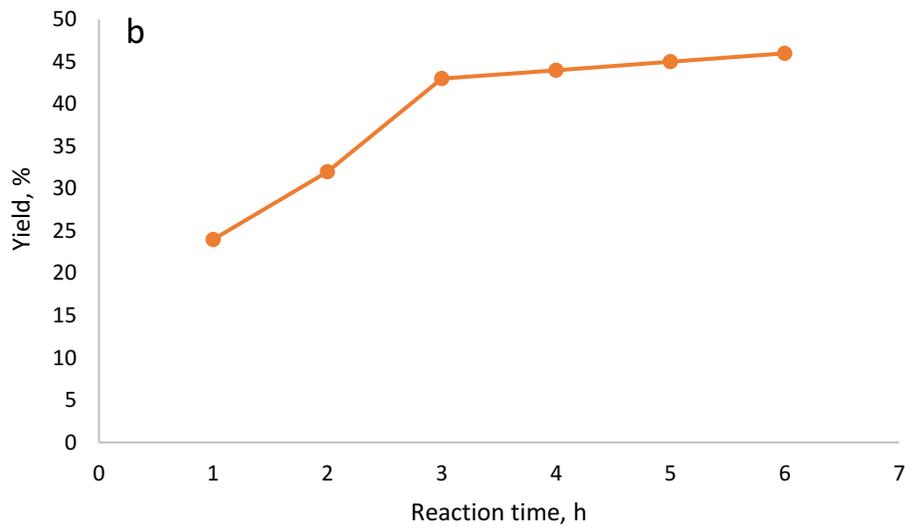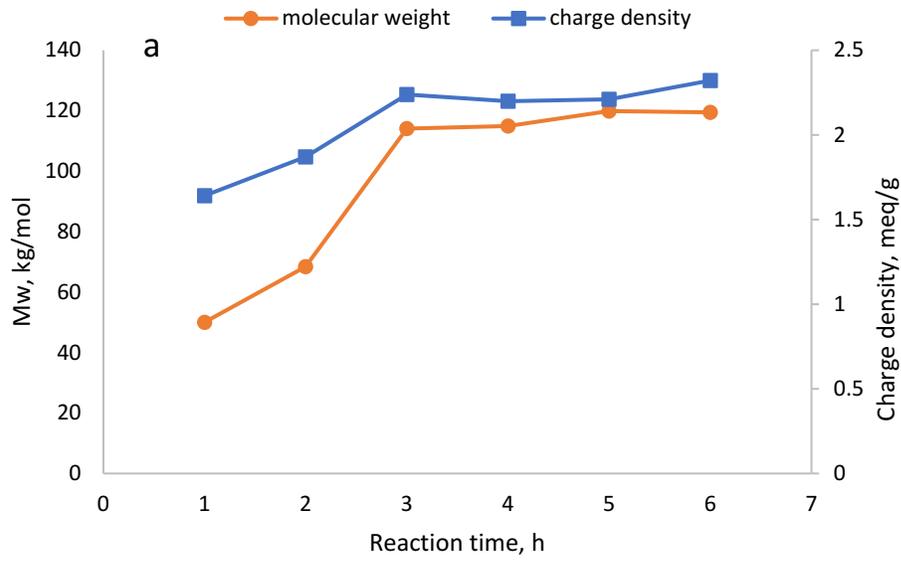
Figure 3.4. The effect of reaction time on KL-AM polymer's a) Mw, and charge density, b) yield

3.5. Hydrolysis of KL-AM polymer

Acidic and alkaline hydrolysis of natural and synthetic polymers were conducted in the past to generate materials with different functionalities. AM side chains of KL-AM polymer can be partially hydrolyzed to produce KL-AM with improved negative charge density. The partially hydrolyzed chains contain polar amide groups and carboxyl groups that impart solubility to the polymer (Zeynali et al., 2002). The ionizable carboxyl groups dissociate to leave negatively charged macromolecules and positively charged counterions, which lead to polyelectrolyte properties in aqueous solutions. Polymers with polyelectrolyte properties gain advantages in flocculation processes as they have more interaction with oppositely charged colloidal particles (Zeynali et al., 2002). In addition, the hydrolysis of grafted AM chains leads to extended conformation in the solution due to the intermolecular repulsion between their carboxylic groups, which enhances bridging between particles and increases the degree of flocculation (Singh et al., 2003; Zeynali et al., 2002). To improve the flocculation efficiency, the optimal hydrolysis of KL-AM polymer is necessary. The hydrolysis conditions and COOH content (mmol/g) in hydrolyzed samples are listed in Table 3.1.

Table 3.1. KL-AM polymer hydrolysis conditions.

Sample	NaOH (M)	Temperature (°C)	Time (h)	COOH content (mmol/g)	Mw (Kg/mol)	Yield (%)
1	3.5	65	4	1.95	1,065	53
2	3.5	80	4	2.27	873	64
3	1.0	90	1	1.75	995	82
4	2.8	90	1	1.86	978	80
5	1.0	90	2	1.93	952	80
6	2.8	90	2	2.13	901	75
7	1.0	90	3	2.27	886	65
8	2.8	90	3	2.45	853	62
9	0.4	90	4	2.73	823	83
10	0.7	90	4	2.98	786	80

11	1.0	90	4	3.10	741	76
12	1.4	90	4	3.25	728	68
13	2.0	90	4	3.52	694	64
14	2.8	90	4	4.84	645	62
15	3.5	90	4	5.07	601	53
16	2.8	95	3	3.26	372	43
17	2.8	95	4	2.97	321	41

The decrease in the polymer molecular weight as the increase in the hydrolysis rate indicates a slight degradation of acrylamide chains in the hydrolysis process (Singh et al., 2003). The hydrolysis rate increased with increasing reaction temperature. At lower temperatures (65 ℃, 80 ℃), the generated products had a smaller COOH content than the products obtained at 90 ℃ indicating lower degree of hydrolysis for them. At a temperature higher than 90 ℃, the molecular weight decreased remarkably in comparison with parent polymer as temperatures higher than 95 ℃ causes the significant degradation of polymer chains as indicated in previous research on synthetic polyacrylamide polymers (Nagase et al.,1965). Raising NaOH concentration improved hydrolysis as products with higher COOH contents was generated. The hydrolysis rate was high at the initial stage and decreased rapidly with the increasing conversion. This declaration in the reaction rate was attributed to the accumulation of negative charges on the polymer, which would exert an electrostatic repulsion effect toward hydroxyl ions in the solution that would lead to a decrease in the conversion rate. As a result, the hydrolysis reaction cannot go to completion (Zeynali and Rabiei, 2002; Kurenkov et al., 2001). The optimal time for hydrolysis was found to be 4 h, as the reaction time longer than 4 h didn't generate products with higher COOH content. Acidic hydrolysis using strong mineral acids, such as sulfuric and hydrochloric acid generated partially or completely insoluble products, which could be attributed to intramolecular imidization (Smet et al., 1959; Kheradmand et al., 1988).

3.6. Polymers properties

The properties of kraft lignin and modified lignin samples are illustrated in Table 3.2. The obtained results by GPC analysis demonstrated that KL had a molecular weight of 20,000 g/mol, which was lower than the reported values (24,000-20,000 g/mol). The difference in the results of this work and those reported in the literature is attributed to the variations in the origins of lignin and pulping process conditions (Inwood et al., 2018). The kraft lignin had a charge density of – 1.2 meq/g. By polymerization with AM, the molecular weight of kraft lignin increased to 1, 564 Kg/mol, and the charge density of the obtained polymer was – 2.33 meq/g. The hydrolysis of KL-AM polymer decreased the molecular weight to 601 Kg/mol, and the charge density was -3.62 as a result of the significant increase in the carboxyl groups of lignin (5.04 mmol/g). The synthesized acrylamide homopolymer (PAM) under the same KL-AM polymerization conditions generated a polymer with a molecular weight of 598 Kg/mol and a charge density of – 0.6 meq/g.

Table 3.2. Molecular weight, charge density, carboxyl, and phenolic hydroxyl groups content (mmol.g^{-1}) of KL, KL-AM, HKL-AM, and PAM polymers.

Polymer	Mw (Kg/mol)	Mw/Mn	Charge density (meq/g)	Carboxylate groups (mmol/g)	Phenolic Hydroxyl (mmol/g)
KL	20	1.674	-1.2	1.37	1.31
KL-AM	1, 064	1.763	- 2.3	1.52	0.53
HKL-AM	601	2.216	-3.62	5.04	0.46
PAM	598	1.563	-0.6	0.75	-

3.7. Elemental analysis

The elemental analysis of KL, KL-AM, and HKL-AM polymers that were generated under the optimal conditions (mentioned in sections 3.3.2 and 3.5) are illustrated in Table 3.3. KL did not have nitrogen element in its structure. Compared to KL, KL-AM polymer showed a considerable

amount of nitrogen indicating that the polymerization reaction successfully altered the elemental component of KL with a high amount of AM being grafted into lignin backbone (253%). The nitrogen content of HKL-AM was lower than that of KL-AM as a result of the hydrolysis of acrylamide chains in KL-AM polymer, which also increased the oxygen content of the product as its carboxylate group increased. The C_9 formula for KL, Kl-AM, and HKL-AM was calculated based on this elemental analysis and are listed in Table 3.3.

Table 3.3. Elemental analysis of polymers.

Elemental analysis	C (wt.%)	H (wt.%)	N (wt.%)	O (wt.%)	S (wt.%)	Molecular formula
KL	53.58	5.77	0	40.39	0.25	$C_9 H_{12}N_0O_{4.8}S_{0.04}$
KL-AM	47.23	7.28	14	31.27	0.20	$C_9 H_{16.62}N_{2.3}O_{4.1}S_{0.04}$
HKL-AM	43.95	8.12	7.5	40.33	0.11	$C_9H_{19.95}N_{1.3}O_{6.1}S_{0.03}$

3.8. Thermal behavior of lignin samples

3.8.1. Thermogravimetric analysis (TGA)

The thermogravimetric analysis provides information on the thermal behavior of lignin polymers. The decomposition and stability behavior of the samples determine the range of applications where the polymers can be used (Yang and Wu, 2009). As illustrated in Figure 3.5.a, the thermogravimetric analysis of lignin, PAM, and modified lignin-acrylamide polymers reveals that grafted lignin polymers were more thermally stable compared to unmodified lignin and polyacrylamide (PAM). Up to 700 °C, 45% weight loss is observed in lignin-acrylamide polymers as compared to 75% weight loss in lignin, and 60% weight loss in PAM. The first 10% weight loss or decomposition below 100 °C in all samples is attributed to the elimination of moisture. The second major decomposition for KL was in the range of 165 to 500 °C with a weight loss of 45 %

is attributed to the degradation of the intra-unit linkage of lignin (Zhang et al., 2014). The main decomposition temperatures for KL and PAM were 340 ℃, 353 ℃, respectively. In the case of KL-AM and HKL-AM polymers, the second decomposition occurred in the range of 230 ℃ and 313 ℃ with 20% weight loss that is attributed to the decomposition of AM segment (Yang, 1998). The third decomposition for KL-AM and HKL-AM polymers occurred in the range of 379 ℃ and 510 ℃, and this degradation is attributed to the decomposition of the polymer backbones. The main decomposition temperature for KL-AM and HKL-AM was higher than that for KL, which proves more thermal stability of polymers where AM segment of the polymers degraded first making the degradation of lignin backbone occurring at a higher temperature (Berbu and Vasile, 2018). KL-AM showed higher thermal stability than HKL-AM at a temperature between 380 ℃ and 500 ℃. HKL-AM contains a higher content of carboxylate groups than KL-AM as indicated in Table 3.2, which makes the polymer less thermally stable as theses groups degrade to CO_2 in this temperature range (Cervantes et al., 2006). Figure (3.5.b) also represents the weight loss rate of KL, KL-AM, and HKL-AM where a noticeable increase occurred in the temperature range of 230 ℃ and 510 ℃ for all sample, with KL representing the highest. The smaller peaks for modified lignin samples in this region compared to KL represent lower weight loss indicating higher thermal stability for modified samples, which can be the result of improved intra-molecular linkage (Berbu and Vasile, 2018). In the case of PAM, the decomposition happens in two stages. The first stage of decomposition is in the range of 220–340°C, where PAM chains remain intact, and the decomposition occurs on pendant amide groups. In the second stage of decomposition (340–430°C), the majority of the weight loss occurs, as main chain breakdown occurs, which is represented by a sharp peak in this region (Van Dyke and Kasperski, 1993).
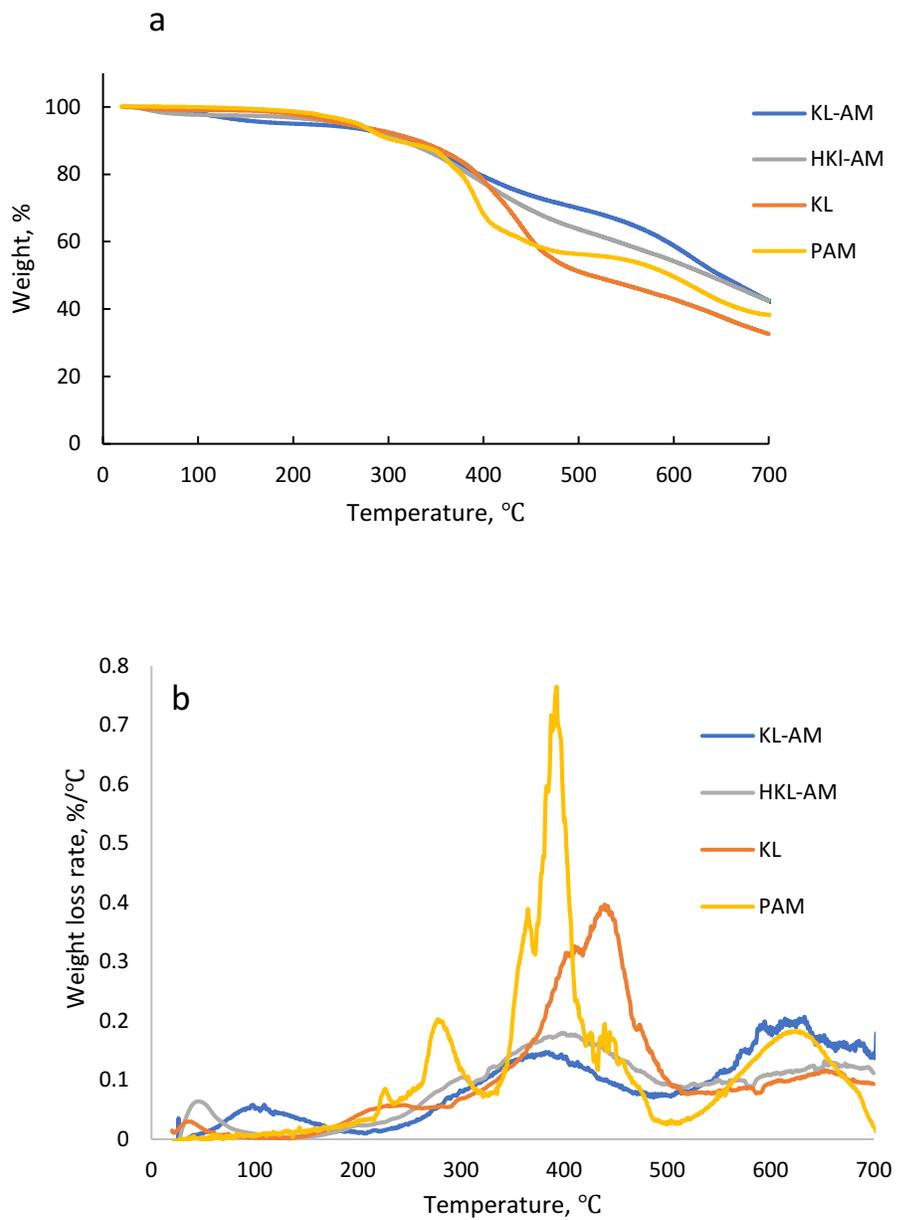
Figure 3.5. a) Weight loss and b) Weight loss rate of KL, KL-AM, and HKL-AM polymers conducted underN$_2$ with the flow rate of 30 mL/min heated at 10 °C/min.

3.8.2. Differential scanning calorimetry (DSC) analysis

To further investigate the thermal behavior of lignin derivatives, the glass transition temperature (T_g) of the samples was analyzed and reported in Table 3.4. Polymers, such as lignin with an amorphous structure, may undergo a transition from a rigid state to a rubbery state at a specific temperature. This temperature is called the glass transition temperature (Fox and Mcdonlad, 2010; Passoni et al., 2016). As reported in different studies, the T_g of lignin varies depending on the type of lignin and the process in which lignin is produced (Tejado et al., 2007). The T_g of kraft lignin is usually reported in the range from 90 to170 °C (Laurichesse and Averous, 2014; Gellerstedt, 2015). As shown in Table 3.4, the T_g of lignin was found to be 151.33 °C. The grafting of acrylamide chains onto lignin's backbone elevated the T_g of KL-AM and HKL-AM to 244.91 and 245.56 °C, respectively. As proven in different studies, the T_g of polymers is affected by the polymer's molecular weight, crosslinking structure, and hydrogen bonding performance (Gordobil et al., 2017; Heitner et al., 2010). The high content of acrylamide chains and carboxyl groups in KL-AM and HKL-AM increased T_g significantly as a result of increased hydrogen bonding. In addition to T_g, the heat capacity of lignin derivatives was determined in DSC analysis. The heat capacity, C_p, is a measure of the heat required to raise the temperature of a substance by one degree. The reported heat capacity of kraft lignin is usually around 0.2573 to 0.292 J/g.°C (Hatakeyama and Quinn, 1995). The C_p of Kraft lignin as measured was 0.2901 J/g.° C. It can be seen that the heat capacity of modified lignin increased compared to unmodified lignin, which indicates improved thermal stability of the samples as the molecular weight and grafting ratio of the polymer improved. The measured T_g and heat capacity of polyacrylamide (PAM) were 153 °C and 0.312 J/g.° C, respectively. Modified lignin polymers were shown to have high thermal stability compared to unmodified kraft lignin and polyacrylamide.

Table 3.4. Glass transition temperature and heat capacity of KL, KL-AM, and HKL-AM

Lignin	T_g (°C)	Heat capacity, Cp (J/g. °C)
KL	151.3	0.290
KL-AM	244.9	0.588
HKL-AM	246.8	0.406
PAM	153.6	0.312

3.9. Fourier transform infrared spectroscopy (FTIR)

Grafting of acrylamide onto lignin was confirmed by comparing the IR spectra of unmodified lignin with KL-AM and HKL-AM polymers. The IR spectra of KL, KL-AM, and HKL-AM are shown in Figure 3.6. The band at 1496, 1425, and 1593 cm^{-1} correspond to the aromatic skeleton vibration of KL, which also exist in the spectra of KL-AM and HKL-AM polymers (Singh et al., 2006). The band at 2926 cm^{-1} is assigned to C-H stretching in the methyl groups of both lignin and modified polymers. The –CH$_2$ vibrations of acrylamide appear around 1460 cm^{-1} (Singh et al., 2006). The most significant band in IR spectra of KL-AM and HKL-AM is around 1600 cm^{-1}. This band is assigned to N-H stretching vibrations of the amide group, which was absent in the IR spectra of unmodified kraft lignin (el-Zaway and Ibrahim, 2012). The band at 1676 cm^{-1} is attributed to the carbonyl group in both lignin and modified polymers (el-Zaway and Ibrahim, 2012). The presence of –CH$_2$ and N-H band in the modified polymers IR spectra confirms that acrylamide monomer was grafted onto kraft lignin.
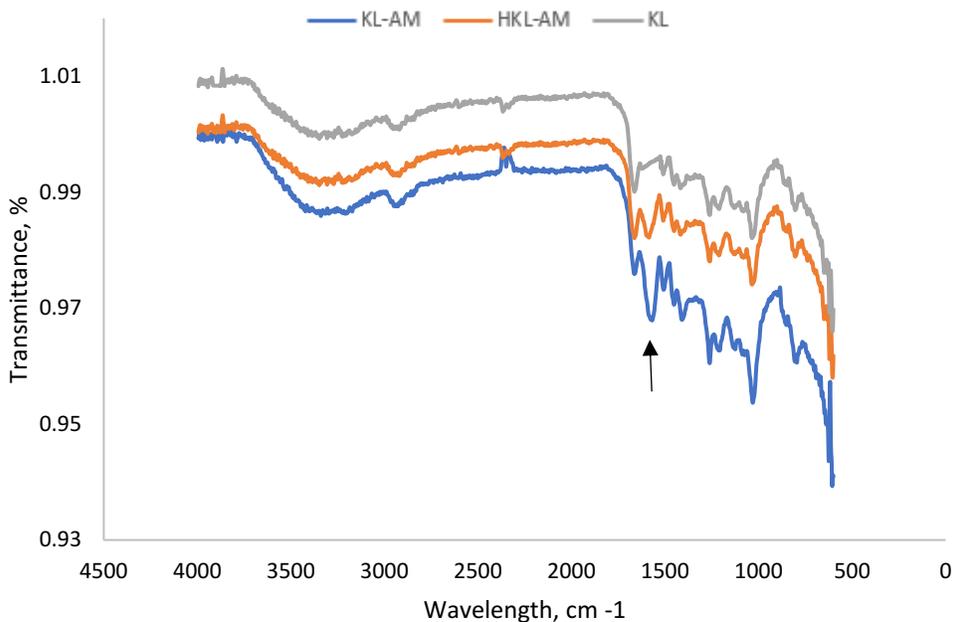
Figure 3.6. FTIR of KL, KL-AM, and HKL-AM.

3.10 . ^{1}H -NMR

Figure 3.7 shows ^{1}H-NMR spectra for KL, KL-AM, and HKL-AM polymers. The peaks at 6.9, 7.07, and 7.06 ppm in the KL spectra are attributed to aromatic protons. The peaks at 6.15 and 5.75 are attributed to H$_\beta$ and Hα of the cinnamyl alcohol unit of lignin and β-5 structure. Methoxy groups protons of kraft lignin appear at 3.70 and 3.30 ppm. Hydroxyl protons peak appeared at 4.00 ppm (Runge and Ragauskas, 1999; Hu et al., 2014; Wang et al., 2016). The Peaks at 4.5 and 4.9 ppm were assigned to the solvent (D$_2$O). In KL-AM and HKL-AM spectra, new peaks were observed at 1.6 and 2.2 ppm, which were absent in the KL spectrum. These two peaks are attributed to Cα and Cβ of acrylamide. The presence of these two peaks indicates that acrylamide was successfully introduced to the backbone of kraft lignin. This peak is weaker in HKL-AM's spectrum compared to KL-AM's, which is a result of acrylamide hydrolysis.
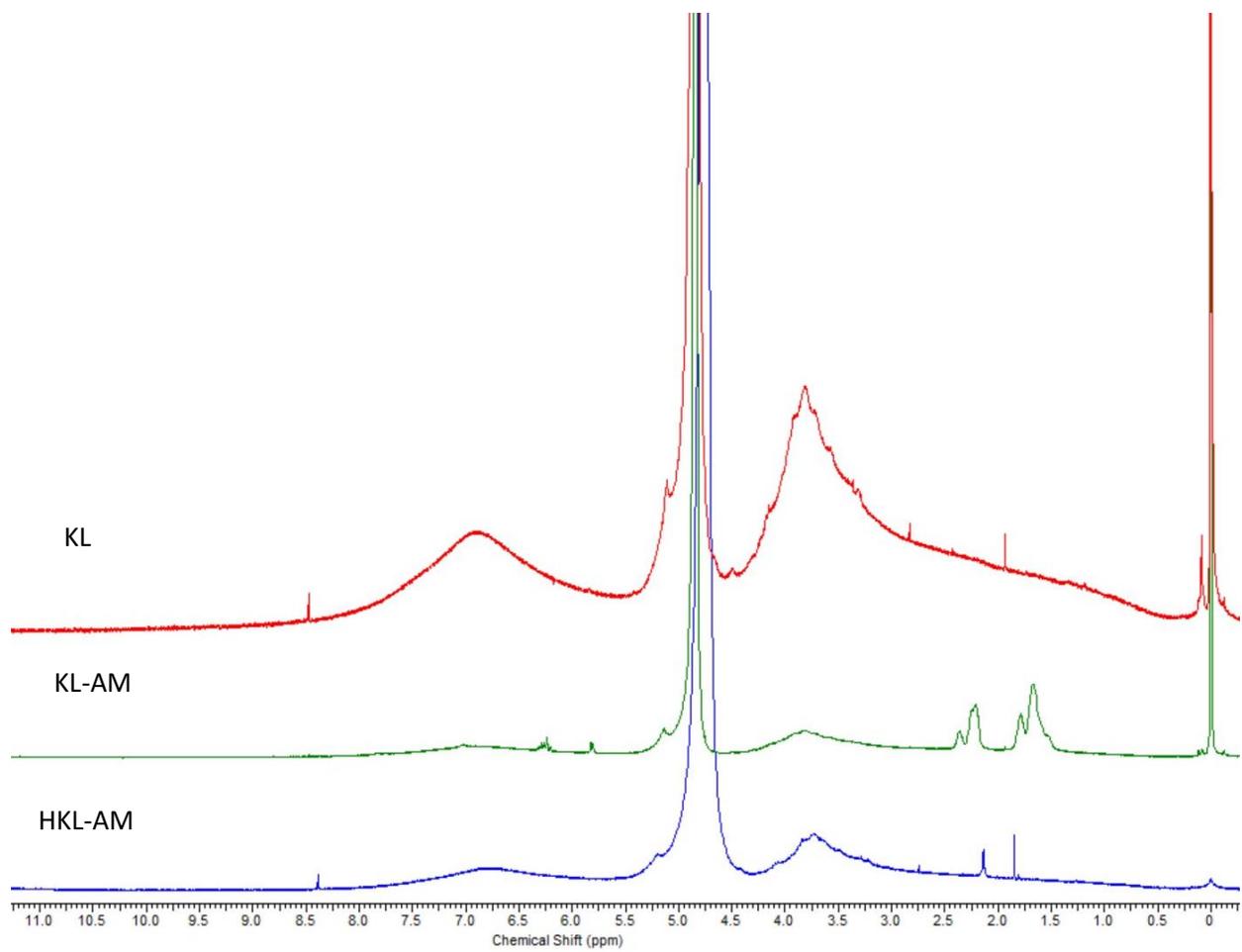
Figure 3.7. ^{1}H-NMR spectra of KL, KL-AM, and HKL-AM.

3.11. Adsorption analysis

To better understand the interaction between anionic lignin-acrylamide polymers and alumina particles, the impact of alumina suspensions' pH on the flocculation behavior should be examined. The isoelectric point (IEP) of alumina is at pH 8.6 (Wiśniewska et al., 2012). Above this pH, the particles carry a net negative charge due to the formation of Al-O⁻ groups, and below this pH, alumina surface carries a net positive charge due to the formation of $Al-OH_2^+$ (Hogg, 2013). Wiśniewska et al. (2012) proved that the adsorption of anionic polyacrylamide on alumina particles was decreased with increasing pH, whereas the adsorption of cationic polyacrylamide was increased at a higher pH. It was also found that the greatest effect of destabilizing alumina suspension was obtained at pH 6 in the presence of polymers with anionic polyacrylamide chains (Ouyang et al., 2009; Chibowski et al., 2014). Figure 3.8 presents the adsorption of KL, PAM, and anionic lignin-derived polymers on alumina particles at pH 6 as a function of polymer concentration. As shown, polymer adsorption on alumina was enhanced with increasing polymer concentration until adsorption reaches a plateau for all polymers at a concentration of 64 mg/L. The limited adsorption (2.4 mg/g) shown by unmodified Kraft lignin is mainly attributed to kraft lignin's limited solubility. Grafted acrylamide chains onto lignin backbone alter kraft lignin's solubility. The functional groups of amide ($-CONH_2$) and their ability to adsorb on alumina surface is greatly enhanced by the integration of other functional groups, such as carboxyl ($-COO-$), and hydroxyl ($-OH$) groups, in hydrolyzed acrylamide polymers (Chen et al., 2003). In other reports, the adsorption of polyacrylic acid and sulfonated lignin on alumina particles was enhanced by increasing polymer's charge density as a result of increased electrostatic interaction between polymers and suspended charged particles (Kazzaz et al., 2018; Kazzaz and Fatehi, 2018). Other studies that investigated the adsorption of synthetic polyacrylamide on alumina particles

demonstrated the effect of high molecular weight in achieving higher adsorption performance (Li et al., 2008). As the molecular weight of polymers increases, the area that the polymers occupy on the surface of particles increases, the net result being that fewer of the large polymers are needed to cover the surface of particles (Inwood, 2014; Matsushita and Yasuda, 2005). As shown in Figure 3.8, HKL-AM polymer with a charge density of -3.6 meq/g, and a molecular weight of 601 kg/mol has the highest adsorption on alumina particles compared to KL-AM polymer with much higher molecular weight (1,064 Kg/mol), and lower charge density (- 2.3 meq/g) as indicated in Table 3.2). By comparing the adsorption of PAM that has a similar molecular weight to HKL-AM, but a low charge density (-0.6 meq/g), PAM shows lower adsorption. This indicates that the molecular weight of polymers was not a significant factor in achieving higher adsorption and that the adsorption of polymers on alumina was mainly influenced by charge density, where polymers with high charge density achieved higher adsorption regardless of their molecular weight.
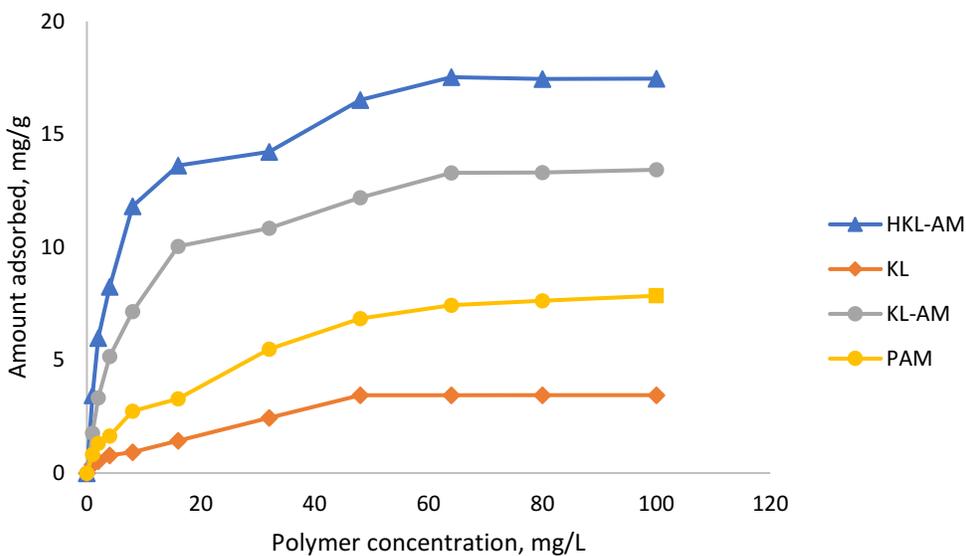

Figure. 3.8. Adsorption isotherms of KL, KL-AM, HKL-AM, and KL on alumina particles conducted at pH 6, and room temperature.

3.12. Zeta potential as a function of polymer concentration

Zeta potential is the potential difference between the double electrical layer surrounding the particles (diffused layer of ions) and the solution. This value is significant for flocculation as the magnitude of the zeta potential indicates the stability of the colloidal system (Singh et al., 2003). If the zeta potential of a system falls below a certain level, the colloidal particles will aggregate due to the attractive forces (Van der Waals forces); conversely, a very high zeta potential, either a negative or positive value, maintains a stable system as the suspended particles repel each other. It was stated in previous studies that when polymers adsorb on the surface of particles, polymers with high charge density had the most significant impact on altering the zeta potential of the colloidal system (Singh et al., 2003). Also, by doing a correlation between the zeta potential of a system, and its relative turbidity, the point at which van der Waals and electrical forces balance at a specific polymer concentration, or what is known as the critical flocculation concentration (CFC), can be identified (López-Maldonado et al., 2014). Figure 3.9 shows alumina suspension's zeta potential as a function of polymer concentration. As these experiments were carried out at pH 6, alumina suspension has a positive zeta potential of ≈30 mV due to its positively charged surface (Kazzaz et al., 2018). By increasing the concentration of KL-AM, and HKL-AM polymers, a significant reduction in the zeta potential of alumina suspension was observed. Changes in the zeta potential were more pronounced for HKL-AM polymer with the higher charge density. This reduction in the suspension zeta potential is attributed to HKL-AM's high adsorption, as shown in Figure 3.8, which results in higher accumulation of anionic charge in the diffused layer around alumina particles.
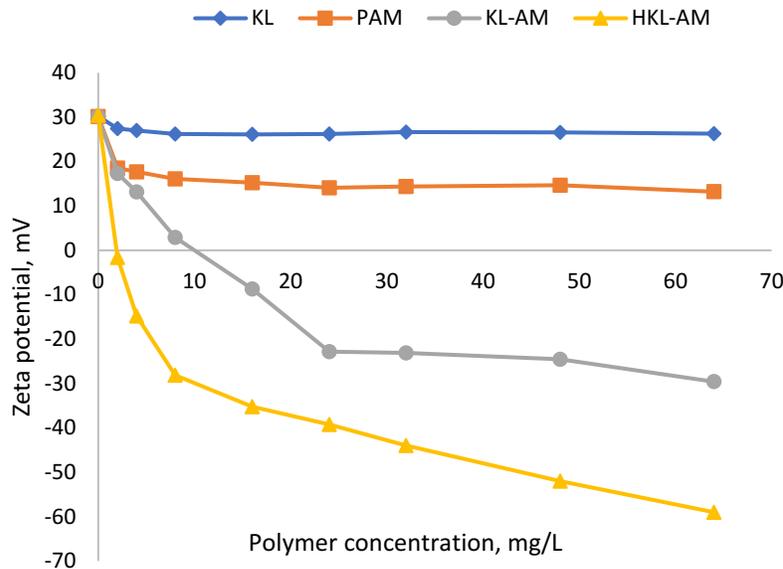
Figure 3.9. Alumina suspension's zeta potential as a function of polymer concentration conducted under the conditions of pH 6, 30 min incubation at 30 °C, and 1 g/L of alumina concentration.

Similarly, KL-AM polymer reduces the zeta potential of the suspension to -29 mV at a polymer concentration higher than 64 mg/L. Unmodified kraft lignin (KL) showed an insignificant impact on the zeta potential of the suspension due to its limited adsorption (Figure 3.8). In the case of acrylamide homopolymer (PAM), the overall zeta potential of alumina suspension remained cationic (16.11 mV) after PAM adsorption on alumina surface. The polymer was unable to change the zeta potential of alumina suspension due to its limited adsorption and low charge density. In another study on cationic lignin acrylamide polymers in bentonite and kaoline suspensions, changes in the zeta potential were more pronounced for polymers with higher charge density, as the zeta potential value increased from -35 mV to +40 mV in bentonite suspension and 30 mV in the kaolin system (Hassan and Fatehi, 2018). These results indicate that the electrostatic attraction between the positively charged polymers and negative surface sites of clay particles neutralized

the surface charge of particles and led to an accumulation of cationic charges in the diffused layer, in the case of highly charged polymers (Hasan and Fatehi, 2018).

3.13. Influence of polymer dosage on relative turbidity

Relative turbidity is a measure of the relative clarity of a liquid, and it is used to monitor the efficiency of flocculation process (Farrokhpay, 2009). The relative turbidity of alumina suspension was plotted as a function of polymer dosage in Figure 3.10 a. As can be seen, the relative turbidity of alumina suspension decreased by increasing the polymers dosage in the suspension. Generally, a dosage of 3 mg/g of HKL-AM polymer was sufficient to reduce the relative turbidity of the suspension dramatically to 0.12. In the case of KL-AM and PAM polymers, the relative turbidity of alumina suspension was reduced to 0.23 and 0.4, respectively, at a higher dosage (10 mg/g). As shown, unmodified kraft lignin didn't impact the relative turbidity of alumina suspension, which is attributed to unmodified kraft lignin's limited adsorption on alumina surface, as indicated in section 3.8. By comparing the results obtained in the relative turbidity and adsorption analysis, it is evident that polymers with higher adsorption, such as HKL-AM, lowered the relative turbidity of the suspension the most, and as indicated previously, the charge density of the polymers was a significant factor in achieving higher adsorption. In another report, anionic polyacrylic acid polymer was used to flocculate anionic alumina particles at a pH above 8.6 (Yu and Somasundaran, 1997). In this work, the most pronounced result in reducing the relative turbidity of the suspension was obtained by polymers that contained the highest anion groups among all polymers tested. Other studies have also shown the effect of high molecular weight on the performance of anionic polyacrylamide flocculants in alumina suspension where the high molecular weight of polymers facilitates the bridging of particles to form large aggregates, and lower relative turbidity (Wiśniewska et al., 2012; Hogg, 2013).

To further investigate if lignin-acrylamide polymers can act as flocculants in the alumina suspension, the removal of alumina was investigated as a function of polymer dosage (Figure 3.10 b). HKL-AM polymer has the highest alumina removal, and 3 mg/g of the polymer was sufficient to remove 92% of alumina. In the case of KL-AM and PAM polymer, 75% and 54% alumina removals, respectively, were obtained at the same dosage. In another report, a complete clay removal (100%) was reported in a study, which investigated the impact of charge density of cationic polyacrylamide polymers on clay removal (Güngör and Karaoğlan, 2001).
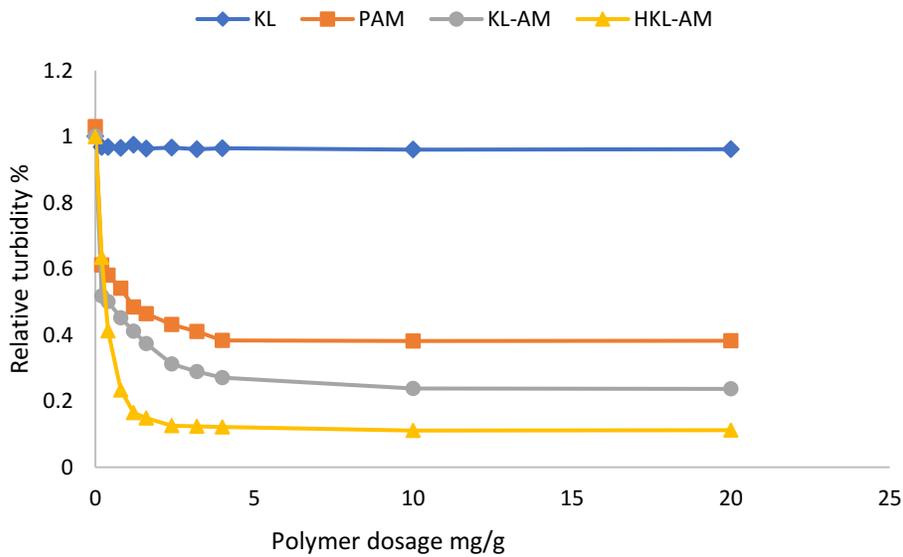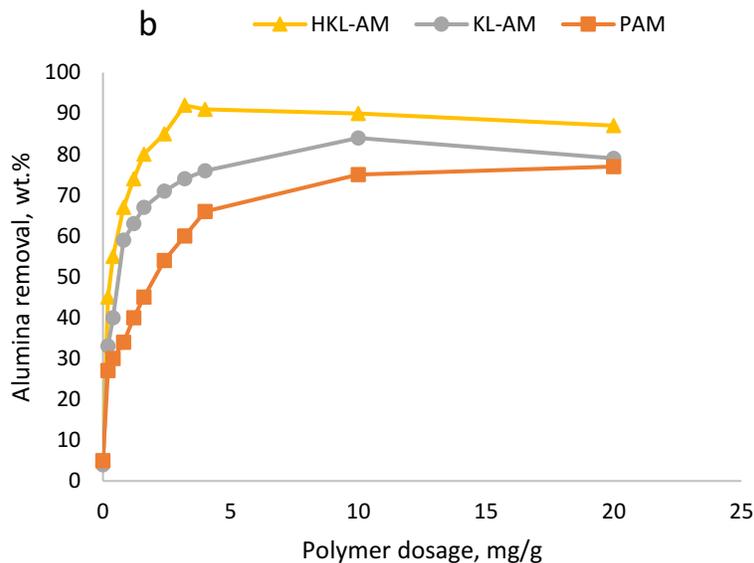
Figure 3.10. a) Influence of polymer dosage on the relative turbidity of alumina suspension, b) alumina removal as a function of polymer dosage. The experiments were conducted under the conditions of 25 °C for 2h at pH 6.

3.14. Correlation between zeta potential and relative turbidity

The relative turbidity of alumina suspensions as a function of zeta potential is plotted in Figure 3.11. This relationship is used to determine the dominant flocculation mechanism in the suspension. As shown, the relative turbidity of alumina suspension drops with reducing its zeta potential. However, the minimum relative turbidity was not achieved at zero potential value. The minimum relative turbidity of alumina suspension occurred at reversed values of -22mV, and -28 mV for KL-AM, and HKL-AM polymers, respectively, indicating that patching or bridging mechanisms were the main reasons for the reduction in the relative suspension turbidity. HKL-AM polymer with the highest charge density (- 3.6 meq/g) achieved the lowest relative turbidity, which is attributed to the polymer's higher adsorption. PAM with a low (-0.6 meq/g) charge

density had the least effect on the suspension relative turbidity and zeta potential as a result of limited adsorption as previously illustrated in Figure 3.8. It can be seen in Figure 3.11 that PAM slightly reduces the relative turbidity of the suspension by neutralizing some of the positive sites on alumina surface as the zeta potential of the system drops from 30.43 to 15.23 mV but doesn't reach 0 mV. This implies that higher adsorption, such as in the case of HKL-AM, and KL-AM leads to bridging effect between particles, which results in a higher reduction in the suspension relative turbidity.
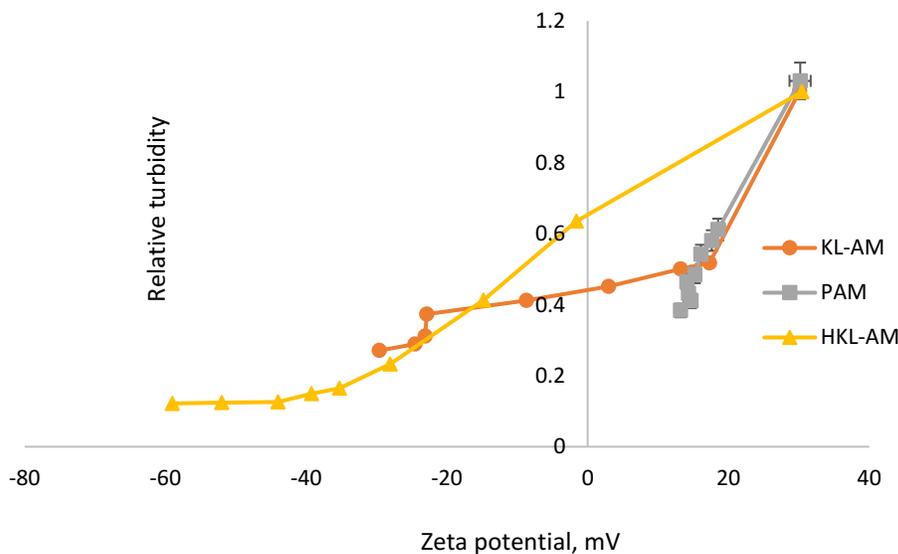
Figure 3.11. Relationship between zeta potential and relative turbidity of alumina suspensions for KL-AM, PAM, HKL-AM polymers.

3.15. Correlation between relative turbidity and the amount of adsorbed polymer

The relationship between the amount of adsorbed polymer and the relative turbidity of alumina suspension is shown in Figure 3.12. It can be seen that a significant drop in the relative turbidity of alumina suspension was obtained in the adsorption amount from 0.1 mg/g to 5.0 mg/g. The points (S) on each curve represents the relative turbidity of alumina suspension at the maximum

adsorption amount. The relative turbidity did not change after the maximum adsorption indicating that unadsorbed polymers in the suspension did not play a role in reducing the relative turbidity of the suspension (Hasan and Fatehi, 2018). As shown in Figure 3.10, the lowest relative turbidity (0.16) was obtained by HKL-AM polymer, which has higher adsorption compared to KL-AM, and PAM. These results indicate that higher adsorption of polymer results in a higher reduction in the relative turbidity of the suspension.
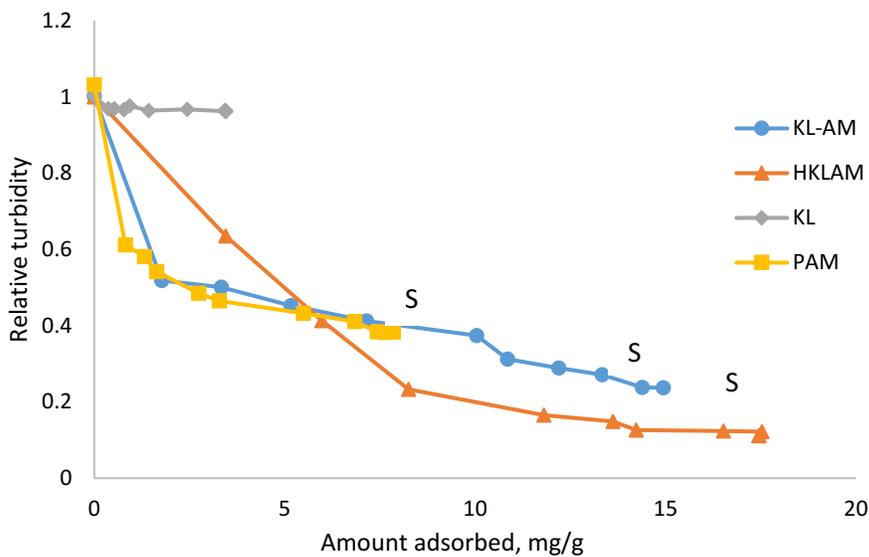
Figure 3.12. Relationship between the relative turbidity of alumina suspension and the amount of adsorbed polymer.

3.16. Floc characterization

Figure 3.13a shows the chord length distribution of the formed flocs using HKL-AM, KL-AM, and PAM polymers at two polymer dosages of 10 and 20 mg/g, as shown in Figure 3.10. In the case of HKL-AM and KL-AM polymer, a significant increase in alumina particles' chord length from 23 to 130 and 98 μm, respectively, were observed. This increase in the chord length was also

associated with a significant drop in alumina's particle counts. This increase in the particles chord length indicates that particles agglomerate in the suspension to a great extent. The larger chord length was measured via adding HKL-AM polymer to the suspension. This implies that HKL-AM generated the larger flocs compared to other polymers. It can be claimed that the higher adsorption of HKL-AM facilitated bridging due to its negative charge, which caused larger and more compact aggregates to form as illustrated in the correlation between the suspension relative turbidity and zeta potential. On the other hand, it can be seen that KL didn't impact alumina particles' chord length and had an insignificant impact on particle counts due to its limited adsorption on alumina surface. In the case of homopolymer (PAM), a 49 μm chord length was obtained. The PAM with a negative charge density of -0.6 meq/g had limited adsorption on alumina surface. Some of the charge neutralization that was caused by PAM led to a limited aggregation between alumina particles, and the formed aggregates were fragile flocs, not closely bond together, which explains the slight drop in particle counts and the moderate increase in particles' chord length (Liimatainen et al., 2009; Nasser and james, 2007).

Figure 3.13.b shows the chord length distribution of alumina particles after increasing the polymer dosage above the optimal. The chord length decreases in alumina samples, when KL-AM and HKL-AM polymers were used. This implies a reduction in the flocculation efficiency caused by the electrostatic repulsion, as a result of the accumulated negative charge on the surface of alumina particles.
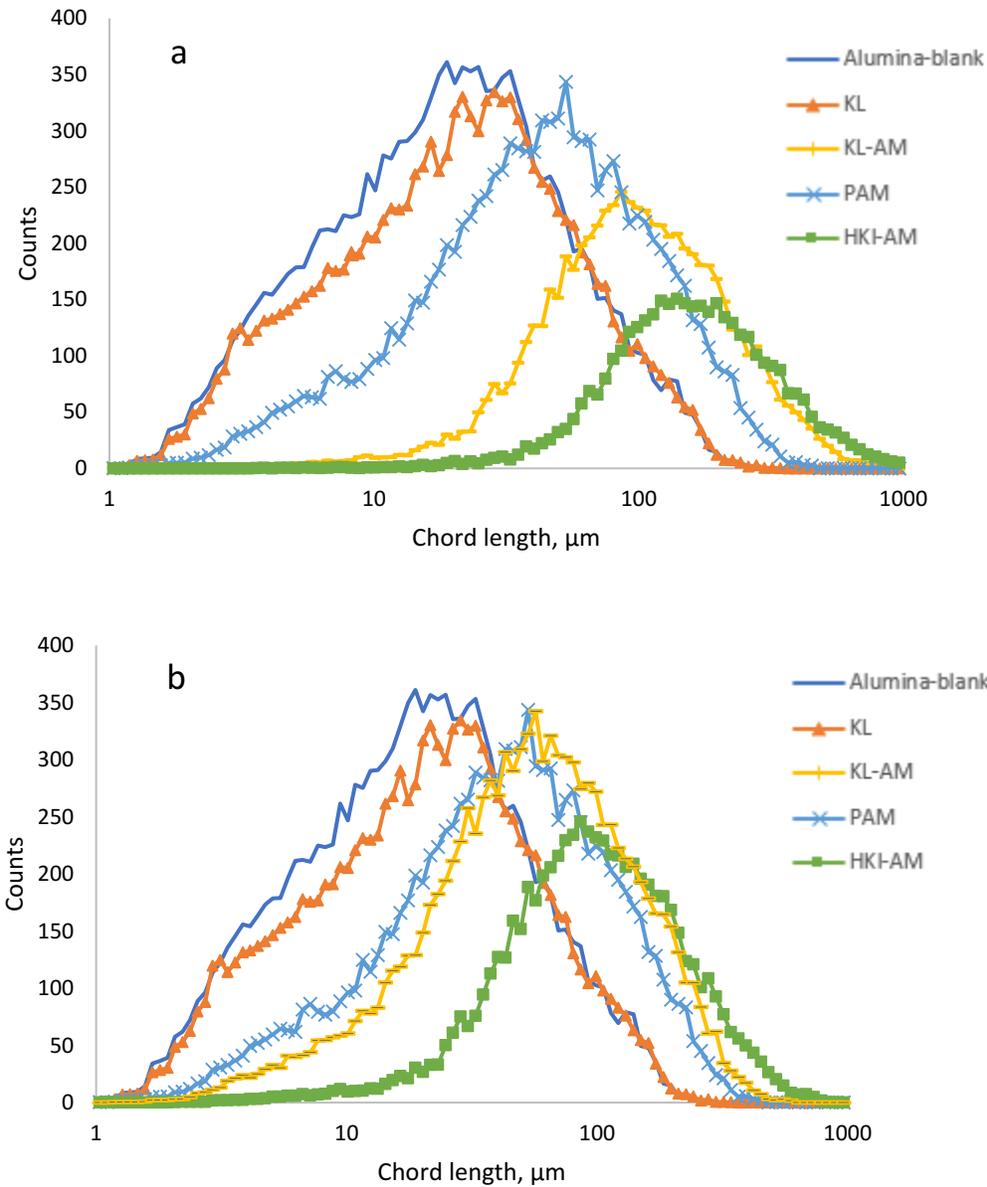
Figure 3.13. Chord length distribution of aluminum oxide flocs formed under a) polymer dosage of a)10 mg/g, and b) 20 mg/g.

3.17. Flocs strength and recoverability

The kinetics of the chord length of alumina particles (μm) were shown in Figure 3.14. The results show that the chord length of alumina particles increased significantly in the presence of HKL-AM and KL-AM polymers at 250 rpm. This increase in the median chord length indicates the

dynamic balance between floc strength and effective shear rate (Blanco et al., 2002). In previous studies, it was stated that flocculants with high charge density have a high particle to polymer bonding strength, which results in the formation of larger and stronger flocs based on the affinity of the polymer layer to elongate and withstand shear forces (Liimatainen et al., 2009). As was found in the adsorption analysis, polymers' charge density was a significant factor in adsorption regardless of polymers' molecular weight. KL-AM polymer with a charge density of 2.3 meq/g increased the median chord length of alumina particles to 100 μm (Figure 3.14). However, the most significant impact on the floc size was obtained by HKL-AM, where the median chord length increased to 132 μm. This higher increase indicates that higher adsorption of HKL-AM resulted in more and larger but compact aggregates. Floc size and strength has shown to be the most important parameters to monitor flocculation efficiency, as it has been concluded in many studies that larger and stronger flocs will promotee flocculation as a result of flocs increased resistance to deformation under shear forces (Wu et al., 2003; Nasser and James 2006). When the shear force was enhanced to 750 rpm, there was a rapid reduction in particles' chord length as a result of floc breakage. When the shear force was restored to 250 rpm, floc regrowth occurred only to a limited extent.

Adjusting the evolution of particles chord length in the deflocculation and re-flocculation curves to exponential equations (3.9), and (3.10) allow us to determine T_{df}, and T_{rf} values to analyze the flocs resistance to shear forces and regrowth. There is a dynamic equilibrium between the formation and breakage of flocs. T_{df} value represents the difference between the rate of flocs formation and breakage; simultaneously, thus when the reformation of flocs is negligible, a higher T_{df} value means higher flocs strength (Alfano et al., l999). Similarly, T_{rf} parameter indicates the difference between flocs' reformation and breakage when the shear forces decrease. However,

when flocs breakage is negligible at the existing shear force, T_{rf} value is used to measure flocs re-flocculation tendency. Therefore, flocs reversibility can be determined using T_{rf} value or by comparing the median chord size of particles before deflocculation and after re-flocculation (Alfano et al., l999; Blanco et al., 200).
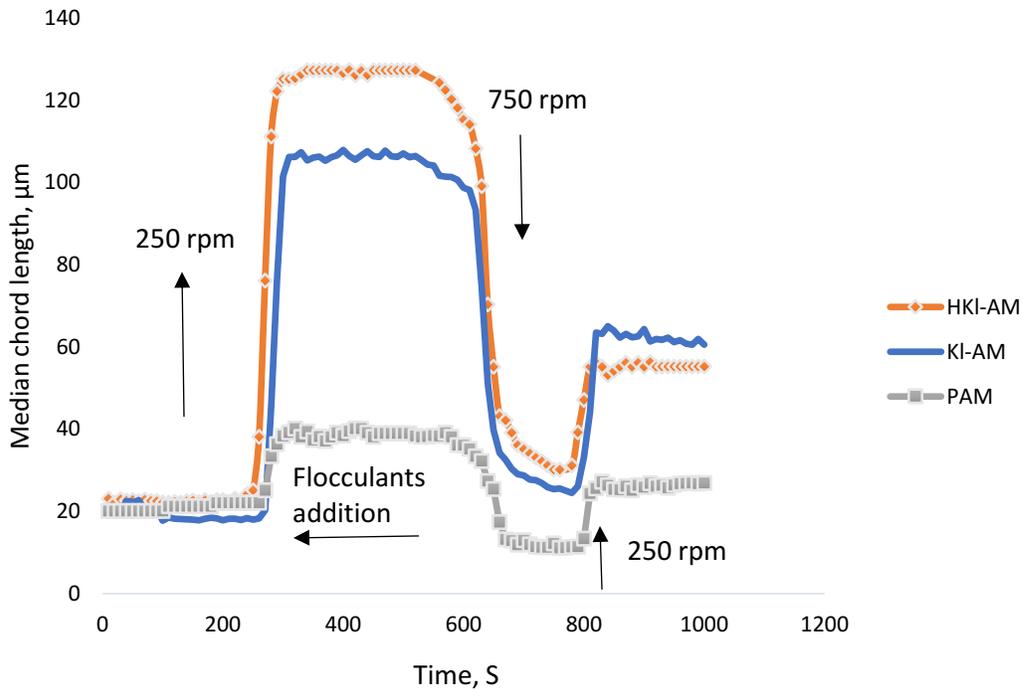
Figure 3.14. Evolution of flocculation process for different flocculants in alumina suspension.

As indicated in Figure 3.15 a, the flocs formed by HKL-AM has a higher T_{df} value at 750 rpm, indicating stronger and more resistant flocs to shear forces compared to flocs formed by KL-AM and PAM. The re-flocculation tendency or T_{rf} value also follows a similar trend. The lower the T_{rf} value, the faster the re-flocculation process. As shown in Figure 3.15 b, HKL-AM polymer generated flocs with higher re-flocculation tendency than KL-AM and PAM. Rasteiro et al. (2008) reported that cation polyacrylamide polymers with a higher charge and molecular weight produced

stronger flocs in calcium carbonate suspensions with higher re-flocculation tendency. Polymers with a higher charge density and molecular weight tend to form stronger flocs with higher re-flocculation tendency (Lee et al., 2014).
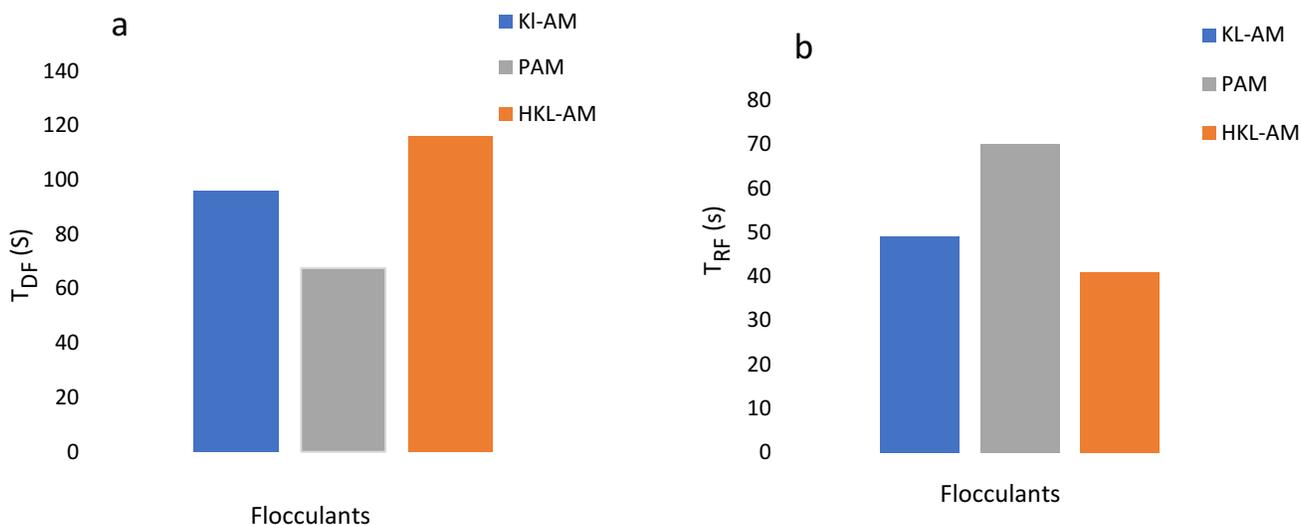
Figure 3.15. a) Flocs formation tendency (T_{df}), and b) flocs re-flocculation tendency (T_{rf}) values for KL-AM, PAM, and HKL-AM polymers.

3.18. Conclusions

In this chapter, the effect of different reaction parameters, such as pH, time, temperature, AM /KL molar ratio on the properties of KL-AM polymer were investigated. KL-AM polymer was hydrolyzed under different conditions to increase the charge density of the polymer. The hydrolysis reaction increased the polymer's carboxyl groups to 3.26 mmol/g and its charge density to -3.62 meq/g. The characteristics of modified lignin samples were investigated using TGA, elemental analysis, Fourier transform infrared spectroscopy (FTIR), proton nuclear magnetic resonance (^{1}H-NMR) which all confirmed the grafting of acrylamide monomer onto kraft lignin

backbone. Modified lignin polymers (KL-AM and HKL-AM) showed higher thermal stability and thermal resistance in the temperature range of 200 and 500 °C where the majority of unmodified kraft lignin and acrylamide homopolymer (PAM) was degraded. The adsorption of modified lignin samples on alumina particles was examined. Polymers' molecular weight was not a significant factor in achieving high adsorption. The adsorption of polymers was mainly influenced by their charge density. HKL-AM polymer with the highest charge density showed higher adsorption (17 mg/g) compared to PAM polymer with a similar molecular weight. In addition, the changes in the suspension's relative turbidity and zeta potential were more pronounced in the case of HKL-AM polymer. The minimum relative turbidity of alumina suspension (0.12) was achieved by using HKL-AM. The effect of shear stress on flocs formation, breakage, and re-flocculation was examined. In the case of polymers with a high charge density and adsorption affinity (HKL-AM), larger flocs (130, and 106 μm), and higher re-flocculation tendency (T_{rf}) were obtained indicating higher flocculation efficiency of this polymer.

References

Abidinet, A. Z., Puspasari, T., & Nugroho, W. A. (2012). Polymers for enhanced oil recovery technology. *Procedia Chemistry*, *4*, 11-16.

Alfano, J. C., Carter, P. W., & Gerli, A. (1998). Characterization of the flocculation dynamics in a paperma king system by non-imaging reflectance scanning laser rnicroscopy (SLM). *Nordic Pulp & Paper Research Journal*, 13(2), 159-165.

Alfano, J. C., Carter, P. W., & Whitten, J. E. (1999). Use of scanning laser microscopy to investigate microparticle flocculation performance. *Journal of pulp and paper science*, 25(6), 189-195.

Alkhalifa, Z. 2017. Copolymerization of pretreated kraft lignin and acrylic acid to produce flocculants for suspension and solution systems. Lakehead university. Mater thesis.

Baklouti, S., Romdhane, M. R. B., Boufi, S., Pagnoux, C., Chartier, T., & Baumard, J. F. (2003). Effect of copolymer dispersant structure on the properties of alumina suspensions. *Journal of the European Ceramic Society*, 23(6), 905-911.

Blanco, A., Fuente, E., Negro, C., & Tijero, J. (2002). Flocculation monitoring: focused beam reflectance measurement as a measurement tool. *Canadian journal of chemical engineering*, 80(4), 734-740.

Bratby, J. (2016). Coagulation and Flocculation in Water and Wastewater Treatment. *Water Intelligence Online*, 15(0), 341.

Brebu, M., & Vasile, C. (2010). Thermal degradation of lignin—a review. *Cellulose Chemistry & Technology*, 44(9), 353.

Brostow, W., Lobland, H. H., Pal, S., & Singh, R. P. (2009). Polymeric flocculants for wastewater and industrial effluent treatment. *Journal of Materials Education*, 31(3-4), 157-166.

Buback, M. (1990). Free-radical polymerization up to high conversion. A general kinetic treatment. *Die Makromolekulare Chemie: Macromolecular Chemistry and Physics*, *191*(7), 1575-1587.

Caskey, J. A., & Primus, R. J. (1986). The effect of anionic polyacrylamide molecular conformation and configuration on flocculation effectiveness. *Environmental progress*, 5(2), 98-103.

Cervantes-Uc, J. M., Cauich-Rodríguez, J. V., Vázquez-Torres, H., & Licea-Claveríe, A. (2006). TGA/FTIR study on thermal degradation of polymethacrylates containing carboxylic groups. *Polymer degradation and stability*, 91(12), 3312-3321.

Chen, H. T., Ravishankar, S. A., & Farinato, R. S. (2003). Rational polymer design for solid–liquid separations in mineral processing applications. *International Journal of Mineral Processing*, *72*(1-4), 75-86.

Chibowski, S., Wiśniewska, M., & Urban, T. (2014). Effect of the presence of cationic polyacrylamide on the surface properties of aqueous alumina suspension-stability mechanism. *Applied Surface Science*, 320, 843-851.

Das, R., Ghorai, S., & Pal, S. (2013). Flocculation characteristics of polyacrylamide grafted hydroxypropyl methyl cellulose: An efficient biodegradable flocculant. *Chemical engineering journal*, 229, 144-152.

El-Zawawy, W. K., & Ibrahim, M. M. (2012). Preparation and characterization of novel polymer hydrogel from industrial waste and copolymerization of poly (vinyl alcohol) and polyacrylamide. *Journal of Applied Polymer Science*, 124(5), 4362-4370.

Fang, R., Cheng, X. S., Fu, J., & Zheng, Z. B. (2009). Research on the graft copolymerization of EH-lignin with acrylamide. *BioResources*, 1(1), 17-22.

Farrokhpay, S. (2009). A review of polymeric dispersant stabilisation of titania pigment. *Advances in Colloid and Interface Science*, *151*(1-2), 24-32.

Fox, C., McDonald, A.G. (2010). Chemical and thermal characterization of three industrial lignins and their corresponding lignin ester. *Bioresource*, 5(2), 990-1009.

Gellerstedt, G. (2015). Softwood kraft lignin: Raw material for the future. *Industrial Crops and Products*, *77*, 845-854.

Gordobil, O., Herrera, R., Llano-Ponte, R., & Labidi, J. (2017). Esterified organosolv lignin as hydrophobic agent for use on wood products. *Progress in Organic Coatings*, 103, 143-151.

Güngör, N., & Karaoğlan, S. (2001). Interactions of polyacrylamide polymer with bentonite in aqueous systems. *Materials Letters*, *48*(3-4), 168-175.

Hasan, A., & Fatehi, P. (2018). Cationic kraft lignin-acrylamide copolymer as a flocculant for clay suspensions:(2) Charge density effect. *Separation and Purification Technology*, 210, 963-972.

Hatakeyama, H., & Hatakeyama, T. (2009). Lignin structure, properties, and applications. *Biopolymers* 31(5), 42-63.

Hatakeyama, T., Nakamura, K., & Hatakeyama, H. (1982). Studies on heat capacity of cellulose and lignin by differential scanning calorimetry. *Polymer*, *23*(12), 1801-1804.

Heitner, C., Dimmel, D., & Schmidt, J. (2016). Lignin and lignans. *Advances in Chemistry,* 67, 324-369.

Hogg, R. (2013). Bridging flocculation by polymers. *KONA Powder and Particle Journal*, *30*, 3-14.

Hu, L., Pan, H., Zhou, Y., & Zhang, M. (2011). Methods to improve lignin's reactivity as a phenol substitute and as replacement for other phenolic compounds: A brief review. *BioResources*, 6(3), 3515-3525.

Huang, J., Xu, J., Wang, D., Li, L., & Guo, X. (2013). Effects of amphiphilic copolymer dispersants on rheology and stability of coal water slurry. *Industrial & Engineering Chemistry Research*, 52(25), 8427-8435.

Inwood, J. (2014). Sulfonation of kraft lignin to water-soluble value-added products. Lakehead university. Masters thesis.

Inwood, J. P., Pakzad, L., & Fatehi, P. (2018). Production of sulfur containing kraft lignin products. *BioResources*, *13*(1), 53-70.

Kazzaz, A. E., Feizi, Z. H., Kong, F., & Fatehi, P. (2018). Interaction of poly (acrylic acid) and aluminum oxide particles in suspension: Particle size effect. *Colloids and Surfaces A: Physicochemical and Engineering Aspects*, *556*, 218-226.

Kheradmand, H., François, J., & Plazanet, V. (1988). Hydrolysis of polyacrylamide and acrylic acid-acrylamide copolymers at neutral pH and high temperature. *Polymer*, 29(5), 860-870.

Konduri, M. K., & Fatehi, P. (2015). Production of water-soluble hardwood Kraft Lignin via Sulfomethylation using formaldehyde and sodium sulfite. *ACS Sustainable Chemistry & Engineering*, 3(6), 1172-1182.

Kong, F., Wang, S., Price, J. T., Konduri, M. K., & Fatehi, P. (2015). Water soluble kraft lignin–acrylic acid copolymer: Synthesis and characterization. *Green Chemistry*, 17(8), 4355-4366.

Kong, F., Wang, S., Price, J. T., Konduri, M. K., & Fatehi, P. (2015). Water soluble kraft lignin–acrylic acid copolymer: Synthesis and characterization. *Green Chemistry*, 17(8), 4355-4366.

Kurenkov, V. F., Hartan, H. G., & Lobanov, F. I. (2001). Alkaline hydrolysis of polyacrylamide. *Russian Journal of Applied Chemistry*, 74(4), 543-554.

Laurichesse, S., & Avérous, L. (2014). Chemical modification of lignins: Towards biobased polymers. *Progress in polymer science*, *39*(7), 1266-1290.

Lee, C. S., Robinson, J., & Chong, M. F. (2014). A review on application of flocculants in wastewater treatment. *Process Safety and Environmental Protection*, *92*(6), 489-508.

Lee, K. E., Morad, N., Teng, T. T., & Poh, B. T. (2012). Development, characterization and the application of hybrid materials in coagulation/flocculation of wastewater: A review. *Chemical Engineering Journal*, 203, 370-386.

Li, H., Long, J., Xu, Z., & Masliyah, J. H. (2008). Effect of molecular weight and charge density on the performance of polyacrylamide in low-grade oil sand ore processing. *The Canadian Journal of Chemical Engineering*, *86*(2), 177-185.

Liimatainen, H., Haapala, A., Tomperi, J., & Niinimäki, J. (2009). Fibre floc morphology and dewaterability of a pulp suspension: role of flocculation kinetics and characteristics of flocculation agents. BioResources, 4(2), 640-658.

Lin, H. R. (2001). Solution polymerization of acrylamide using potassium persulfate as an initiator: kinetic studies, temperature and pH dependence. *European polymer journal*, *37*(7), 1507-1510.

Lindstrom, T. (1989). Some fundamental chemical aspects on paper forming. *Fundamental Research Symposium*, 5(2), 309-412.

Liu, Z., Xu, D., Xu, L., Kong, F., Wang, S., & Yang, G. (2018). Preparation and Characterization of Softwood Kraft Lignin Copolymers as a Paper Strength Additive. *Polymers*, 10(7), 743.

López-Maldonado, E. A., Oropeza-Guzman, M. T., Jurado-Baizaval, J. L., & Ochoa-Terán, A. (2014). Coagulation–flocculation mechanisms in wastewater treatment plants through zeta potential measurements. *Journal of hazardous materials*, *279*, 1-10.

Lou, T., Cui, G., Xun, J., Wang, X., Feng, N., & Zhang, J. (2018). Synthesis of a terpolymer based on chitosan and lignin as an effective flocculant for dye removal. *Colloids and Surfaces A: Physicochemical and Engineering Aspects*, 537, 149-154.

Ma, X. (2011). Effect of a low-molecular-weight polyacrylic acid on the coagulation of kaolinite particles. *International Journal of Mineral Processing*, 99(1-4), 17-20.

Mai, C., Milstein, O., & Hüttermann, A. (2000). Chemoenzymatical grafting of acrylamide onto lignin. *Journal of Biotechnology*, *79*(2), 173-183.

Matsushita, Y. (2015). Conversion of technical lignins to functional materials with retained polymeric properties. *Journal of Wood Science*, *61*(3), 230.

Mishra, S., Mukul, A., Sen, G., & Jha, U. (2011). Microwave assisted synthesis of polyacrylamide grafted starch (St-g-PAM) and its applicability as flocculant for water treatment. *International Journal of Biological Macromolecules*, *48*(1), 106-111.

Moens, J., & Smets, G. (1957). Alkaline and acid hydrolysis of polyvinylamides. *Journal of polymer science*, *23*(104), 931-948.

Nagase, K., & Sakaguchi, K. (1965). Alkaline hydrolysis of polyacrylamide. *Journal of Polymer Science Part A: General Papers*, *3*(7), 2475-2482.

Nakabayashi, K., & Mori, H. (2013). Recent progress in controlled radical polymerization of N-vinyl monomers. *European Polymer Journal*, *49*(10), 2808-2838.

Nasser, M. S., & James, A. E. (2006). The effect of polyacrylamide charge density and molecular weight on the flocculation and sedimentation behaviour of kaolinite suspensions. *Separation and purification technology*, 52(2), 241-252.

Nasser, M. S., & James, A. E. (2007). Effect of polyacrylamide polymers on floc size and rheological behaviour of kaolinite suspensions. *Colloids and Surfaces A: Physicochemical and Engineering Aspects*, 301(1-3), 311-322.

Ouyang, X., Zaixiong, L. I. N., Yonghong, D. E. N. G., Dongjie, Y. A. N. G., & Xueqing, Q. I. U. (2010). Oxidative degradation of soda lignin assisted by microwave irradiation. *Chinese Journal of Chemical Engineering*, *18*(4), 695-702.

Passoni, V., Scarica, C., Levi, M., Turri, S., Griffini, G. 2016. Fractionation of industrial softwood kraft lignin: Solvent selection as a tool for tailored material properties. *ACS Sustainable Chemistry and Engineering*, 4(4), 2232-2242

Patnaik, S. K., Murthy, P. V. R., & Vidyasagar, P. (2000). Importance of synthetic flocculants in alumina industry.*Separation and purification technology,* 32(1), 214-654.

Price, J. T., Gao, W., & Fatehi, P. (2018). Lignin-g-poly (acrylamide)-g-poly (diallyl dimethyl-ammonium chloride)Synthesis, Characterization, and Applications. *ChemistryOpen*, 7(8), 645-658.

Rabiee, A. (2010). Acrylamide-based anionic polyelectrolytes and their applications: A survey. *Journal of Vinyl and Additive Technology*, 16(2), 111-119.

Ragnar, M., Lindgren, C. T., & Nilvebrant, N. O. (2000). pKa-values of guaiacyl and syringyl phenols related to lignin. *Journal of wood chemistry and technology*, *20*(3), 277-305.

Renault, F., Sancey, B., Charles, J., Morin-Crini, N., Badot, P. M., Winterton, P., & Crini, G. (2009). Chitosan flocculation of cardboard-mill secondary biological wastewater. *Chemical Engineering Journal*, 155(3), 775-783.

Rong, H., Gao, B., Zhao, Y., Sun, S., Yang, Z., Wang, Y., ... & Li, Q. (2013). Advanced lignin-acrylamide water treatment agent by pulp and paper industrial sludge: Synthesis, properties, and application. *Journal of Environmental Sciences*, 25(12), 2367-2377.

Runge, T. M., & Ragauskas, A. J. (1999). NMR analysis of oxidative alkaline extraction stage lignins. *Holzforschung*, 53(6), 623-631.

Sang, Y., & Xiao, H. (2008). Clay flocculation improved by cationic poly (vinyl alcohol)/anionic polymer dual-component system. *Journal of colloid and interface science*, 326(2), 420-425.

Sharma, B. R., Dhuldhoya, N. C., & Merchant, U. C. (2006). Flocculants—an ecofriendly approach. *Journal of Polymers and the Environment*, 14(2), 195-202.

Singh, R. P., Nayak, B. R., Biswal, D. R., Tripathy, T., & Banik, K. (2003). Biobased polymeric flocculants for industrial effluent treatment. *Materials Research Innovations*, 7(5), 331-340.

Singh, V., Tiwari, A., Pandey, S., & Singh, S. K. (2006). Microwave-accelerated Synthesis and Characterization of Potato Starch-g-poly (acrylamide). *Starch-Stärke*, *58*(10), 536-543.

Smets, G., & Hesbain, A. M. (1959). Hydrolysis of polyacrylamide and acrylic acid–acrylamide copolymers. *Journal of Polymer Science*, 40(136), 217-226.

Swerin, A., & Ödberg, L. (1993). Flocculation and floc strength in suspensions A flocculated by retention aids. *Nordic Pulp & Paper Research Journal*, 8(1), 141-147.

Tejado, A., Pena, C., Labidi, J., Echeverria, J. M., & Mondragon, I. (2007). Physico-chemical characterization of lignins from different sources for use in phenol–formaldehyde resin synthesis. *Bioresource Technology*, 98(8), 1655-1663.

Van Dyke, J. D., & Kasperski, K. L. (1993). Thermogravimetric study of polyacrylamide with evolved gas analysis. *Journal of Polymer Science Part A: Polymer Chemistry*, *31*(7), 1807-1823.

Wang, H. M., MIN, X. B., CHAI, L. Y., & SHU, Y. D. (2011). Biological preparation and application of poly-ferric sulfate flocculant. *Transactions of Nonferrous Metals Society of China*, 21(11), 2542-2547.

Wang, J. P., Chen, Y. Z., Yuan, S. J., Sheng, G. P., & Yu, H. Q. (2009). Synthesis and characterization of a novel cationic chitosan-based flocculant with a high water-solubility for pulp mill wastewater treatment. Water research, 43(20), 5267-5275.

Wang, S., Sun, Y., Kong, F., Yang, G., & Fatehi, P. (2016). Preparation and characterization of lignin-acrylamide copolymer as a paper strength additive. *BioResources*, 11(1), 1765-1783.

Wiśniewska, M., Chibowski, S., & Urban, T. (2012). Impact of anionic and cationic polyacrylamide on the stability of aqueous alumina suspension—comparison of adsorption mechanism. *Colloid and Polymer Science*, 293(4), 1171-1179.

Wu, C. C., Wu, J. J., & Huang, R. Y. (2003). Effect of floc strength on sludge dewatering by vacuum filtration. *Colloids and Surfaces A: Physicochemical and Engineering Aspects*, 221(1-3), 141-147.

Yang, M. H. (1998). The two-stages thermal degradation of polyacrylamide. *Polymer testing*, 17(3), 191-198.

Yang, Q., & Wu, S. (2009). Thermogravimetric characteristics of wheat straw lignin. *Cellulose Chemistry & Technology*, *43*(4), 133.

Yang, Y., Li, Y., Zhang, Y. M., & Liang, D. W. (2010). Applying hybrid coagulants and polyacrylamide flocculants in the treatment of high-phosphorus hematite flotation wastewater (HHFW): Optimization through response surface methodology. *Separation and Purification Technology*, 76(1), 72-78.

Yang, Z., Yang, H., Jiang, Z., Cai, T., Li, H., Li, H., ... & Cheng, R. (2013). Flocculation of both anionic and cationic dyes in aqueous solutions by the amphoteric grafting flocculant carboxymethyl chitosan-graft-polyacrylamide. *Journal of hazardous materials*, *254*, 36-45.

Yu, X., & Somasundaran, P. (1996). Role of polymer conformation in interparticle-bridging dominated flocculation. *Journal of Colloid and Interface Science*, *177*(2), 283-287.

Zeynali, M. E., & RABIEI, A. (2002). Alkaline hydrolysis of polyacrylamide and study on poly (acrylamide-co-sodium acrylate) properties.

Zhang, J., Feng, L., Wang, D., Zhang, R., Liu, G., & Cheng, G. (2014). Thermogravimetric analysis of lignocellulosic biomass with ionic liquid pretreatment. *Bioresource technology*, *153*, 379-382.

Zhong, J., Sun, X., & Wang, C. (2003). Treatment of oily wastewater produced from refinery processes using flocculation and ceramic membrane filtration. *Separation and Purification Technology*, 32(1-3), 93-98.

Zoia, L., Salanti, A., Frigerio, P., & Orlandi, M. (2014). Exploring allylation and Claisen rearrangement as a novel chemical modification of lignin. *BioResources*, *9*(4), 6540-6561.

Chapter 4

4.1. Abstract

Kraft lignin is an underutilized material that is mainly combusted in the pulping industry for the production of heat. However, kraft lignin can be extracted from the pulping process and converted to value-added products, but its insolubility in water limits its end-use applications. In this work, the modification of kraft lignin (KL) through oxidation and carboxymethylation for the production of anionic water-soluble products was investigated. These modification methods generated water-soluble polymers (OKL, and CMKL) with a charge density of – 1.6, and -1.9 meq/g, respectively. These products functioned as dispersants in an alumina suspension where the relative turbidity of the suspension was altered from 1 to 1.46, and 1.23 via adding 10 mg/g of the polymers. These modified lignin samples were subsequently polymerized with acrylamide (AM) monomer for the production of anionic lignin-based polymers to be used as flocculants in the alumina suspension. The properties of polymers were characterized using, GPC, elemental analysis, TGA, DSC, and NMR. The polymerization of OKL and CMKL polymers with acrylamide increased the molecular weight of polymers to 684 and 387 kg/mol with a grafting ratio of 155%, and 99% respectively. OKL-AM and CMKL-AM polymers were applied as flocculants in alumina suspension. The chord length of particles increased the most in suspension by the adsorption of OKL-AM polymer with the highest molecular weight. The flocs strength analysis via FBRM revealed that the flocculation process was reversible for both OKL-AM and CMKL-AM polymers. Flocculation analysis demonstrated that the molecular weight of polymers could influence the turbidity of the suspension dramatically where the minimum relative turbidity occurred at high negative zeta potential values.

4.2. Introduction

After cellulose, lignin is the most abundant biopolymer on earth. It is a complex and three-dimensional polymer that is mainly linked by ether bonds (Bentivenga et al., 2003). Currently, lignin is either incinerated to generate heat, or treated in wastewater systems, which introduces extra costs and challenges to pulping processes (Zhou, 2014). Kraft lignin, a by-product of the kraft pulping process, is a water-insoluble product, and for this, it has limited practical applications in industry (Zhou, 2014). However, kraft lignin contains a variety of functional groups, including aliphatic, phenolic hydroxyl, carbonyl, carboxyl, and methoxy groups that can facilitate the modification of lignin to alter its chemical and physical properties to characteristics that promote its broader application in industry, especially as flocculants for wastewater treatment. There have been different methods reported in the literature to increase the reactivity of lignin and to produce soluble products, such as phenolation, sulfation, sulfomethylation, and hydroxymethylation (Shin and Rowell, 2005; Hu et al., 2011). However, due to the rigorous conditions of these reactions including a high temperature, and the use of expensive catalysts and organic solvents, the large scale production of modified lignin following these reactions was not economically feasible (Hu et al., 2011). Oxidation and carboxymethylation are popular procedures for improving the properties of lignin under mild conditions (Konduri et al., 2015; He et al., 2017). The oxidation of lignin was reported to reduce the steric hindrance of lignin's structure and produce products with a lower molecular weight and higher reactivity (He and Fatehi, 2015). It was also reported that oxidation forms reactive catechol groups on lignin (Nagieb and Egypt, 1985; Olivares et al., 1988). Various oxidation pathways, including oxygen with catalysts, nitrobenzene, and metal oxides, were performed on lignin to improve its properties (Sun et al., 1995; Mahmood et al. 2016). However, with these procedures, undesirable by-products were formed during the oxidation

reactions. A report on the oxidation of nonwood lignin showed that hydrogen peroxide (H_2O_2) oxidation increased the carboxylate groups of lignin and thus its water solubility (Araujo et al., 2002; Dalimova, 2005). In this work, the modification of kraft lignin via carboxymethylation was also examined (Da et al., 2011). In a similar study, sugarcane bagasse-based lignin was carboxymethylated with monochloroacetic acid. The anionic water-soluble products were applied successfully as stabilizing agents in aqueous ceramic suspensions, and as an adsorbent for the removal of dyes (Da et al ., 2011; Cerrutti et al., 2012).

Although oxidation and carboxymethylation of lignin produce reactive and water-soluble products, they do not significantly increase products' molecular weight, which is an important parameter in the production of efficient flocculants (Lee and Schlautman, 2015). Polyacrylamide is a highly used polymer in industry, as it is very cost-effective compared to other water-soluble monomers. It is applied in many applications, especially in wastewater treatment, due to its efficiency and rapid dissolution (Singh et al., 2006). However, the long exposure to polyacrylamide at high dosages was found carcinogenic in animals (Xiong et al., 2018). Since there is no legal limitation yet on the use of polyacrylamide in industry, the harmful effect of polyacrylamide on the environment can be minimized by reducing the used dosages of polyacrylamide (Xiong et al., 2018). This study involves the pre-treatment of lignin via oxidation and carboxymethylation to increase lignin charge density, and subsequently polymerize it with acrylamide to produce novel anionic polymers. This work focuses on the polymerization of acrylamide monomer with a readily available natural polymer (lignin) to produce efficient flocculants for wastewater treatment. This work also involves the characterization of these products by TGA, DSC, NMR, and the assessment of their performance as flocculants in synthetic alumina suspension.

4.3. Materials and methods

4.3.1. Materials

In this work, softwood kraft lignin (KL) was supplied by FPInnovations from its pilot plant facilities located in Thunder Bay, ON, and it was produced by LigniForce[TM] technology (Kouisni et al. 2012). Sodium hydroxide (98%) and sulfuric acid (98%) were purchased from Sigma Aldrich, and they were diluted to 1 M concentration before use. Potassium hydroxide solution (8 M), para-hydroxybenzoic acid, Alumina particles (1 μm), potassium persulfate ($K_2S_2O_8$) (analytical grade), sodium hydroxide and sodium chloroacetate (SCA), acrylamide (99.0 % purity), hydrogen peroxide solution (30%), poly diallyl dimethyl ammonium chloride (PDADMAC,100,000-200,000 g/mol) were all purchased from Sigma Aldrich and were used as received. Dialysis membranes with the molecular weight cut-off of 1000 g/mol were purchased from Spectrum labs.

4.3.2. Carboxymethylation of lignin

The carboxymethylation of kraft lignin was conducted as described in the literature for the carboxymethylation of other biomass resources (Lange and Schweers; 1980 Konduri et al., 2015). First, 1 g of kraft lignin was dissolved in sodium hydroxide solution, and then sodium chloroacetate was added to the solution. The conditions for the reaction was 4 h, 40 °C, 3 mol/mol SCA/lignin ratio, 0.15 M NaOH(aq), and lignin concentration of 16.7 g/L. The reaction was carried out at a constant stirring of 150 rpm. Upon completion, the solution was cooled down to room temperature, and its pH was adjusted to 7.0 using 1M sulfuric acid solution. Then, the sample was dialyzed for 48 h using membrane dialysis to separate unreacted reagents. The water of the system was changed every 6 h. The dialyzed sample was dried overnight in an oven at 105 °C, and the obtained product was denoted as CMKL.

4.3.3. Lignin oxidation

A specific amount of KL was mixed with hydrogen peroxide and sodium hydroxide solution in a 250 mL three-neck flask at room temperature. The temperature of the reaction was controlled by using a hot plate equipped with a thermometer. The conditions followed for lignin oxidation was 80 °C, $NaOH/H_2O_2$ ratio of 0.77 mol/mol, and H_2O_2/lignin ratio of 2.8 mol/mol, and 2 h reaction (He et al., 2017). Once the reaction was completed, the solution was allowed to cool to room temperature, and the pH of the solution was adjusted to 7.0 using 1M sulfuric acid solution. Finally, the mixture was dialyzed using the membrane to purify the produced oxidized KL, and the sample was then dried in the oven overnight at temperature 105 °C. This product was denoted as OKL.

4.3.4. Polymerization of modified lignin with acrylamide (AM)

Pretreated lignin samples (OKL and CMKL) were dissolved into 50 mL of deionized water in a three-neck glass flask at 280 rpm. Then, a specific amount of acrylamide was added to the solution, and the pH of the solution was adjusted to 10. The mixture was purged with nitrogen for 15 min. Subsequently, $K_2S_2O_8$ was added to the solution as an initiator, and the reaction mixture was purged under nitrogen for half an hour. The optimal polymerization reaction conditions were AM/ KL ratio of 7 mol/mol, 80 °C, 3 h, 3 wt. % of $K_2S_2O_8$ (based on lignin mass) as discussed in the previous chapter. Upon completion, the pH of the solution was adjusted to 7.0 using 1M sulfuric acid solution. The polymerized lignin samples were then placed in dialysis membranes for 2 days for purification. The solution was dried in an oven at 150°C, and the obtained products were denoted as OKL-AM, and CMKL-AM.

4.3.5. Solubility of unmodified lignin and modified polymers analysis

The solubility of the modified samples was measured by mixing 0.2 g of each sample with 19.8 mL of deionized water. The samples were stirred at 150 rpm, and 30 °C for 2 h in a water bath shaker. Afterward, the samples were centrifuged at 1000 rpm for 10 min. The filtrates were separated from the precipitates and used to determine the solubility of the samples following equation 4.1:

$$solubility\ (wt.\%) = \frac{mass\ of\ dissolved\ lignin}{Intial\ mass\ of\ lignin} \times 100 \tag{4.1}$$

4.3.6. Charge density and elemental analysis

For charge density analysis, 0.2 g of each sample was mixed with 20 mL of deionized water, and the charge density of samples was measured using a particle charge detector (Mütek PCD 04, Germany) with a standard PDADMAC solution (0.0050 M) at pH 7 (Wang et al., 2011). The elemental composition of the samples was determined using an elemental analyzer (Elementar, Vario Micro, Germany). In this set of experiments, the samples were dried in a 105 °C oven overnight to remove any moisture. Approximately, 2 mg of the samples were used for this analysis to determine carbon, hydrogen, oxygen, and nitrogen contents of the samples based on a previously established method (Fadeeva et al., 2008; Jahan et al., 2012). Based on the measured nitrogen content (%), the grafting ratio of AM in OKL-AM and CMKL-AM polymers was determined following equation 4.2:

$$Grafting\ ratio\ mol\ \% = \frac{\frac{N}{14} \times M_w}{100 - N/14 \times M_w} \times 100 \tag{4.2}$$

Where N is the nitrogen content of the sample (wt%), and Mw is the molecular weight of AM, 71.08 g/mol.

4.3.7. Molecular weight analysis

The molecular weight of modified lignin samples was measured using a gel permeation chromatography (Malvern, GPCmax VE2001 Module + Viscotek TDA305) with UV, RI, and viscometer detectors. In this experiment, about 23 mg of the samples were dissolved in 10 mL of 5% $NaNO_3$ solution by stirring at 200 rpm for 24 h and room temperature. The samples were filtered with a nylon 0.2 μm filter (13 mm diameter), and the resulting solutions were used for the molecular weight analysis. The columns of PolyAnalytic PAA206 and PAA203 were used for analysis, and 0.1 mol/L $NaNO_3$ solution was used as eluent at a flow rate of 0.7 mL/min. The column temperature was set at 35 °C for the systems, and polyethylene oxide was used as a standard sample for calibrating the instrument.

4.3.8. Determination of phenolic hydroxyl and carboxylate groups

An automatic potentiometer (Metrohm, 728 Titrado, Switzerland) was used to measure the content of phenolic hydroxyl and carboxylate groups of lignin-based samples. In a 200 mL beaker, 0.06 g of the sample was dissolved in 1 mL of potassium hydroxide (0.8 M), and 4 mL of para-hydroxybenzoic acid (0.5%) was added as an internal standard. Then, 100 mL of deionized water was added, and the mixture was titrated against HCl (0.1 M). The content of phenolic hydroxyl and carboxylate groups (mmol/g) was measured according to the method explained by Konduri et al. (2015). Based on the measured carboxylate group content (mmol/g), the degree of substitution (DS) for CMKL was determined following equation 4.3:

$$Degree\ of\ substitution\ (DS) = \frac{M \times A}{1 - 0.081 \times A} \qquad (4.3)$$

where A is the total carboxylate group content (mmol/g), 0.081 (g/mmol) is the net increase in lignin mass for each sodium carboxymethyl group attached (Peng et al., 2011), and M is the mass of the basic unit of lignin (g/mmol).

4.3.9. H-NMR

KL-AM sample was dried overnight at 105 ℃ to remove any moisture. The sample was dissolved into D_2O at 40-50 mg/mL concentration. The solution was stirred for 30 min, and the ^{1}H-NMR spectrum of the samples was recorded at room temperature using an INOVA-500 MHz instrument (Varian, USA) with a 45° pulse, and the interpulse delay time of 1.0 s.

4.3.10. Thermal analysis (DSA and TGA)

To determine the thermal stability of lignin-based polymers, around 10-20 mg of each sample was dried for 48 h at 60 ℃ to remove moisture. Then, samples were moved to a platinum crucible, and their thermogravimetric analysis was performed using a TGA, (Instrument Specialist Inc i-1000 series). The samples were heated from 100 to 700 ℃ at a constant rate of 10 ℃/minute under nitrogen (at 35 mL/ min flow rate). The thermal behavior of polymers was also investigated by differential scanning calorimeter (TA instrument, Q2000). Samples were dried overnight at 150 ℃, and then the samples were placed in Tzero aluminum pan. The DCS analysis was performed between 50 and 250 ℃ at a rate of 5 ℃/min and under a nitrogen flow of 50 mL/min.

4.3.11. Alumina removal and Turbidity analysis

The removal of alumina from its suspension was investigated as a function of polymer dosage by mixing different dosages (0.2-20 mg/g) of polymers with 50 mL of alumina suspension (1 g/L) at pH 6, and 30 ℃ for 2 h. After mixing, the suspensions were allowed to settle for an hour. Then, 10 mL of each sample was collected before and after settlement and oven-dried at 105 ℃. The alumina particle's concentrations were

tested to investigate the removal of alumina by developing a mass balance. All reported values are the mean of three experiments.

Turbidity analysis of alumina suspension was carried out at pH 6 using a photometer dispersion analyzer (PDA 3000, Rank Brothers Ltd), which was connected to a dynamic drainage jar (DDJ) having a 70 mm mesh screen. Then, 480 mL of distilled water was transferred to the DDJ container and circulated through a 3 mm plastic tube from DDJ to PDA at a constant flow rate of 20 mL/min. Afterward, 20 mL of 25 g/L alumina suspension was added to the DDJ resulting in a 1 g/L alumina suspension that was stirred at 300 rpm. The addition of alumina caused the decrease of the initial DC voltage of PDA from (V_0) to a new Voltage (V_i). After 100 s, the different concentrations of polymers were added into the DDJ, and the final DC voltage (V_f) was recorded. The relative turbidity of the suspension was assessed following equation 4.4 (Wang et al., 2009).

$$\text{Relative turbidity} = \frac{\ln(V_0/V_f)}{\ln(V_0/V_i)} \qquad (4.4)$$

4.3.12. Zeta potential analysis

The zeta potential analysis of alumina suspension was performed using a NanoBrook Zeta PALS (Brookhaven Instruments Corp, USA). In this analysis, the different dosages of kraft lignin and modified lignin samples were added to 50 mL of a 25 g/L alumina suspension at pH 6. After stirring at 250 rpm and room temperature for 10 minutes, 1 mL of each sample was collected and mixed with 10 mL of KCl solution (1 mM) before zeta potential measurement. The zeta potential results are the average of three independent tests.

4.3.13. Adsorption analysis

The adsorption of polymers onto alumina particles was studied as a function of polymer concentration at room temperature. In this analysis, different concentrations (2-100 mg/L) of kraft

lignin and modified lignin samples were added to 50 mL alumina suspension (1 g/L). The mixtures were incubated at 30 °C and 150 rpm for an hour. Then, the mixture was centrifuged at 1500 rpm for 10 minutes. The samples were filtered using Whatman filters #1, and the polymer concentrations remaining in the filtrate samples were measured using a UV-Vis spectrophotometer at 280 nm and 25 °C. The amount of adsorbed polymers on alumina particles was calculated according to the previously established procedure (Fengel and Wegener, 1984).

4.3.14. Flocculation analysis under dynamic conditions

The flocculation of alumina particles by anionic lignin-based polymers was studied under dynamic conditions using a focused beam reflectance measurement (FBRM, Mettler-Toledo E25). In this analysis, the chord length of particles was determined, and the data were acquired over the range of 1–1000 μm by the iC-FBRM software (version 4.4.29). In this set of experiments, the laser probe with a diameter of 25 mm was inserted into 200 mL of alumina suspension (25 g/L) stirring at 250 rpm, and the scan duration was set at 3 s. In the FBRM analysis, the optimal dosage of the polymer was added, and the analysis was conducted for 30 min after adding the polymer. The beam rotated around the axis of the probe at a scanning speed of 2 m/s, and a scanning diameter of 5 mm and median chord length of particles was evaluated as defined by iC-FBRM software (Alfano et al., l998; Alfano et al., l999).

4.4. Results and discussion

4.4.1. Properties of unmodified, and modified lignin polymers

Table 4.1 lists the properties of unmodified kraft lignin (KL) and modified lignin polymers (CMKL-OKL, OKL-AM, and CMKL-AM). The carboxylate group content of unmodified lignin (KL) and carboxymethylated lignin (CMKL) was found to be 1.37, and 1.98 mmol/g, respectively.

The degree of substitution (DS) for CMKL based on the measured carboxylate group content was found to 0.42 g/mmol. The noticeable decrease in the content of phenolic hydroxyl groups in CMKL polymer indicates that the majority of carboxymethyl groups substitution took place at the phenolic hydroxyl groups in lignin (Chien et al., 2012). The results on the molecular weight (Mw) and charge density analysis show that CMKL polymer had a slightly higher molecular weight of 28,000 g/mol and a higher charge density of -1.9 meq/g compared to those of kraft lignin. Such increases are attributed to the attachment of carboxymethyl groups and the possible condensation of lignin during carboxymethylation reactions (Chien et al., 2012).

The contents of phenolic hydroxyl and carboxyl groups in OKL were 1.87 and 1.5 mmol/g as a result of hydrogen peroxide oxidation of lignin (Gellerstedt et al., 1980). The change in these groups resulted in an increase in the polymer charge density to -1.6 meq/g. The Mw of KL decreased by oxidation to 16,000 g/mol, and this change is related to the partial decomposition of KL during oxidation via the breakage of ether bonds of kraft lignin (Wu et al. 2012).

The elemental analysis of OKL-AM polymer, as indicated in Table 4.1, shows that the amount of nitrogen in the polymer increased to 12% (from 0 % in KL), which provides evidence for the success of polymerization reaction. Following equation 4.2, the grafting ratio of AM onto OKL-AM polymer was 155%. In the case of CMKL-AM polymer, the elemental analysis showed a 10% nitrogen amount, which corresponds to a 99% grafting ratio. The higher polymerization efficiency of OKL-AM, which was followed by a higher grafting ratio and Mw, can be attributed to that OKL contains higher phenolic hydroxyl groups required for the polymerization reaction.

Table 4.1. Properties of lignin samples.

Sample	Elemental analysis					Charge density (meq/g)	M_w (kg/mol)	Mw/Mn	Phenolic Hydroxyl (mmol/g)	Carboxylate groups (mmol/g)
	N (wt.%)	C (wt.%)	H (wt.%)	S (wt.%)	O (wt.%)					
KL	0	53.58	6.77	0.26	39.39	-1.2	20	1.67	1.31	1.37
OKL	0	50.25	7.20	0.11	42.43	-1.6	16	2.05	1.87	1.50
CMKL	0	49.51	5.97	0.19	44.33	-1.9	28	1.85	0.84	1.98
OKL-AM	12	74.35	3.9	0.12	32.12	-2.6	684	3.25	0.54	1.28
CM-AM	10	54.35	3.7	0.13	37.32	-2.4	387	2.21	0.53	1.74

4.4.2. ^{1}HNMR analysis

^{1}H-NMR spectra of unmodified kraft lignin, CMKL, OKL, OKL-AM, and CMKL-AM polymers are shown in Figure 4.1a and 4.1b. The two peaks at 3.5 and 7 ppm in unmodified kraft lignin correspond to the protons of the methoxy groups and aromatic ring protons (Dali et al., 2006). The peak at 4.7 ppm corresponds to the solvent (D_2O) in all spectra. The peaks at 3.5, and 7 ppm in carboxymethylated lignin (CMKL) were somewhat weaker compared to unmodified kraft lignin, which might be attributed to the breakage of the aromatic ring and methoxy groups during the carboxymethylation reaction (Li and Lundquist, 1999). Furthermore, a new peak at 3.8 ppm is observed in carboxymethylated kraft lignin, which corresponds to the protons of carboxymethyl groups attached to lignin, which was absent in unmodified kraft lignin (Li and Lundquist, 1999). Thus, ^{1}H-NMR analysis confirms the attachment of carboxymethyl groups to lignin during carboxymethylation reaction. In ^{1}H-NMR spectra of CMKL-AM polymer, two additional peaks at 1.6, and 2.2 pp were observed. These peaks are assigned to the to Cα and Cβ protons connecting the amide groups of the polymer (Song et al., 2007). The presence of these peaks indicates that

acrylamide was introduced to the lignin backbone. In oxidized kraft lignin (OKL), the peak at 2 ppm, which corresponds to aliphatic CH_2, was weaker compared to that of unmodified kraft lignin as a result of the breakage of lignin to smaller units and the formation of OH, and COOH groups on lignin. The peak at 8.5 ppm attributed to phenolic hydroxyl groups was higher in oxidized lignin compared to unmodified kraft lignin. As illustrated in Figure. 4.1, the content of phenolic hydroxyl groups in oxidized kraft lignin was higher due to the cleavage of the β-aryl ether bonds (Stärk et al., 2010). The observed new peaks at 1.6 and 2.2 ppm for OKL-AM, as mentioned above, indicated the polymerization of oxidized kraft lignin with acrylamide.

b
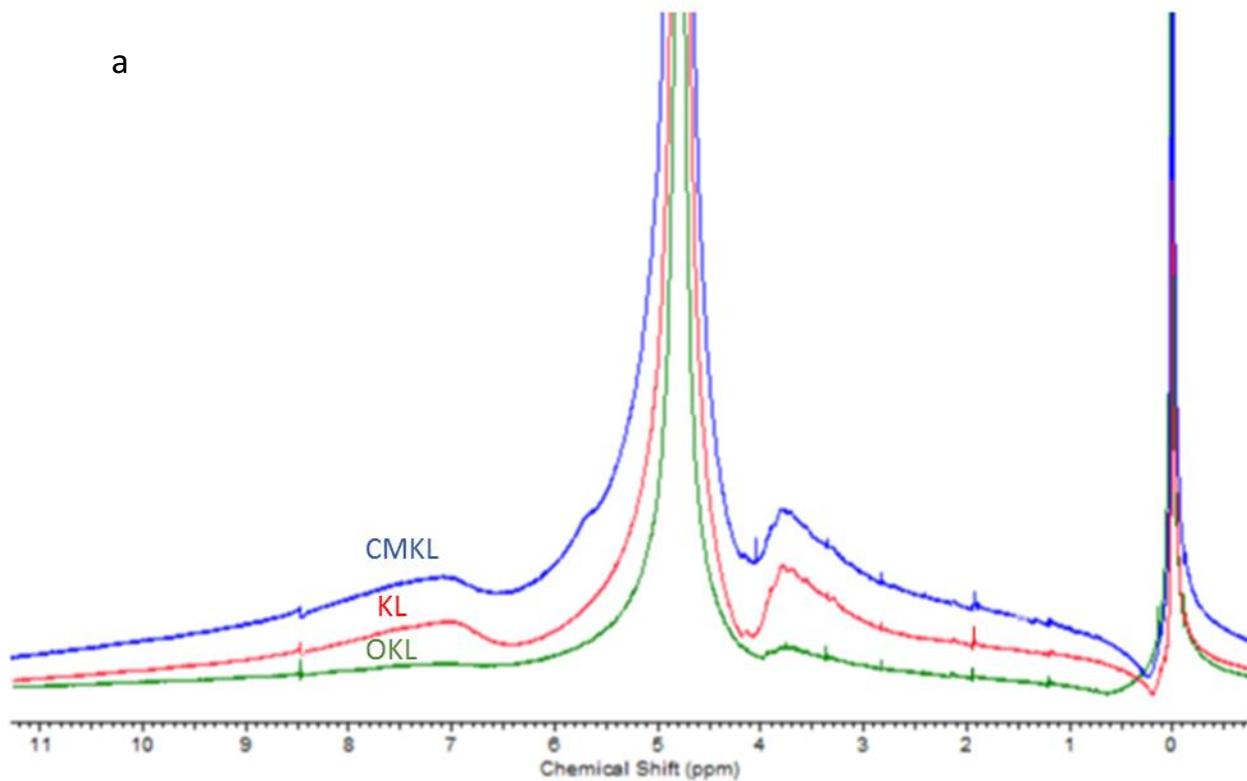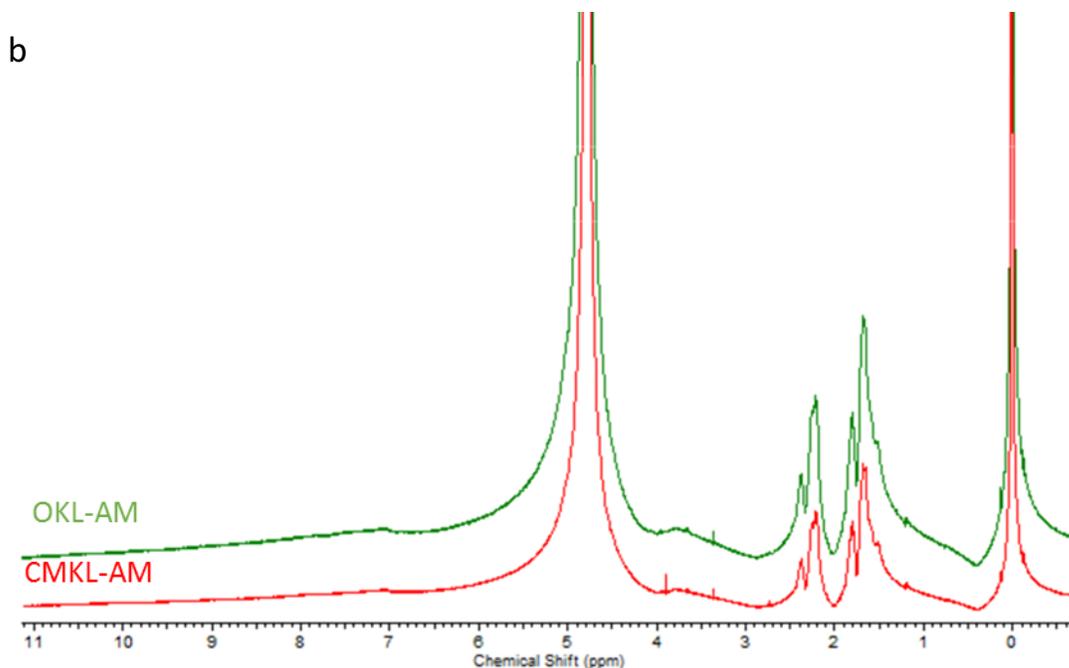
Figure 4.1. a). ^{1}H-NMR spectra of CMKL, KL, OKL, and b) ^{1}H-NMR spectra of CMKL-AM, and OKL-AM.

4.4.3. Thermogravimetric and differential scanning analysis

The thermal characteristics of kraft lignin and modified lignin samples are presented in Figure 4.2. All modified lignin samples showed higher thermal stability than KL. The weight loss below 100 °C in all samples is attributed to the elimination of water. In KL sample, a small peak between 140-200°C is observed, where the propanoid side chain of kraft lignin would start to decompose (Brebu et al., 2010). The degradation of KL started at a temperature higher than 200 °C where 60% of the sample was degraded between 260 and 600 °C, and this weight loss was attributed to the degradation of lignin backbone (Zhang et al., 2014). The thermal degradation of OKL and CMKL started at 275 °C. However, the major degradation of these samples was between 400 and 600°C. In general, OKL polymer showed a similar degradation pattern to CMKL polymer. However, CMKL showed higher thermal stability between 350 and 600 °C, where 40% weight loss was

observed compared to 55% for OKL sample. Higher thermal stability observed for CMKL can be attributed to the degradation of ether bonds linkage formed during carboxymethylation reactions (Petal et al., 2010). In a study that involved the thermal analysis of polyether ether ketone, it was reported that ether bonds decomposition occurred at a temperature higher than 600 °C (Patel et al., 2010).

Acrylamide polymerization increased the decomposition temperature for both OKL and CMKL polymers, as seen in Figure 4.2 a. The introduction of acrylamide into lignin molecule reduced the number of hydrogen bonds in lignin, where the first decomposition step occurs (Laurichesse et al., 2014). The main decomposition temperature for both OKL-AM and CMKL-AM was 400 °C. Approximately, 20% of OKL-AM polymer decomposed between 400 and 600 °C compared to 35 % weight loss for CMKL-AM. The higher thermal stability of OKL-AM with 50 % residue at 700 °C can be attributed to its higher grafting ratio, as indicated in Table 4.1. In another study that involved the grafting of acrylamide onto xanthan gum, the main thermal degradation temperature of polymers increased with increasing the grafting ratio of acrylamide (Maia et al., 2012).
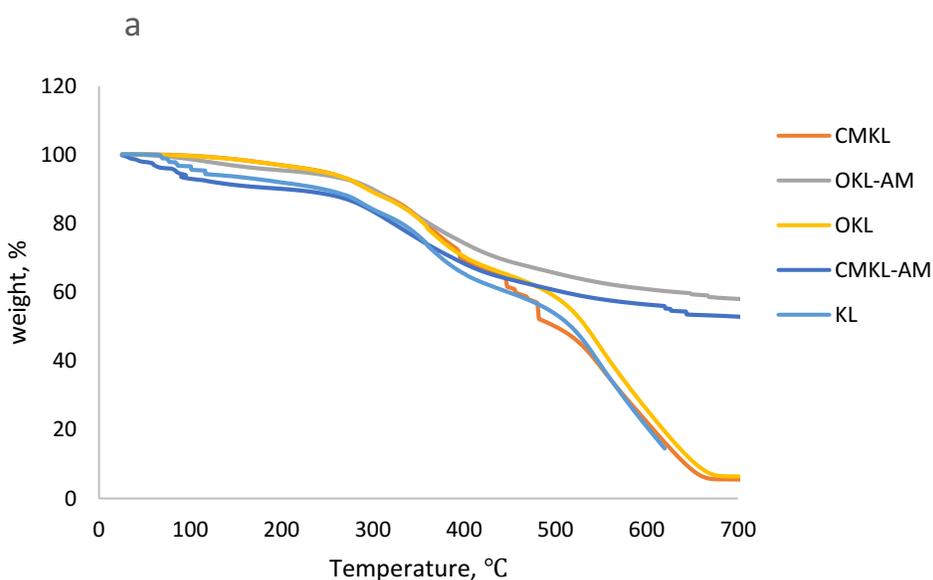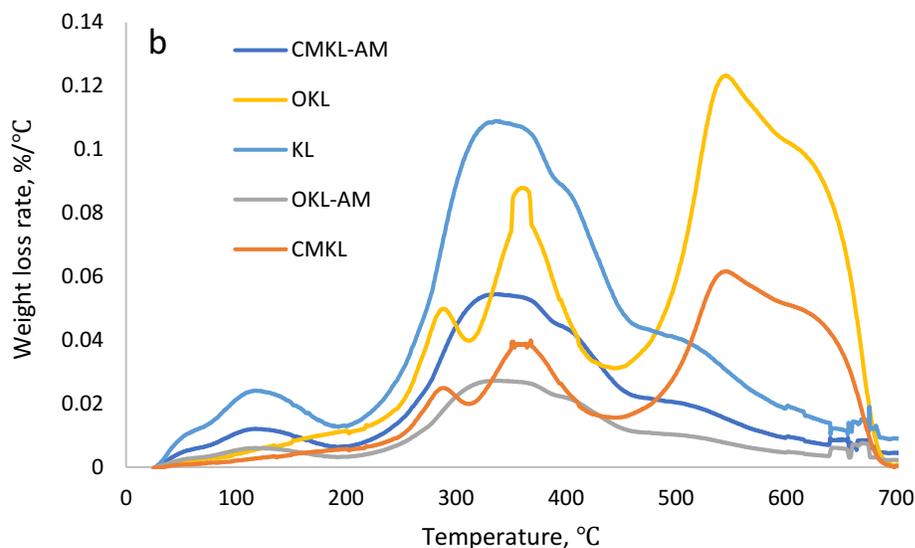
Figure 4.2. a) weight loss and b) weight loss rate of polymers at a nitrogen flow rate of 35 mL/min.

To further investigate the changes in the thermal behavior of lignin derivatives, the glass transition temperature (T_g) of the polymers was analyzed, and the results are reported in Table 4.2. As reported previously, the glass transition temperature of lignin varies depending on the source of lignin, and the process in which lignin is produced (Passoni et al., 2016). Kraft lignin's glass transition temperature (T_g) was reported to be in the range between 90 and 170 °C. As shown in Table 4.2, the T_g of KL was found to be 151 °C. Interestingly, an increase in T_g happened for all modified lignin samples except for OKL polymer, where the T_g decreased from 151 to 117 °C. The decrease in T_g for OKL can be attributed to the decrease in lignin's molecular weight that happens during the oxidation reaction. This was illustrated by Flory–Fox equation, which relates the average molecular mass of polymer to its glass transition temperature where a lower molecular mass gives a lower T_g value (Lu and Jiang, 1991).

Contrary to OKL, carboxymethylated lignin (CMKL) showed a higher T_g, which can be attributed to the formed ether linkage that raised the polymer's thermal stability (Lange and Schweers, 1980).

The highest T_g for modified lignin samples was obtained for OKL-AM (258 °C). It was reported that the T_g of the polymer was affected by its molecular weight, hydrogen bonding, and crosslinking (Heitner et al., 2010). OKL-AM polymer has a high molecular weight, which resulted in higher Tg. In addition, glass transition temperature depends on the flexibility and mobility of polymeric chains or what's known as free volume. Free volume is a measure of the space in which a polymer chain moves in relationship to the other polymeric chains around it (Praharaj and Mishra, 2015). If the polymeric chains can move easily, the glassy state of a polymer can be converted to a rubbery state at a lower temperature, i.e., a lower glass transition temperature (Balani et al., 2014). A polymer with a higher molecular weight and long chains has a less free volume that raises its T_g (Praharaj and Mishra, 2015; Aslanzadeh et al., 2016). As illustrated in Table 4.1, OKL-AM had the highest molecular weight and grafting ratio of AM, which justified its highest T_g.

The heat capacities (C_p) of modified lignin samples at constant pressure were also illustrated in Table 4.2. The heat capacity (C_p) values show the amount of heat needed to change the sample's temperature over a temperature gradient (Gordobil et al., 2017). The reported heat capacity of kraft lignin is around 0.25 to 0.29 J/g.°C (Hatakeyama, 2009). The heat capacity of kraft lignin was 0.29 (J/g.°C). The C_p increased for all modified lignin sample except for OKL sample. As mentioned earlier, as the reduction in the polymer's molecular weight reduces its glass transition temperature, it also lowers polymer's heat capacity (Balani et al., 2014). OKL-AM polymer, on the other hand, demonstrated the highest heat capacity (0.63 J/g.°C), as a result of larger molecular weight, and the higher presence of stiffening groups in the polymer chains, such as amide groups, which reduces the flexibility of the chain resulting in higher heat capacity as well as higher glass transition

temperature (Balani et al., 2014). Such results indicate higher thermal stability of OKL-AM compared to other modified lignin samples.

Table 4.2: Thermal properties of kraft lignin, and modified lignin polymers measured by DSC.

Sample	Tg (°C)	Heat capacity (J/g.°C)
KL	151	0.29
OKL	117	0.25
CMKL	189	0.33
OKL-AM	258	0.63
CMKL-AM	245	0.59

4.4.4. Adsorption analysis

The adsorption performance of KL and modified lignin samples on alumina particles at pH 6 is illustrated in Figure 4.3. The adsorption of modified lignin samples was significantly higher than unmodified lignin. As mentioned previously, the limited adsorption shown by KL is mainly attributed to lignin's limited solubility. In all modified lignin samples, the adsorption of polymers increased by increasing polymer concentration until the adsorption reaches a plateau at a concentration higher than 64 mg/L. OKL and CMKL polymers with a molecular weight of 16,000, and 28,000 g/mol, respectively, had higher adsorption on alumina particles than did OKL-AM and CMKL-AM with higher molecular weights. This indicates that a lower molecular weight of polymers facilitated its higher adsorption on alumina particles. By comparing the adsorption of OKL-AM and CMKL-AM, it is evident that polymer's charge density played a significant role in adsorption. OKL-AM with the highest charge density of -2.6 meq/g and a molecular weight of 684,000 g/mol showed higher adsorption values compared to CMKL-AM with a lower molecular weight (387×10^3 g/mol), and lower charge density (-2.4 meq/g). The main driving force for

adsorption on alumina particles is the electrostatic interaction between the cationic charges associated with alumina particles and anionic charges of lignin polymers. In the previous chapter, the adsorption of polymers on alumina particles was mainly affected by polymers' charge density. Polymers with a higher charge density had higher adsorption, regardless of their molecular weights. In this work, adsorption analysis also demonstrated that polymers' charge density significantly affected their adsorption behavior. Also, the lower molecular weight of polymers such as OKL, and CMKL facilitated higher adsorption on alumina particles. In a similar study that investigated the interaction of oxidized lignin and alumina, the adsorption of oxidized lignin samples with similar charge densities, but varied molecular weights (26000- 50000 g/mol) was studied (Alzahrani, 2018). Higher adsorption was observed for the polymer with a lower molecular weight (Alzahrani, 2018). In another study, it was stated that lowering the molecular weight of polymers would minimize the electrostatic repulsion between polymer's charged chains that might limit polymers adsorption on charged particles (Kim and Carty, 2016).
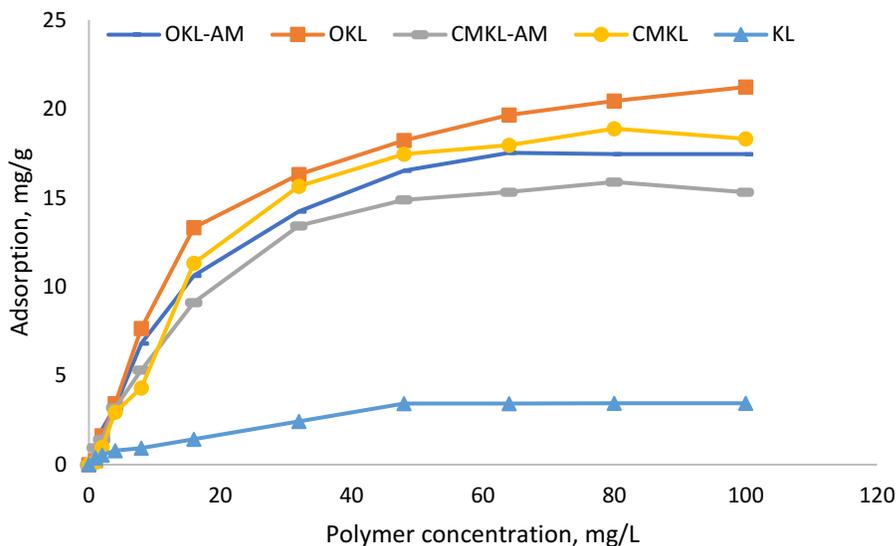

Figure. 4.3. Adsorption isotherms of KL, OKL, OKL-AM, CMKL, and CMKL-AM on alumina particles conducted at pH 6, and room temperature.

4.4.5. Zeta potential as a function of polymer concentration

Figure 4.4 shows the zeta potential of alumina suspension as a function of polymer concentration. The zeta potential is mainly used for describing the ionic strength of colloidal particles, which directly affects the stability of particles in any suspensions (Singh et al., 2003). Generally, an alumina suspension has a positive zeta potential of 30 mV at pH 6 due to its positively charged surface (Wiśniewska et al., 2012). By adding lignin samples, the zeta potential of the suspension dropped to negative values except for unmodified kraft lignin, in which the impact on the suspension's zeta potential was insignificant. The most pronounced effect on the zeta potential was achieved by OKL and CMKL polymers where the zeta potential of alumina suspension dropped from 30 mV to -39, and -42 mV, respectively. The zeta potential was clearly affected by the amount of adsorbed lignin on particles (Perez et al., 2016; Konduri and Fatehi, 2017). As OKL had higher adsorption, it affected the zeta potential of the suspensions more significantly.
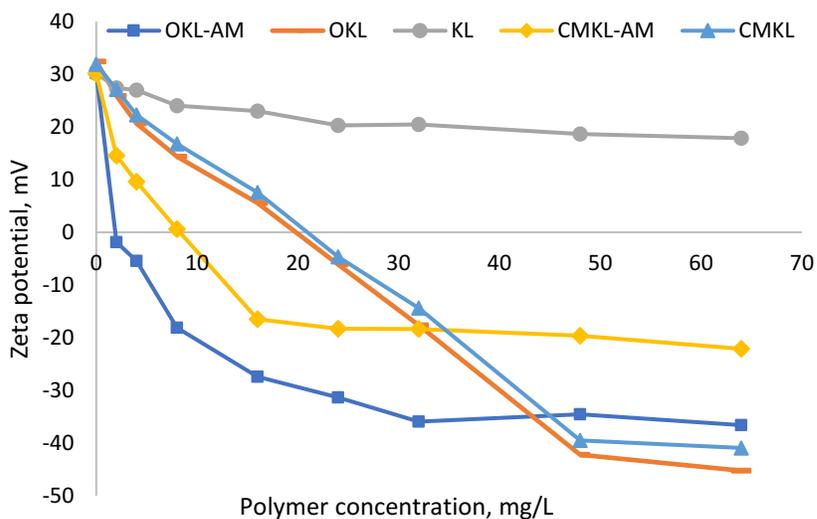

Figure 4.4. Alumina suspension's zeta potential as a function of polymer concentration, which was conducted under the conditions of pH 6, 30 min incubation at 30 °C, and 1 g/L of alumina concentration.

4.4.6. Influence of polymer dosage on alumina's relative turbidity

The effect of the addition of lignin samples on alumina suspension's relative turbidity is illustrated in Figure 4.5a. As shown, KL had an insignificant impact on the relative turbidity of alumina suspension due to lignin's limited adsorption on alumina particles (Figure 4.3). With increasing the dosage of OKL-AM and CMKL-AM polymers in the alumina suspension, a significant reduction in suspension's relative turbidity was observed. At the dosage of 4 mg of OKL-AM, the relative turbidity of alumina suspension was reduced to 0.21. Increasing OKL-AM dosage beyond 4 mg/g caused a slight increase in the relative turbidity. This increase can be attributed to OKL-AM's higher charge density (-2.6 meq/g), which might cause repulsion between alumina particles. In the case of CMKL-AM polymer, at a higher dosage of 10 mg/g, the relative turbidity of alumina suspension decreased to 0.48. OKL and CMKL polymers showed an opposite effect on the suspension's relative turbidity. OKL and CMKL polymers increased the relative turbidity of alumina particles from 1 to 1.46, and 1.23 at the polymer dosage of 10 mg/g, respectively. It is also evident that OKL and CMKL polymers acted as dispersants in alumina suspension in which they improved the stability of the system. As explained earlier, the lower molecular weight of OKL and CMKL facilitated their adsorption, which caused a significant reduction in the zeta potential and improvement in the repulsion between particles. In a similar work that investigated the effect of anionic polymers on stabilizing a ceramic suspension, the suspension's relative turbidity increased as the zeta potential of the suspension decreased to more negative values (Tyliszczak et al., 2012). In addition, OKL and CMKL polymers may be used as dispersants in the mining industry (ore suspensions), cement admixture, cement admixture, and many other applications (Hubbe et al., 2011; Li and Ge, 2011).

For polymers (OKL-AM, CMKL-AM) that shows flocculation behavior, alumina removal was investigated as a function of polymer dosage in Figure 4.5b. At the same dosages that achieved the lowest relative turbidity in Figure 4.5a, OKL-AM showed 86% alumina removal compared to 70 % removal achieved by CMKL-AM. The higher flocculation efficiency of OKL-AM than CMKL-AM was mainly attributed to the higher molecular weight of the polymer. It was reported that the molecular weight of polymers has a significant effect in bridging particles, and thus minimizing colloidal suspensions' relative turbidity (Divakaran and Pillai 2001; Wong et al., 2006).
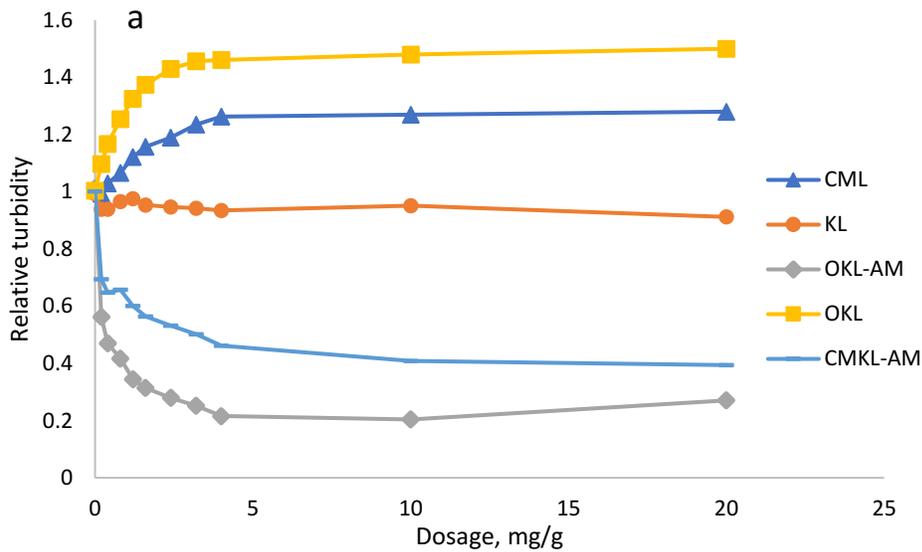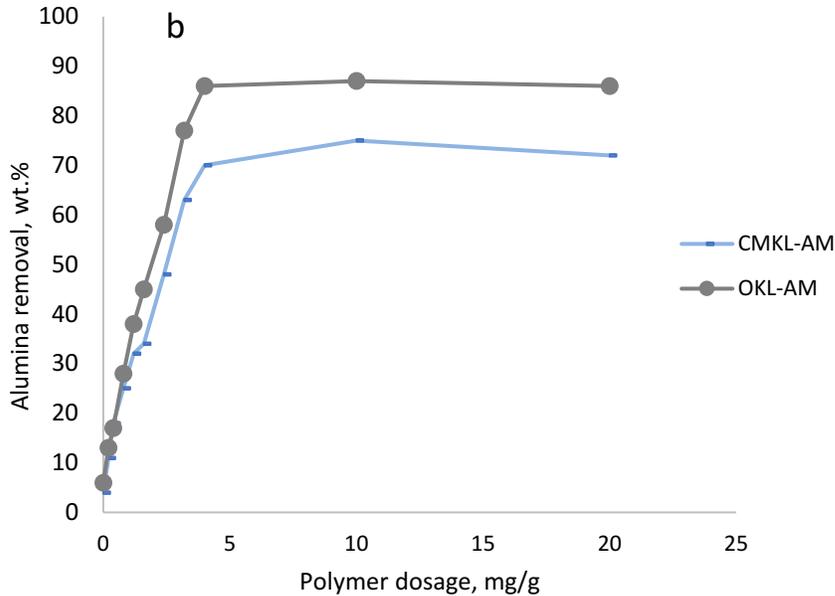
Figure 4.5. a) Influence of polymers dosages on alumina suspension relative turbidity, b) Alumina removal as a function of polymers dosage. The experiments were conducted under the conditions of 25 °C for 2h at pH 6.

To understand the mechanism underlying the ability of modified lignin samples (OKL-AM and CMKL-AM) in decreasing the relative turbidity of alumina suspension, the relative turbidity of the suspension was plotted as a function of alumina suspension's zeta potential. As illustrated in Figure 4.6, by reducing the zeta potential of the suspension with increasing polymer concentration, the relative turbidity of the suspension dropped. However, the minimum relative turbidity of alumina suspension was not achieved at neutral zeta potential. It was reported that suspension with a zeta potential of ±30 mV to be stable due to the repulsion forces between particles (Araki et al., 1998; Sharma et al., 2014). OKL-AM and CMKL-AM polymers altered the relative turbidity of alumina suspension to - 48, and 24 mV, respectively, due to their high adsorption, and accumulation of negative charge in the diffuse layer of particles. The minimum relative turbidity for these polymers was achieved at these values of zeta potential (-48, and -24 mV) indicating that

the flocculation happens through batching or bridging mechanism facilitated by OKL-AM and CMKL-AM high molecular weight and not through charge neutralization mechanism.
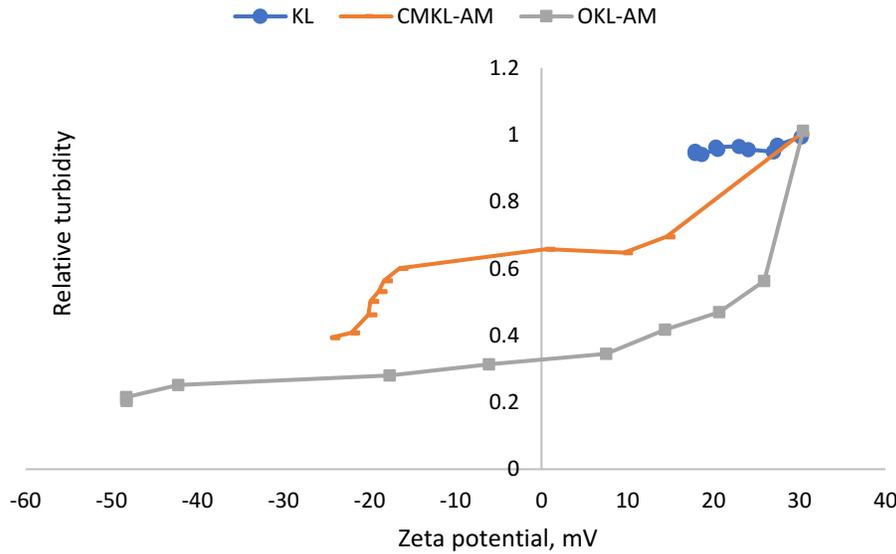

Figure 4.6. Correlation between the relative turbidity and zeta potential of alumina suspensions for KL, OKL-AM, and CMKL-AM polymers.

4.4.7. Flocculation under dynamic conditions

Focused beam reflectance measurement (FBRM) was used to investigate the performance of polymers in alumina suspension under dynamic conditions. Figure 4.7 illustrates the size distribution of particles obtained after adding OKL, CMKL, OKL-AM, and CMKL-AM polymers at pH 6 and 250 rpm. As can be seen, the blank sample of alumina suspension has around 1200 counts with the mean size of 21 μm. By adding 10 mg/g of OKL and CMKL polymers, the number of counts increased to approximately 2000, and the chord length of particles decreased to 10 μm, and 14 μm for OKL and CMKL, respectively. These results were in accordance with the results obtained in the relative turbidity analysis for OKL and CMKL, where the relative turbidity of

alumina suspension increased, indicating a better separation of particles and higher stability. Moreover, the same dosage of OKL-AM and CMKL-AM polymers that led to the minimum relative turbidity was added to this system, and the chord length was ramped up, and the number of particles in the suspension diminished. This change provides evidence of alumina flocculation by OKL-AM and CMKL-AM polymers. OKL-AM shows a higher flocculation efficiency compared to CMKL indicating that its higher molecular weight facilitated flocculation and the formation of larger flocs by bridging of alumina particles (Wong et al., 2006).
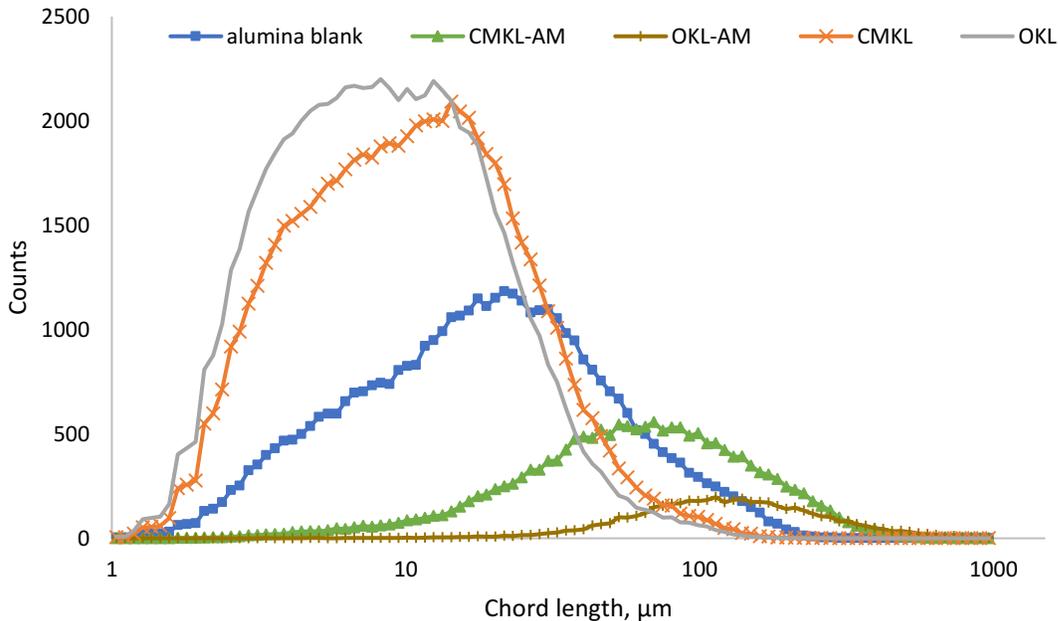

Figure 4.7. Chord length distribution of aluminum oxide particles formed under polymers optimal dosages used in relative turbidity analysis.

Figure (4.8) presents the formation, breakage, and reformation of flocs generated in alumina suspension as a function of time in the presence of OKL-AM, and CMKL-AM polymers. Different shear rates were applied to investigate the effect of shear rate on the formation and breakage of flocs. As shown, the formation of the floc occurs faster in alumina suspension for OKL-AM than for CMKL-AM. Floc formation reached a steady state at 250 rpm where the floc chord length was

constant at 140 and 70 μm for OKL-AM and CMKL-AM, respectively, indicating a dynamic balance between floc growth and breakage (Blanco et al., 200). Generally, the chord length of particles decreased via increasing the share rate to 750 rpm. Floc breakages were more significant via increasing the share rates in the suspension where CMKL-AM was used. As shown, the chord length of formed flocs using CMKL-AM dropped to 23 μm, and that of OKL-AM dropped to 46 μm, indicating stronger flocs (higher T_{df} value) in the case of OKL-AM as indicated in Figure 4.9.a. After reducing the share rate to 250 rpm, we noticed a higher re-flocculation tendency (lower T_{rf}) in the system where OKL-AM flocculant was used. The regrowth of flocs took less time (140 s, and larger flocs (95 μm) were reformed.
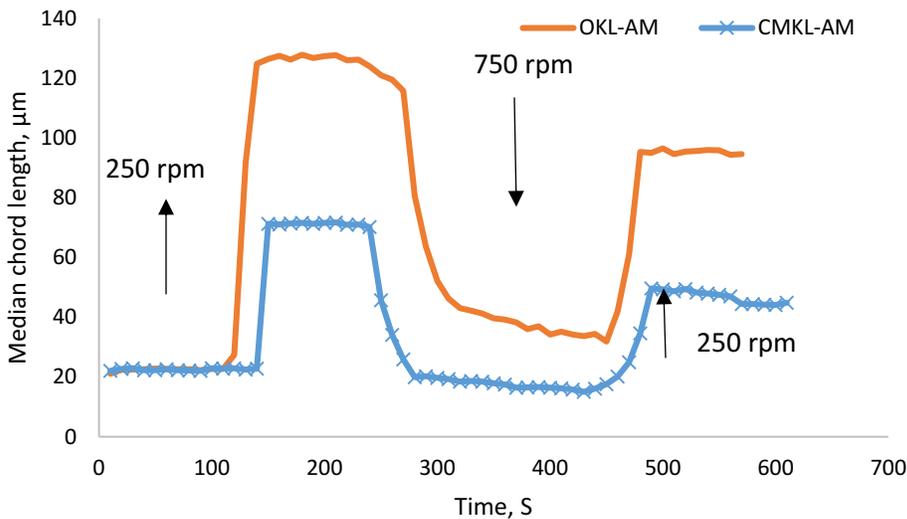

Figure 4. 8. Flocculation evolution OKL-AM, and CMKL flocculants in alumina suspension.
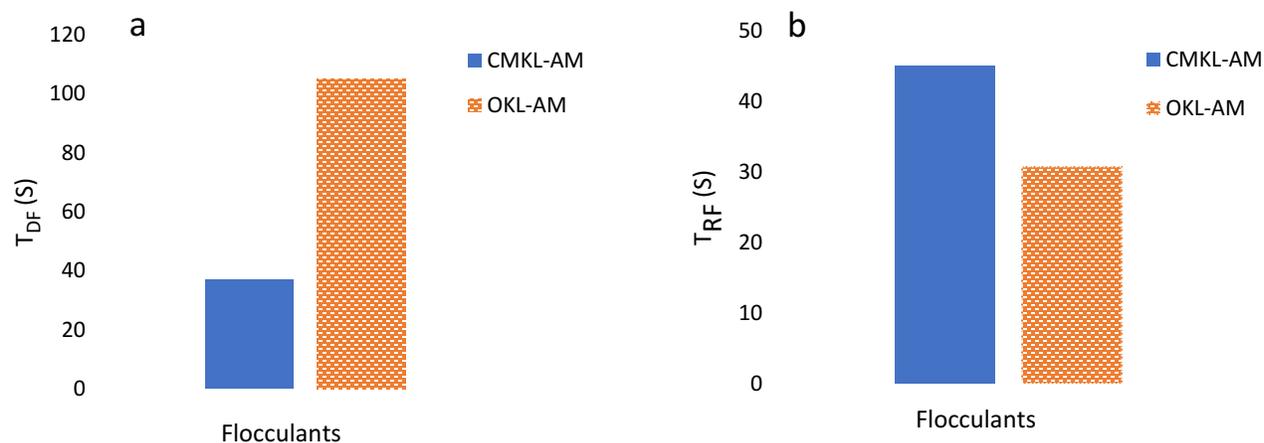
Figure 4.9. a) Flocs formation tendency (T_{df}) and b) flocs reflocculation tendency (T_{rf}) values for CMKL-AM, OKL-AM polymers.

4.4.8. Conclusions

In this chapter, Kraft lignin's limited solubility and low charge density were altered via chemical modification methods of oxidation and carboxymethylation. The effect of pretreated kraft lignin polymers (OKL, CMKL) on the relative turbidity and zeta potential of alumina suspension was studied. Oxidized kraft lignin that had the highest adsorption value (20.5 mg/g) increased the relative turbidity of the suspension to 1.46 at a zeta potential value of – 42. mV, resulting in a more stable system. Carboxylmethylated kraft lignin (CMKL) also functioned as a dispersant in alumina suspension with increased relative turbidity (1.23) at a zeta potential value of – 39 mV. The significant change in the suspension's zeta potential demonstrated by OKL and CMKL polymers was the result of their higher adsorption on alumina particles that was facilitated by the polymers' low molecular weight. The produced OKL-AM and CMKL-AM polymers with a high molecular

weight were applied as a flocculant in alumina suspension where alumina suspension's relative turbidity decreased significantly compared to unmodified kraft lignin that had no impact on suspension's relative turbidity. The minimum relative turbidity (0.2) achieved by OKL-AM confirms the impact of polymer's high molecular weight in increasing flocculants efficiency. This reduction in the relative turbidity resulted in 86 %, and 75% alumina removal for OKL-AM, and CMKL-AM, respectively. Flocs strength and flocculation process' reversibility under various shear rates were studied. The formed flocs demonstrated high strength even under a higher shear rate of 750 rpm, and high re-flocculation tendency where the flocs reformation occurs after 150 s of returning the shear rate to its initial state (250 rpm).

References

Alfano, J. C., Carter, P. W., & Gerli, A. (1998). Characterization of the flocculation dynamics in a paperma king system by non-imaging reflectance scanning laser rnicroscopy (SLM). *Nordic Pulp & Paper Research Journal*, 13(2), 159-165.

Alfano, J. C., Carter, P. W., & Whitten, J. E. (1999). Use of scanning laser microscopy to investigate microparticle flocculation performance. *Journal of pulp and paper science*, 25(6), 189-195.

Alzahrani, P. (2018). Dispersion and flocculation affinity of anionically charged kraft lignin. Lakehead University. Master thesis.

Araki, J., Wada, M., Kuga, S., & Okano, T. (1998). Flow properties of microcrystalline cellulose suspension prepared by acid treatment of native cellulose. *Colloids and Surfaces A: Physicochemical and Engineering Aspects*, *142*(1), 75-82.

Araujo, E., Rodríguez-Malaver, A. J., González, A. M., Rojas, O. J., Peñaloza, N., Bullón, J., ... & Dmitrieva, N. (2002). Fenton's reagent-mediated degradation of residual Kraft black liquor. *Applied biochemistry and biotechnology*, *97*(2), 91-103.

Araujo, E., Rodríguez-Malaver, A. J., González, A. M., Rojas, O. J., Peñaloza, N., Bullón, J., ... & Dmitrieva, N. (2002). Fenton's reagent-mediated degradation of residual Kraft black liquor. *Applied biochemistry and biotechnology*, *97*(2), 91-103.

Balani, K., Verma, V., Agarwal, A., & Narayan, R. (2014). Physical, Thermal, and Mechanical Properties of Polymers. *Materials Research Innovations,* 42, 54-67.

Bentivenga, G., Bonini, C., D'Auria, M., & De Bona, A. (2003). Degradation of steam-exploded lignin from beech by using Fenton's reagent. *Biomass and Bioenergy*, *24*(3), 233-238.

Blanco, A., Fuente, E., Negro, C., & Tijero, J. (2002). Flocculation monitoring: focused beam reflectance measurement as a measurement tool. *Canadian journal of chemical engineering*, 80(4), 734-740.

Brebu, M., & Vasile, C. (2010). Thermal degradation of lignin—a review. *Cellulose Chemistry & Technology*, *44*(9), 353.

Cerrutti, B. M., De Souza, C. S., Castellan, A., Ruggiero, R., & Frollini, E. (2012). Carboxymethyl lignin as stabilizing agent in aqueous ceramic suspensions. *Industrial Crops and Products*, *36*(1), 108-115.

Chien, S. N., Amidon, T. E., & Lai, Y. Z. (2012). Fractionation of wood polymers by carboxymethylation: Exploring the strategy. *TAPPI JOURNAL*, *11*(1), 29-37.

Da Silva, L. G., Ruggiero, R., Gontijo, P. D. M., Pinto, R. B., Royer, B., Lima, E. C., ... & Calvete, T. (2011). Adsorption of Brilliant Red 2BE dye from water solutions by a chemically modified sugarcane bagasse lignin. *Chemical Engineering Journal*, *168*(2), 620-628.

Dali, S., Lefebvre, H., Gharbi, R. E., & Fradet, A. (2006). Synthesis of poly (glycolic acid) in ionic liquids. *Journal of Polymer Science Part A: Polymer Chemistry*, *44*(9), 3025-3035.

Dalimova, G. N. (2005). Oxidation of hydrolyzed lignin from cotton-seed husks by hydrogen peroxide. *Chemistry of natural compounds*, *41*(1), 85-87.

Divakaran, R., & Pillai, V. S. (2001). Flocculation of kaolinite suspensions in water by chitosan. *Water Research*, *35*(16), 3904-3908.

Fadeeva, V. P., Tikhova, V. D., & Nikulicheva, O. N. (2008). Elemental analysis of organic compounds with the use of automated CHNS analyzers. *Journal of analytical chemistry*, *63*(11), 1094-1106.

Fengel, D., & Wegener, G. (1984). Wood Chemistry, ultrastructure, reactions.*Walter de Gruyter, Berlin and New York*, p 613.

Gellerstedt, G., & Agnemo, R. (1980). The reactions of lignin with alkaline hydrogen peroxide. Part III. The oxidation of conjugated carbonyl structures. Acta Chem. Scand. B, 34(0), 4.

Gordobil, O., Herrera, R., Llano-Ponte, R., & Labidi, J. (2017). Esterified organosolv lignin as hydrophobic agent for use on wood products. *Progress in Organic Coatings*, *103*, 143-151.

Hatakeyama, H., & Hatakeyama, T. (2009). Lignin structure, properties, and applications. *In Biopolymers* (pp. 1-63). Springer, Berlin, Heidelberg.

He, W., Gao, W., & Fatehi, P. (2017). Oxidation of kraft lignin with hydrogen peroxide and its application as a dispersant for kaolin suspensions. *ACS Sustainable Chemistry & Engineering*, *5*(11), 10597-10605.

Hu, L., Pan, H., Zhou, Y., & Zhang, M. (2011). Methods to improve lignin's reactivity as a phenol substitute and as replacement for other phenolic compounds: A brief review. *BioResources*, *6*(3), 3515-3525.

Hubbe, M. A., Hasan, S. H., & Ducoste, J. J. (2011). Cellulosic substrates for removal of pollutants from aqueous systems: A review. 1. Metals. *BioResources*, *6*(2), 2161-2287.

Jahan, M. S., Liu, Z., Wang, H., Saeed, A., & Ni, Y. (2012). Isolation and characterization of lignin from prehydrolysis liquor of kraft-based dissolving pulp production. *Cellul. Chem. Technol*, *46*(3-4), 261-267.

Kim, U., & Carty, W. M. (2016). Effect of polymer molecular weight on adsorption and suspension rheology. *Journal of the Ceramic Society of Japan*, *124*(4), 484-488.

Konduri, M. K., & Fatehi, P. (2015). Production of water-soluble hardwood Kraft Lignin via Sulfomethylation using formaldehyde and sodium sulfite. *ACS Sustainable Chemistry & Engineering*, *3*(6), 1172-1182.

Konduri, M. K., & Fatehi, P. (2017). Dispersion of kaolin particles with carboxymethylated xylan. *Applied Clay Science*, 137 (4), 183-191.

Konduri, M. K., Kong, F., & Fatehi, P. (2015). Production of carboxymethylated lignin and its application as a dispersant. *European Polymer Journal*, *70*, 371-383.

Lange, W., & Schweers, W. (1980). The carboxymethylation of organosolv and kraft lignins. *Wood Science and Technology*, *14*(1), 1-7.

Laurichesse, S., Huillet, C., & Avérous, L. (2014). Original polyols based on organosolv lignin and fatty acids: new bio-based building blocks for segmented polyurethane synthesis. *Green Chemistry*, *16*(8), 3958-3970.

Lee, B., & Schlautman, M. (2015). Effects of polymer molecular weight on adsorption and flocculation in aqueous kaolinite suspensions dosed with nonionic polyacrylamides. *Water*, *7*(11), 5896-5909.

Li, S., & Lundquist, K. (1994). A new method for the analysis of phenolic groups in lignins by 1H NMR spectroscopy. *Nordic Pulp & Paper Research Journal*, *9*(3), 191-195.

Li, Z., & Ge, Y. (2011). Extraction of lignin from sugar cane bagasse and its modification into a high performance dispersant for pesticide formulations. *Journal of the Brazilian Chemical Society*, *22*(10), 1866-1871.

Lu, X., & Jiang, B. (1991). Glass transition temperature and molecular parameters of polymer. *Polymer*, *32*(3), 471-478.

Mahmood, N., Yuan, Z., Schmidt, J., & Xu, C. C. (2016). Depolymerization of lignins and their applications for the preparation of polyols and rigid polyurethane foams: A review. *Renewable and Sustainable Energy Reviews*, *60*, 317-329.

Maia, A. M., Silva, H. V., Curti, P. S., & Balaban, R. C. (2012). Study of the reaction of grafting acrylamide onto xanthan gum. Carbohydrate polymers, 90(2), 778-783.

Nagieb, Z. A. (1985). Demethylation of thiolignin by reaction with potassium dichromate—a kinetic study. *Wood science and technology*, *19*(3), 233-242.

Olivares, M. A. R. C. E. L. A., Guzman, J. A., Natho, A. R. T. U. R. O., & Saavedra, A. (1988). Kraft lignin utilization in adhesives. *Wood Science and Technology*, *22*(2), 157-165.

Passoni, V., Scarica, C., Levi, M., Turri, S., & Griffini, G. (2016). Fractionation of industrial softwood kraft lignin: Solvent selection as a tool for tailored material properties. *ACS Sustainable Chemistry & Engineering*, *4*(4), 2232-2242.

Patel, P., Hull, T. R., McCabe, R. W., Flath, D., Grasmeder, J., & Percy, M. (2010). Mechanism of thermal decomposition of poly (ether ether ketone)(PEEK) from a review of decomposition studies. Polymer Degradation and Stability, 95(5), 709-718.

Peng, X. W., Ren, J. L., Zhong, L. X., Peng, F., & Sun, R. C. (2011). Xylan-rich hemicelluloses-graft-acrylic acid ionic hydrogels with rapid responses to pH, salt, and organic solvents. *Journal of agricultural and food chemistry*, *59*(15), 8208-8215.

Petzold, K., Schwikal, K., Günther, W., & Heinze, T. (2005). Carboxymethyl Xylan-Control of Properties by Synthesis. In *Macromolecular symposia*, 232 (1), 27-36.

Praharaj, M., & Mishra, S. (2015). Comparative study of molecular interaction in ternary liquid mixtures of polar and non-polar solvents. *Journal of Pure and Applied Ultrasonics*, *37*, 68-77.

Sharma, S., Shukla, P., Misra, A., & Mishra, P. R. (2014). Interfacial and colloidal properties of emulsified systems: pharmaceutical and biological perspective. *Colloid and interface science in pharmaceutical research and development* 154 (2), 149-172.

Singh, R. P., Nayak, B. R., Biswal, D. R., Tripathy, T., & Banik, K. (2003). Biobased polymeric flocculants for industrial effluent treatment. *Materials Research Innovations*, *7*(5), 331-340.

Singh, V., Tiwari, A., Pandey, S., & Singh, S. K. (2006). Microwave-accelerated Synthesis and Characterization of Potato Starch-g-poly (acrylamide). *Starch-Stärke*, *58*(10), 536-543.

Song, H., Zhang, S. F., Ma, X. C., Wang, D. Z., & Yang, J. Z. (2007). Synthesis and application of starch-graft-poly (AM-co-AMPS) by using a complex initiation system of CS-APS. *Carbohydrate Polymers*, *69*(1), 189-195.

Stärk, K., Taccardi, N., Bösmann, A., & Wasserscheid, P. (2010). Oxidative depolymerization of lignin in ionic liquids. *ChemSusChem*, *3*(6), 719-723.

Sun, R., Lawther, J. M., & Banks, W. B. (1995). The effect of alkaline nitrobenzene oxidation conditions on the yield and components of phenolic monomers in wheat straw lignin and compared to cupric (II) oxidation. *Industrial Crops and Products*, *4*(4), 241-254.

Tyliszczak, B., Sobczak-Kupiec, A., Bialik-Was, K., & Kasprzyk, W. (2012). Stabilization of ceramics particles with anionic polymeric dispersants. *Journal of nanoscience and nanotechnology*, *12*(12), 9312-9318.

Wang, B. Y., Lim, D. S., & Oh, Y. J. (2009). Effect of the molecular weight of dispersant to the slurry for lead-free transparent dielectric films. *Molecular Crystals and Liquid Crystals*, *514*(1), 190-520.

Wang, H. M., MIN, X. B., CHAI, L. Y., & SHU, Y. D. (2011). Biological preparation and application of poly-ferric sulfate flocculant. *Transactions of Nonferrous Metals Society of China*, 21(11), 2542-2547.

Wang, J., Yao, K., Korich, A. L., Li, S., Ma, S., Ploehn, H. J., ... & Tang, C. (2011). Combining renewable gum rosin and lignin: Towards hydrophobic polymer composites by

controlled polymerization. *Journal of Polymer Science Part A: Polymer Chemistry*, *49*(17), 3728-3738.

Wiśniewska, M., Chibowski, S., & Urban, T. (2015). Impact of anionic and cationic polyacrylamide on the stability of aqueous alumina suspension—comparison of adsorption mechanism. *Colloid and Polymer Science*, 293(4), 1171-1179.

Wong, S. S., Teng, T. T., Ahmad, A. L., Zuhairi, A., & Najafpour, G. (2006). Treatment of pulp and paper mill wastewater by polyacrylamide (PAM) in polymer induced flocculation. *Journal of Hazardous Materials*, *135*(1-3), 378-388.

Xiong, B., Loss, R. D., Shields, D., Pawlik, T., Hochreiter, R., Zydney, A. L., & Kumar, M. (2018). Polyacrylamide degradation and its implications in environmental systems. *NPJ Clean Water*, *1*(1), 17.

Zhang, J., Feng, L., Wang, D., Zhang, R., Liu, G., & Cheng, G. (2014). Thermogravimetric analysis of lignocellulosic biomass with ionic liquid pretreatment. *Bioresource technology*, *153*, 379-382.

Zhou, X. (2014). Oxidation of lignin-carbohydrate complex from bamboo with hydrogen peroxide catalyzed by Co (salen). *Hemijska industrija*, *68*(5), 541.

Chapter 5: Conclusions and recommendations

5.1. Summary of conclusion

In this work, the effect of different reaction parameters on the polymerization of kraft lignin and acrylamide was investigated. The optimal conditions for kraft lignin-acrylamide (KL-AM) polymerization was found to be 7 mol/mol AM/KL molar ratio, 80 °C, 3 h, pH 10, 3 wt. % (based on lignin) of $K_2S_2O_8$ as an initiator. The grafting of acrylamide into lignin backbone was confirmed by GPC, FTIR, NMR, and elemental analysis. The properties of kraft lignin that hinder its use as a flocculant, such as limited solubility, low charge density, and low molecular weight were significantly altered by polymerization with AM where the obtained polymer had a molecular weight of $1,064 \times 10^3$ g/mol, and a charge density of -2.33 meq/g. The increase in the molecular weight and charge density of kraft lignin after AM polymerization resulted in better flocculation efficiency that was illustrated in the reduction of alumina suspension's relative turbidity from 1 to 0.3, and 84 % alumina removal, while unmodified kraft lignin had no impact on altering the relative turbidity or the zeta potential of alumina suspension.

To further increase the polymer's charge density, KL-AM was hydrolyzed. The hydrolysis of KL-AM was associated with a reduction in the polymer's molecular weight. However, the polymer's charge density increased from -2.33 to -3.62 meq/g due to the increase of carboxyl groups content (5.04 mmol/g). The thermal properties of KL-AM and HKL-AM polymers were analyzed using DSC and TGA by which polymers showed higher thermal stability, especially in the range of 200-500 °C, and the majority of unmodified kraft lignin and acrylamide homopolymer (PAM) was degraded.

This work also involved the polymerization of oxidized and carboxymethylated lignin and acrylamide under the optimal polymerization conditions mentioned above. The pretreatment of kraft lignin via oxidation and carboxymethylation was investigated to increase kraft lignin charge density prior to acrylamide polymerization. The oxidation of kraft lignin was exploited under the reaction conditions of 0.77 mol/mol NaOH/H_2O_2 ratio, 80 ºC, and 2.85 mol/mol H_2O_2/lignin ratio for 2 h. The obtained oxidized kraft lignin (OKL) had a charge density of -1.6 meq/g and phenolic hydroxyl groups content of 1.87 mmol/g. In the synthesis of carboxymethylated kraft lignin, sodium chloroacetate was used to introduce carboxymethyl groups into lignin. The reaction conditions were 3 mol/mol SCA/lignin ratio, 0.15 M NaOH(aq), 4 h, 40 °C, and 16.7 g/L lignin concentration. The pretreatment of kraft lignin via carboxymethylation increased the molecular weight and charge density of lignin as a result of the attachment of carboxymethyl group to lignin (1.98 mmol/g). The subsequent polymerization of pretreated lignin samples with acrylamide was more efficient with oxidized kraft lignin compared to carboxymethylated lignin. The higher reactive sites in oxidized lignin resulted in higher grafting ratio and larger molecular weight for OKL-AM.

CMKL-AM and OKL-AM polymers showed higher thermal stability than OKL and CMKL. Only 20% of OKL-AM and 35% of CMKL-AM decomposed in the temperature range of 400 and 600 °C. This thermal stability was attributed to the improvement of intermolecular linkages in these samples. DSC results also showed an increase in T_g and C_p of all modified lignin polymers except oxidized kraft lignin, where the reduction in polymer's molecular weight reduced its glass transition temperature and heat capacity.

The adsorption analysis of modified lignin samples was significantly affected by the polymer's charge density. Polymers of HKL-AM and OKL-AM had high adsorption affinity. In addition, the

lower molecular weight of OKL and CMKL compared to other polymers facilitated their adsorption on alumina particles, which resulted in significant alteration of the zeta potential of the alumina suspension. The reduction in the zeta potential of alumina suspension from +30 mV to - 45, and – 39 mV in OKL and CMKL, respectively, increased the relative turbidity of the suspension due to increased electrostatic repulsion between particles. In the case of polymers with higher molecular weight (HKL-AM, KL-AM, OKL-AM, and CMKL-AM), the flocculation (i.e., minimum relative turbidity) was obtained at high negative values; indicating a bridging mechanism. Two of the lignin-acrylamide flocculants (HKL-AM, and OKL-AM) significantly outperformed the other lignin flocculants by producing larger flocs and removing more alumina particles. The minimum relative turbidity showed by these polymers (0.13, and 2.1) resulted in 92 %, and 86% alumina removal. Flocculation under dynamic conditions was also assessed to investigate flocs strength and re-flocculation tendency as a function of time. The modified lignin polymers with high charge density (i.e., HKL-AM, and OKL-AM) showed more tendency for aggregation, which led to the formation of larger flocs. A larger chord length of 140 -126 μm was observed using these polymers with less time to re-flocculate. In the case of CMKL, OKL polymers, the chord length of alumina particles was reduced from 21 μm to 14 and 10 μm, respectively, with increased counts indicating higher stability and more dispersed particles.

5.2. Recommendation for future work

In this thesis, synthetic alumina suspension was used as a model to asses the flocculation performance of anionic kraft lignin -acrylamide based flocculants. However, industrially produced suspensions may have different compositions and conditions, thus affecting flocculation behavior differently. Testing these polymers on industrial samples of alumina suspensions and other

industrial suspensions are recommended to generate a deeper understanding and more industrially

attractive results.